

CONTENTS

A Study of the Invariance Property  
of the  $\beta$  -decay Interaction under  
Time-Reversal.

|  |        |
|--|--------|
| 1. Parity  | page 1 |
| (i) Strong Interactions  | 2      |
| (ii) Weak Interactions   | 5      |
| 2. The Two Component Neutrino Theory and the<br>PCT Theorem                            | 8      |
| 3. Consequences of the Conservation of Parity<br>and the Two Component Neutrino Theory |        |
| (i) Theory   | 10     |
| (ii) Experiment  | 14     |
| 4. Coupling Types present in Weak Interactions   | 18     |
| 5. Helicity  | 23     |
| 6. The Universal Fermi Interaction   | 26     |
| 7. Time-Reversal   |        |
| (i) Strong Interactions  | 31     |
| (ii) Weak Interactions   | 32     |

submitted by

VIOLET A. BRIGLMEN, B.Sc.

for the degree of  
DOCTOR OF PHILOSOPHY

INTRODUCTION TO EXPERIMENT

|                  |    |
|------------------|----|
| 1. General       | 41 |
| 2. Apparatus     | 44 |
| 3. Choice of ... | 47 |

University of Edinburgh

August, 1960.



CONTENTS.PRELIMINARY MEASUREMENTS.Chapter I.INTRODUCTION: RECENT CHANGES AND DEVELOPMENTS IN  
BETA-DECAY THEORY.

|  |        |
|--|--------|
| 1. Parity  | page 1 |
| (i) Strong Interactions  | 2      |
| (ii) Weak Interactions   | 5      |
| 2. The Two Component Neutrino Theory and the<br>PCT Theorem                                | 8      |
| 3. Consequences of the Non-Conservation of Parity<br>and the Two Component Neutrino Theory |        |
| (i) Theory   | 10     |
| (ii) Experiment  | 14     |
| 4. Coupling Types present in Weak Interactions   | 18     |
| 5. Helicity  | 23     |
| 6. The Universal Fermi Interaction   | 26     |
| 7. Time-Reversal   |        |
| (i) Strong Interactions  | 31     |
| (ii) Weak Interactions   | 32     |

Chapter II.INTRODUCTION TO EXPERIMENT.

|                     |    |
|---------------------|----|
| 1. General          | 41 |
| 2. Apparatus        | 44 |
| 3. Choice of Source | 47 |

ACKNOWLEDGMENTSREFERENCES

Chapter III.PRELIMINARY MEASUREMENTS.

|   |         |
|---|---------|
| 1. Adjustment of Voltages on the<br>Photomultiplier Tubes | page 49 |
| 2. Resolving Times of the Coincidence Channels            | 49      |
| 3. Source Preparation                                     | 50      |
| 4. Choice of Scattering Foils                             | 51      |
| 5. Instrumental Asymmetries                               | 52      |

Chapter IV.EXPERIMENTAL PROCEDURE AND TREATMENT OF RESULTS.

|   |    |
|---|----|
| 1. Normalization and Correction Factors | 56 |
| 2. Results                              | 67 |

Chapter V.DISCUSSION OF POSSIBLE SOURCES OF INSTRUMENTAL  
ASYMMETRIES AND FURTHER RESULTS.

|                             |    |
|-----------------------------|----|
| 1. Instrumental Asymmetries | 73 |
| 2. Further Observations     | 80 |

Chapter VI.DISCUSSION OF RESULTS.

|   |    |
|---|----|
| 1. Comparison of the Present Results with Those<br>of Other Experimenters | 86 |
| 2. Consideration of Coulomb Correction Terms                              | 91 |

|                 |    |
|-----------------|----|
| ACKNOWLEDGMENTS | 95 |
|-----------------|----|

|            |    |
|------------|----|
| REFERENCES | 96 |
|------------|----|

## Chapter I.

### Introduction:

#### Recent Changes and Developments in Beta-Decay Theory.

##### 1. Parity.

Prior to 1956 it was generally accepted that parity was conserved in both weak and strong interactions; however in that year Lee & Yang<sup>(1)</sup> reviewed the experimental data then available, in particular that concerning the decay of the  $\theta$  - and  $\tau$ -mesons, and questioned the validity of this assumption.

The  $\theta$  - and  $\tau$ -mesons have almost identical masses and half-lives but decay differently, the  $\theta$  decay being a two body decay, ( $\theta^{\pm} \rightarrow \pi^{\pm} + \pi^0$ ), and the  $\tau$  decay being a three body one, ( $\tau^{\pm} \rightarrow \pi^{\pm} + 2\pi$ ). Since pimesons are pseudoscalar particles of odd parity the  $\theta$  - and  $\tau$ -mesons must have different parities and therefore, on the grounds of strict parity conservation, cannot be the same particle. If, however, parity is not conserved, then all atomic and nuclear states must be mixtures containing mainly the states they are normally assigned, together with a small percentage of states of opposite parity. Under this condition the  $\theta$  - and  $\tau$ -mesons can be considered as the same particle in opposite parity states.

If all states are mixtures then their wave functions can be written in the form  $\psi = \psi_{\text{regular}} + \eta\psi_{\text{irregular}}$ ,

where  $\eta$  denotes the mixing ratio of the two parity states, and Lee & Yang's hypothesis of mixed states can be tested by determining the magnitude of  $\eta$ , or  $\eta^2$ , in suitable interactions. This can be done either by looking for interactions which are absolutely forbidden by parity selection rules and which can therefore occur only through the irregular part of the wave function, or by studying interactions which are allowed to both parts of the wave function and observing some phenomenon which indicates interference between the two components.

(i) Strong Interactions.

Experiments of the first type have been carried out by Wilkinson<sup>(2)</sup> and by Tanner<sup>(3)</sup> who studied the  $\text{He}^4(\alpha \gamma)\text{Li}^6$  and  $\text{F}^{19}(\text{p } \alpha)\text{O}^{16}$  reactions respectively.

The second excited state of  $\text{Li}^6$  is an  $0^+$  state at 3.56 MeV which, by parity conservation, is rigorously forbidden to break up into an alpha particle and a deuteron. If such a decay did occur, since the alpha particle has zero spin and even parity and the deuteron has spin 1, in order to conserve <sup>angular</sup> momentum the deuteron would have to possess an <sub>orbital</sub> angular momentum and hence would have odd parity. Such a decay would therefore violate parity conservation and could only occur through the irregular part of the wave function, having a probability of  $\eta^2$  relative to the corresponding allowed

$\gamma$ -transition. By looking for this forbidden transition Wilkinson found an upper limit to  $\bar{\gamma}^2$  of  $1 \times 10^{-7}$ .

The  $F^{19}(p\alpha)O^{16}$  reaction proceeds through a  $J = 1$ , even parity state of  $Ne^{20}$  which normally decays by an  $\alpha_1$  group to a 6.14 MeV level in  $O^{16}$ . However a parity impurity in the wave function of either the  $Ne^{20}$  excited state or of the  $O^{16}$  or  $He^4$  ground states would allow a resonant  $\alpha_0$  group to the ground state of  $O^{16}$ . Tanner looked for evidence of this resonant  $\alpha_0$  transition and from his results obtained an upper limit to  $\bar{\gamma}^2$  of  $4 \times 10^{-8}$ .

An experiment of a similar nature was performed by Segel et al. <sup>(4)</sup> who bombarded  $Be^7$  with neutrons and looked for the  $Be^7(n\alpha)He^4$  reaction which is forbidden on the grounds of parity conservation. This experiment also led to a value of  $\bar{\gamma}^2 \leq 1 \times 10^{-7}$ .

Wilkinson has also studied allowed transitions in an attempt to find some phenomenon which shows interference between the two components of the wave function, and also effects which depend only on the irregular part. In the first case <sup>(5)</sup> he looked for circular polarization of gamma-rays following the bombardment of unpolarized target nuclei by unpolarized particles. He studied the  $B^{11}(pp)B^{11}$  and  $F^{19}(p\alpha)O^{16}$  reactions and obtained values of  $\bar{\gamma}^2$  of  $\leq 1 \times 10^{-7}$  and  $3 \times 10^{-8}$  respectively. In the second case <sup>(6)</sup> he studied the  $Li^7(pp)Li^7$  reaction and

and observed the angular distribution of the gamma-rays of the lithium de-excitation relative to the direction of the bombarding proton beam. If parity is conserved this distribution cannot contain odd powers of  $\cos \theta$ , whereas if parity is not conserved an angular distribution of the form  $1 + \alpha \cos \theta$ , where  $\alpha$  is proportional to  $\eta^2$ , may be expected. This experiment led to an upper limit to  $\eta^2$  of  $1 \times 10^{-4}$ .

An earlier experiment by Chamberlain et al.<sup>(7)</sup> in 1954 on the scattering of a beam of polarized protons by nuclei also led to a value of  $\eta^2$  of  $\leq 10^{-4}$ .

The above mentioned experiments all measured the degree of parity mixing in strong interactions.

A much more sensitive test of parity mixing is given by an experiment which was reported by Purcell & Ramsay<sup>(8)</sup> in 1950 in which an accurate determination was made of the electric dipole moment of the neutron. A violation of parity conservation leads to an electric dipole moment of all systems of order of magnitude  $e \times \eta \times$  the dimensions of the system. In this experiment the value of the electric dipole moment of the neutron was found to be  $e \times 5 \times 10^{-20}$  which gives an upper limit to  $\eta^2$  of  $3 \times 10^{-13}$ .

All these experiments show that, to a high degree of accuracy, parity is conserved in strong interactions.

(ii) Weak Interactions.

In weak interactions, however, since the coupling strengths are reduced by a factor of the order of  $10^{-12}$  a violation of parity conservation would introduce a value of  $\eta^2 < 10^{-24}$  which cannot be readily detected in interactions in which other factors of order one are also present. Therefore, to test for parity conservation in weak interactions, experiments must be devised which can determine whether or not these interactions are invariant with respect to space inversion, i.e. whether they can differentiate between a right-handed and a left-handed set of axes.

Lee & Yang<sup>(1)</sup> suggested experiments of this nature for both meson and beta decay. For meson decay they proposed an experiment on the decay of  $\Lambda^0$ -mesons, ( $\Lambda^0 \rightarrow p + \pi^-$ ), since if parity is conserved the frequency of production of the  $\pi^-$ -mesons will be symmetric with respect to the plane of production of the lambda-mesons which are themselves produced by the reaction  $\pi^- + p \rightarrow \Lambda^0 + \theta$ . For the case of  $\beta$ -decay they suggested the observation of the angular distribution of the electrons from oriented nuclei. An asymmetry, with respect to the polarization of the parent body, in the distribution of the  $\pi^-$ -mesons from the decay of polarized  $\Lambda^0$ -mesons and of the  $\beta$ -radiation from the decay of oriented nuclei would show that these interactions are

not invariant with respect to space inversion and hence that they do not conserve parity.

Since  $\beta$ -decay can be described in terms of operators which, acting on a neutron wave function, lead to a proton wave function, and, similarly, lead to the absorption of an antineutrino and the emission of an electron, the interaction Hamiltonian can be written as the sum of terms of the type  $[(\psi_p^* O \psi_n)(\psi_e^* O \psi_\nu) + \text{complex conjugate.}]$ . Since, however, each of these brackets can take a scalar (S), vector (V), tensor (T), axial vector (A), or pseudoscalar (P) form depending on the Dirac operator used, the total Hamiltonian is given by  $H = g \left[ \sum_i C_i (\psi_p^* O_i \psi_n)(\psi_e^* O_i \psi_\nu) + \text{c.c.} \right]$  where  $i = S, V, T, A, P$  and the constants  $C_i$  measure the relative strengths of the five forms of coupling. If parity is not conserved in  $\beta$ -decay then each of these coupling constants must have two parts, the normal, parity conserving part,  $C_i$ , and a parity non-conserving part  $C_i'$ . To detect parity non-conservation, interference terms of the form  $CC'$  must be observed. The angular distribution of  $\beta$ -radiation from oriented nuclei is proportional to  $(1 + \alpha \cos \theta) \sin \theta d\theta$ , where  $\alpha$  depends on terms of the type  $CC'$ , hence any observation of an electron distribution of this nature with  $\alpha \neq 0$  would give positive proof of a violation of parity conservation in  $\beta$ -decay.

The first experiment of this type to be performed was that of Wu et al. (9) using  $\text{Co}^{60}$  nuclei oriented at low temperatures. In this experiment the asymmetry in the electron distribution as between  $\theta$  and  $180^\circ - \theta$ , where  $\theta$  defines the direction of orientation of the parent nuclei, was measured by reversing the polarizing field. The degree of polarization of the nuclei was measured by observing the anisotropy in the  $\gamma$ -ray distribution. In this experiment a large asymmetry in the electron distribution was found showing that parity was not conserved in the decay.

The first reported case of the detection of parity non-conservation in meson decay is that of Garwin et al. (10) who studied the  $\pi^+ \rightarrow \mu^+ \rightarrow e^+$  decay. This experiment was based on the fact that non-conservation of parity implies that the mesons emitted from stopped pions will be polarized along their direction of motion. Since the angular distribution of the electrons resulting from the decay of the mu-mesons can be used to analyse this polarization Garwin's group studied this angular distribution when a beam of  $\pi^+$ -mesons were stopped in carbon. An asymmetry in this distribution was found showing that the mu-mesons were polarized and therefore that parity is not conserved in meson decay.

(or always parallel) to its momentum, corresponding to

$C_1 = -C_2$  (or  $C_1 = +C_2$ ).

This theory does not conserve parity since under

## 2. The Two Component Neutrino Theory and the PCT Theorem.

In view of this evidence of parity non-conservation Lee & Yang<sup>(11)</sup> put forward a two-component theory of the neutrino. (A similar suggestion was made by Landau<sup>(12)</sup> and by Salam<sup>(13)</sup> at approximately the same time.)

In the old, four component neutrino theory, in which two components are used to describe the neutrino and the other two the antineutrino, the two parts of the neutrino wave function are given by  $\psi_1 = \frac{1}{2}(1 - \gamma_5)\psi_\nu$ ,  $\psi_2 = \frac{1}{2}(1 + \gamma_5)\psi_\nu$ , where  $\psi_\nu = \psi_1 + \psi_2$ , and  $\psi_\nu$  is invariant under the transformation  $\psi_\nu \rightarrow \pm \gamma_5 \psi_\nu$ .

The two component neutrino theory is a special case of the four component theory in which the mass of the neutrino is zero, only  $\psi_1$  <sup>or only  $\psi_2$</sup>  appears in the interactions and the coupling constants are related by  $C_i = + C_i'$  or  $C_i = - C_i'$  depending on the type of interaction involved.

In this theory the neutrino and the anti-neutrino cannot be the same particle since the neutrino (defined as a particle in a positive energy state) has its spin always parallel (or always antiparallel) to its momentum, whilst the antineutrino (defined as a hole in a negative energy state) has its spin always antiparallel (or always parallel) to its momentum, corresponding to  $C_i = - C_i'$  (or  $C_i = + C_i'$ ).

This theory does not conserve parity since under

space inversion (P) the momentum of the neutrino is inverted but its spin remains unchanged, and since, for the neutrino, the two must be always parallel (or antiparallel), the operator P applied to a neutrino state leads to a non-existent state. Similarly the theory is non-invariant under charge conjugation (C) since application of C to a neutrino state changes a particle into an antiparticle without changing its spin or momentum. It may, however, be invariant under CP since this operation changes a particle into an antiparticle and simultaneously reverses the momentum but leaves the spin direction unchanged. By the Lüders-Pauli (PCT) theorem, where T is the time-reversal operator, this means that the theory may be invariant under time-reversal. At the time that Lee & Yang put forward the two-component neutrino theory, however, although non-conservation of parity had been demonstrated in the experiment with oriented  $\text{Co}^{60}$  and in the  $\pi^+ \rightarrow \mu^+ \rightarrow e^+$  decay, and a violation of charge conjugation shown from the magnitude of the asymmetries obtained, no test of time-reversal invariance had been carried out.

By the PCT theorem, which states that interactions are invariant under the combination of these three operations, the existence of an asymmetry in the above experiments implies non-invariance of the interactions under at least one of the operations of charge

conjugation and time-reversal.

The validity of the PCT theorem can be demonstrated by applying these operations in turn to the wave function describing a particle with, say, negative helicity.

The operator  $P$  reverses the momentum and thus leads to a particle with positive helicity,  $C$  changes this particle into an antiparticle without changing the spin or momentum and  $T$  reverses the momentum and the spin thus leading to an antiparticle with positive helicity.

These operations, as well as being applied to the particle itself, must also be applied to the surroundings in which the particle may be observed. Thus the combined operation of  $P$ ,  $C$  and  $T$  leads from a particle of negative helicity in the normal world to an antiparticle of positive helicity in the antiworld, which appears exactly the same to that world as the original particle does to this.

### 3. Consequences of the Non-Conservation of Parity and the Two Component Neutrino Theory.

#### (i) Theory.

Since the first discovery of parity non-conservation, papers have been published by many authors on its effects in beta and meson decay. These include Jackson et al., (14) who pointed out that electrons from the decay of unoriented, as well as oriented nuclei would be longitudinally polarized. For recoil experiments they gave

the expected distribution functions for electron and neutrino directions and electron energy, and for electron energy, angle and polarization for allowed transitions from oriented nuclei, as well as the distribution function for electron and neutrino directions, electron energy and polarization for allowed transitions from unoriented nuclei. In these distribution functions the Coulomb distortion effects and the relativistic corrections for the nucleons were omitted.

In an allowed transition the directions of the  $\beta$  - particle and the antineutrino are correlated, the correlation being of the form  $1 + \lambda \left(\frac{v}{c}\right) \cos \theta$ , where the value of  $\lambda$  depends on the type of interaction present, being  $+1$  for a vector interaction,  $+\frac{1}{3}$  for a tensor interaction,  $-1$  for a scalar interaction and  $-\frac{1}{3}$  for an axial vector interaction. (The pseudoscalar interaction is not included as it is generally accepted that this type of interaction plays very little part in  $\beta$  -decay.) Since angular momentum must be conserved and the spin change of the nucleus is  $0$ , or  $\pm 1$ , and since, by the two component neutrino theory, the antineutrino spin can only have one direction the electron spin direction must also be fixed: for a  $\Delta J = 0$  transition the electron spin direction must be opposite to that of the antineutrino and for a  $\Delta J = 1$  transition it must lie in the same direction as that of the

antineutrino. Averaged over the possible electron directions this leads to a resultant polarization of the electron beam in the direction of the momentum.

Curtis & Lewis<sup>(15)</sup> considered the case of  $\beta$  - particles followed by  $\gamma$  -radiation from unpolarized nuclei. They derived formulae for the longitudinal polarization of electrons in  $\beta$  -decay and for the correlation of the transverse electron polarization with the direction of a  $\gamma$  -ray.

As the electrons produced in  $\beta$  -decay are expected to be longitudinally polarized the daughter nucleus will also be partially polarized and any subsequent  $\gamma$  - radiation or bremsstrahlung is therefore expected to be circularly polarized. Since the angular distribution of  $\gamma$  -rays with respect to the electron direction depends on this circular polarization, the  $\beta$  -  $\gamma$  polarization correlations, as well as the electron distribution and electron polarization functions, from oriented and unoriented nuclei, were given by Alder et al.<sup>(16)</sup> who considered both allowed and first forbidden decays. This circular polarization of the  $\gamma$  -rays has also been considered by Morita<sup>(17)</sup>, who calculated the angular correlation between the electrons and circularly polarized  $\gamma$  -rays in triple cascades, and by Morita & Morita,<sup>(18)</sup> who have given this correlation for double and triple cascades from unoriented nuclei, and who have

also calculated the  $\beta$ -ray angular distribution from oriented nuclei.

Bouchiat<sup>(19)</sup> considered recoil effects in  $\beta$ -decay and K-capture for forbidden transitions in oriented nuclei. In the case of  $\beta$ -decay, he gave formulae for the angular distribution of recoil nuclei, for the recoil  $\chi$ -ray angular correlation and for the polarization of the recoil nucleus. For K-capture he considered the recoil asymmetry for polarized nuclei, the polarization of recoil nuclei and the recoil- $\chi$ -ray polarization correlation.

The angular distributions and polarization of electrons emitted by polarized and aligned nuclei in transitions of any order of forbiddenness has been given by Dolginov<sup>(20)</sup>.

Similar formulae to those mentioned above have been given in papers by Jackson et al.<sup>(21)</sup>, Ebel & Feldman,<sup>(22)</sup> Berestetsky et al.<sup>(23)</sup> and Bincer<sup>(24)</sup>, who include the effects of Coulomb corrections.

Kinoshita & Sirlin<sup>(25)</sup>, and Uberall<sup>(26)</sup>, have discussed the electron polarization in muon decay while Jackson et al.<sup>(27)</sup> proposed an experiment to determine the direction of polarization of mu-mesons in pion decay. Uberall also pointed out that the polarized electrons from muon decay passing through matter will emit bremsstrahlung which will be circularly polarized.

(ii) Experiment.

On the experimental side numerous attempts have been made to observe the polarizations and asymmetries predicted.

Grace et al. (28), using  $\text{Co}^{60}$  polarized in a magnetic field at low temperatures, have confirmed Wu's results on parity failure in  $\beta^-$  decay whilst Ambler et al. (29), and Postma et al. (30), making similar asymmetry measurements on  $\text{Co}^{58}$  and  $\text{Mn}^{52}$  found positron <sup>asymmetry</sup> of opposite sign to that of the electrons in the  $\text{Co}^{60}$  experiments.

The violation of parity conservation in the decay of unoriented nuclei has been detected by observation of a longitudinal polarization of the electrons produced, of the circular polarization of subsequent  $\gamma$ -rays and bremsstrahlung, and of the correlation functions.

Longitudinal electron polarization can be detected by first converting it into a transverse polarization, then scattering the transversely polarized electron beam from a thin foil of high Z value (Mott scattering) and finally observing the resultant asymmetry in the distribution of the scattered electrons.

Three experimental methods have been used to convert the longitudinal electron polarization into a transverse one. Frauenfelder et al. (31) working with

Co<sup>60</sup> and De Waard & Poppema<sup>(32)</sup> using Co<sup>60</sup>, P<sup>32</sup> and Tm<sup>170</sup> as sources, achieved this by deflecting the initial electron beam through 90° in a cylindrical electrostatic field, which also served as an energy selector since only a small section of the beam of deflected electrons was focused onto the scattering foil. The electrons were then single scattered over large angles in this foil, which was perpendicular to the incident beam, and the left-right asymmetry in the resultant electron distribution observed. Conversion from a longitudinal electron polarization to a transverse one can also be obtained by passing the electron beam through crossed electric and magnetic fields. This method was used by Cavanagh et al.<sup>(33)</sup> when looking for the polarization of electrons from the decay of Co<sup>60</sup>. The third method, which was used by de-Shalit et al.<sup>(34)</sup> employs scattering in the Coulomb field of a nucleus. In this experiment the electron beam from a P<sup>32</sup> source was first scattered by a cylindrical aluminium foil to change the longitudinal polarization into a transverse one, which was then observed by means of Mott scattering.

The longitudinal electron polarization has also been detected by means of Møller scattering. In this method the longitudinally polarized electrons are scattered from the polarized electrons in a magnetised foil made from a material of high magnetic permeability.

The scattered and recoil electrons are observed first when the foil is magnetised parallel, and then when it is magnetised antiparallel to the direction of motion of the incident beam since the cross-section for Møller scattering depends on the relative orientation of the spins of the incident and target electrons. The recoil electrons are observed in order to eliminate multiple and Rutherford scattering effects. This method was used by Fraunfelder et al. (35) and Geiger et al. (36) to study the electrons produced in the decay of  $P^{32}$  and  $Pr^{144}$ . Geiger's group also studied the decay of  $Y^{90}$  and  $Au^{198}$ .

Many  $\beta - \chi$  correlation experiments have also been carried out to show parity violation in weak interactions; these include experiments on the decays of  $Co^{60}$ ,  $Co^{58}$ ,  $Au^{198}$ ,  $Hg^{203}$ ,  $Na^{22}$ ,  $Na^{24}$ ,  $V^{48}$ ,  $Mn^{52}$ ,  $Zr^{95}$ ,  $Sb^{124}$ ,  $Sc^{44}$  and  $Sc^{46}$ , (37) - (45) whilst further experiments by Goldhaber et al. (46) and Schopper & Galster (47), using  $Sr^{90} + Y^{90}$  sources, have detected the predicted circular polarization of bremsstrahlung.

Most of the experiments to detect electron polarization and the predicted correlation functions gave results which were consistent with the two component neutrino theory and a maximum violation of parity. There were however some discrepancies, in particular the results obtained by Fraunfelder et al. (48), Boehm &

Wapstra<sup>(38)</sup> & (39), and De Waard & Poppema<sup>(32)</sup> gave polarizations considerably less than the maximum value and seemed to indicate that parity was conserved in Fermi interactions. As a check on this point Boehm et al.<sup>(49)</sup> studied the positron polarization in the decay of  $N^{13}$  by observing the circular polarization of the high energy quanta from annihilation in flight. They chose  $N^{13}$  because it has a mirror transition in which the Fermi matrix element is larger than the Gamow-Teller matrix element so that the positron polarization is mainly determined by the Fermi part of the interaction. Knowing the ratio of the squares of the matrix elements (i.e.  $|M_{GT}|^2 / |M_F|^2$ ) from an analysis of ft values they obtained results which were consistent with full polarization. If only the Gamow-Teller part of the interaction violates parity the expected result would have been approximately one third of that obtained. In this way it was shown that both Fermi and Gamow-Teller interactions violate parity conservation and that they contribute to the electron polarization in the same sense. This similarity between the Fermi and Gamow-Teller interactions has also been shown by Deutsch et al.<sup>(50)</sup> in their studies of the decay of  $Ga^{66}$  and  $Cl^{34}$ .

The electron polarization resulting from muon decay in the  $\pi \rightarrow \mu \rightarrow e$  sequence, where the electron polarization is measured in the rest system of the pion, has

been observed for both natural and artificially produced pi-mesons<sup>(51)</sup> - (56).

From the above mentioned experiments it has been confirmed that parity is not conserved in the  $\beta$ -decay of oriented or unoriented nuclei, both in allowed and forbidden transitions, and in meson decay.

#### 4. Coupling Types present in Weak Interactions.

Since the degree of polarization of the electrons produced in  $\beta$ -decay, of the mu-mesons produced in the decay of stopped pions, and the various correlation functions in  $\beta$ -decay depend on the coupling constants involved in the interactions, it is important to establish the relative magnitude of these constants, to determine whether the <sup>Gamow Teller</sup> interactions are of a tensor (T) or axial vector (A) nature and also whether the <sup>Fermi</sup> interactions are of a scalar (S) or vector (V) nature. The absence of Fierz interference terms, as shown by the linearity of the Kurie plots for allowed  $\beta$ -decays, shows that in the interactions T couplings cannot be present with A nor S with V. In mixed Fermi and Gamow-Teller transitions, it is also important to know the ratio of the Fermi to Gamow-Teller contributions.

Before the discovery of non-conservation of parity most of the evidence seemed to indicate that the Fermi

interaction was predominantly of a <sup>scalar</sup> nature and that the Gamow-Teller interaction was predominantly <sup>tensor</sup>. (57) - (62) As a result of this Alder et al. (16) and Berestetsky (23) in their derivations of the distribution and correlation functions in  $\beta$ -decay assumed an STP interaction. On the other hand Allen et al. (63) in 1949 studying the  $\beta$  -  $\nu$  angular correlation in the decay of  $\text{He}^6$  obtained results which were consistent with an axial vector type of Gamow-Teller interaction. The expected  $\beta$  -  $\nu$  angular correlation for allowed decays, assuming conservation of P, C and T, had been calculated for the different types of interactions (S, T, V, A and P) by Hamilton (64) in 1947.

Morita & Morita (18) in their discussion of the distribution and correlation functions in  $\beta$ -decay considered the STP, VA and STPVA types of interactions separately, with the assumption of no interference between the STP and VA interactions, and concluded that  $\beta$ -interactions were either STP with  $C_i = -C_i'$ , or VA with  $C_j = +C_j'$  or a linear combination of these two possibilities. Morita (65) in three further papers derived correlation functions in  $\beta$ -decay and discussed a large number of possible experimental situations which could be used to determine the types of coupling actually involved in the interactions.

Bouchiat (19) also considered the cases of ST and VA

interactions separately in his discussion of the distributions and correlations in recoil experiments in  $\beta$ -decay and K-capture, and noted the different asymmetries expected from the different types of interactions.

The  $\beta$  -  $\gamma$  correlation function of oriented nuclei was discussed by Curtis and Lewis<sup>(66)</sup> who considered in particular the case of a  $1^+(\beta)1^+(\gamma)0^+$  transition, assuming that both the Fermi and Gamow-Teller interactions were present, and showed that by measuring the  $\beta$ -intensity, the  $\gamma$ -ray anisotropy, the  $\beta$ -asymmetry and the  $\beta$  -  $\gamma$  coincidence asymmetry, the coupling constants present in the  $\beta$ -interaction could, in principle, be determined. They also discussed<sup>(67)</sup> the study of  $\beta$  -  $\gamma$  angular correlation with resonance fluorescence of the  $\gamma$ -ray as a means of obtaining information about the coupling types, whilst Frauenfelder et al.<sup>(68)</sup> considered the possibility of distinguishing between T and A, and between S and V interactions in K-capture and  $\beta$ -emission experiments using unpolarized parent nuclei.

Early experiments taking into account parity non-conservation by Good & Lauer<sup>(69)</sup> and Alford & Hamilton<sup>(70)</sup> on  $\text{Ne}^{19}$  and by Frauenfelder et al.<sup>(31)</sup> on  $\text{Co}^{60}$  also seemed to agree with the assumption of an ST interaction in  $\beta$ -decay. However Herrmannsfeldt et al.<sup>(71)</sup> measured the  $\beta^+$  -  $\gamma$  angular correlation in the decay of  $\text{A}^{35}$ , which occurs mainly through the Fermi matrix

element, and also the energy spectrum of the recoils without selection of the direction of the positron emission. They obtained a  $\beta^+ - \nu$  angular correlation coefficient  $\lambda$  of  $+ 0.9 \pm 0.3$ . They then compared the energy spectrum with that expected for different values of  $\lambda$  and found that it agreed with a value of  $\lambda$  equal to  $+ 0.7 \pm 0.17$ . The result  $\lambda > \frac{1}{3}$ , found in both experiments, implies the existence of a vector interaction independently of any assumptions made about the nuclear matrix elements, since, for any combination SA, ST, AV or TV,  $\lambda$  depends only on the ratio of the Fermi to Gamow-Teller transition probabilities which can be deduced from the known  $ft$  values of the  $0^+ - 0^+$  transitions in  $O^{14}$ ,  $Al^{26}$  and  $Cl^{34}$  and from the  $ft$  value of  $A^{35}$ , since the Fermi matrix element for the  $0^+ - 0^+$  transition is (to within about 10%) twice that of the mirror transition  $A^{35} - Cl^{35}$ .

From a comparison of the experimental results with the theoretical ones for the different types of interactions Herrmannsfeldt was able to show that at least one third of the Fermi interaction was of a vector nature. He then reconsidered the results of the experiments on  $Ne^{19}$  on the same basis as above and showed that they were in fact consistent with either ST or VA interactions.

There still remained, however, a discrepancy between

these results and the results of the  $\text{He}^6$  experiments. In view of this Herrmannsfeldt et al.<sup>(72)</sup> measured the  $\beta - \nu$  angular correlation coefficient in the decay of  $\text{He}^6$ . From theoretical considerations, since  $\text{He}^6$  obeys only Gamow-Teller selection rules, this coefficient  $\lambda$  should be  $+\frac{1}{3}$  for tensor interactions and  $-\frac{1}{3}$  for axial vector interactions. The result obtained in this experiment was  $\lambda = -0.39 \pm 0.02$  showing that the Gamow-Teller interaction is predominantly of an axial vector nature.

A similar result was obtained by Appel et al.<sup>(45)</sup> for the Gamow-Teller transitions in  $\text{Co}^{60}$  and  $\text{Na}^{22}$  by studying the  $\beta - \chi$  circular polarization correlation.

Lauritsen et al.<sup>(73)</sup> studying the decay of  $\text{Li}^8$  showed that this decay was 90% Gamow-Teller in nature whilst Barnes et al.<sup>(74)</sup> were able to show that at least 90% of this Gamow-Teller interaction was of an axial vector nature. Lauterjung et al.<sup>(75)</sup> have confirmed this result.

For the case of muon decay Culligan et al.<sup>(76)</sup>, by measuring the helicity of the positrons from the decay of unpolarized mu-mesons, and Bardon et al.<sup>(77)</sup>, by observing the electron anisotropy from the decay of polarized mu-mesons, have shown that the interactions responsible for mu-meson decay are also of a VA nature.

The results of these experiments are consistent

with the two component theory of the neutrino with  $C_V = C_V'$  and  $C_A = C_A'$ . A further test of the two component theory may however be obtained from a determination of the helicity of the neutrino and also of the muon in the  $\pi - \mu$  decay.

### 5. Helicity.

Kinoshita & Sirlin<sup>(78)</sup> have shown that the predicted muon spectra from the two- and four-component neutrino theories are much the same if the radiative corrections are not considered; if, however, they are taken into account the two-component theory gives a spectrum which is completely defined for the decay of unpolarized muons and depends only on one parameter when the muons are polarized. They have also considered<sup>(79)</sup> the correlation between the electron spectrum and the mu-meson spectrum in the two theories and have shown that the two component theory predicts unambiguously the correlation between the spin and momentum of the mu-meson if lepton conservation is assumed in the  $\pi - \mu - e$  sequence.

Bouchiat<sup>(19)</sup>, in his paper on recoil effects in  $\beta$  - decay and K-capture for the case of first forbidden transitions, has given expressions for the recoil asymmetry, the polarization of the recoil nucleus and the recoil  $\gamma$ -ray polarization correlation, each of which

can be used to determine the neutrino helicity.

Allowed electron capture by an unpolarized nucleus, leading via a Gamow-Teller transition to an excited state of non-zero angular momentum, was considered by Page<sup>(80)</sup>, who proposed an experiment to find the neutrino helicity by detecting the sign of the helicity of the resultant  $\gamma$ -ray.

Treiman<sup>(81)</sup> also considered recoil effects in capture experiments and  $\beta$ -decay, with a view to determining the neutrino helicity. In particular, he discussed the capture reaction  $\mu^- + \text{C}^{12} \rightarrow \text{B}^{12} + \nu$ . The  $\text{B}^{12}$  nucleus in this reaction should have an appreciable longitudinal polarization the sign of which is determined by the neutrino helicity. As  $\text{B}^{12}$  decays rapidly by  $\beta^-$  emission the asymmetry of the electrons about the direction of recoil motion can be used as an analyser of this polarization.

In an experiment to determine the neutrino helicity, Goldhaber et al.<sup>(82)</sup> observed the circular polarization and resonant scattering of  $\gamma$ -rays following orbital electron capture in  $\text{Eu}^{152}$  nuclei. They found that the neutrino was "left-handed", that is, that its polarization was antiparallel to its momentum. Their results also confirmed that the Gamow-Teller interaction is axial vector.

In experiments on polarized neutrons, in which the

correlations between the neutrino direction and the neutron spin and between the electron momentum and the neutron spin were measured, Burgy et al.<sup>(83)</sup> also obtained results which showed that the neutrino spin was negative and that the interaction was V-A. (V-A signifies that  $C_A/C_V = -x$  where  $|x|$  is the ratio in which the Gamow-Teller and Fermi couplings are present in the interaction.) To obtain these results they compared the correlation coefficients determined experimentally with those predicted for left- and right-handed anti-neutrinos for each of the possible combinations of interactions, S+T, S-T, V+A and V-A, on the assumptions that the interaction must be either S and T or V and A, that the antineutrino emitted in the reaction is completely polarized, and that the reaction is invariant under time-reversal. They noted that the accuracy of their results was not sufficient to exclude small deviations from the first two of these assumptions or even fairly large deviations from the third.

The helicity of the electrons and positrons produced in muon decay has been determined by Macq et al.<sup>(84)</sup> by measuring the sense of the circular polarization of their bremsstrahlung when they are stopped in magnetised iron. It was found that the positrons were "right-handed" and the electrons "left-handed".

From the experiments measuring the asymmetry of

the electron distribution in muon decay, it is known that those states are favoured in which the  $\beta$ -particle momentum is antiparallel to the muon momentum in the pion rest frame, hence, since in the reaction  $\mu^+ \rightarrow e^+ + \nu + \bar{\nu}$  the neutrino ( $\nu$ ) and the anti-neutrino ( $\bar{\nu}$ ) have spins in opposite directions and are emitted together in the direction opposite to the electron, if the electron is right-handed then the mu-meson must be left-handed and vice-versa. Macq's results are therefore consistent with the two component neutrino theory of left-handed neutrinos, VA interactions, complete polarization of both positrons and electrons and conservation of leptons.

#### 6. The Universal Fermi Interaction.

In view of the similarity of beta and mu-meson decay processes, Feynman & Gell-Mann<sup>(85)</sup> postulated the existence of a Universal Fermi Interaction. They pointed out that, in the representation of Fermi particles by two-component Pauli spinors satisfying second order differential equations, these spinors act without gradient couplings in  $\beta$ -decay and that this leads to an essentially <sup>unique</sup> four fermion coupling, which is equivalent to equal amounts of V and A couplings with two component neutrinos, conservation of leptons and non-conservation of parity. Owing to the similarity

mentioned above, they assumed this coupling to be "universal" to all weak interactions. Through analogy with electrodynamics they assumed that the total interaction occurred through the self-interaction of a  $\mathbf{J}_\lambda$  current  $J_\lambda$ , where  $J_\lambda$  is a sum of bilinear covariants  $[\bar{\psi}_a \gamma_\lambda \frac{1}{2}(1+\gamma_5) \psi_b]$  over certain pairs of fermions a, b, where (a,b) must be a singly charged pair.  $J_\lambda$  may be split into two parts  $J_\lambda^V$  and  $J_\lambda^A$ , where  $J_\lambda = \frac{1}{2}(J_\lambda^V + J_\lambda^A)$ ,  $J_\lambda^V = \psi_a \gamma_\lambda \psi_b$ , and  $J_\lambda^A = \psi_a i \gamma_\lambda \gamma_5 \psi_b$ .

If the vector current is divergenceless, i.e. if  $\partial J_\lambda^V \equiv 0$ , this theory leads to a universal Fermi coupling constant, for both beta and mu-meson interactions, of  $G = G' = (1.41 \pm 0.01) \times 10^{-49}$  ergs/cm.<sup>3</sup> where the interaction forms are  $(8)^{\frac{1}{2}}G(\bar{\psi}_n \gamma_\lambda \frac{1}{2}(1+\gamma_5) \psi_p)$   $\times (\bar{\psi}_r \gamma_\lambda \frac{1}{2}(1+\gamma_5) \psi_e)$  and  $(8)^{\frac{1}{2}}G'(\bar{\psi}_\mu \gamma_\lambda \frac{1}{2}(1+\gamma_5) \psi_r)$   $\times (\bar{\psi}_r \gamma_\lambda \frac{1}{2}(1+\gamma_5) \psi_e)$ , respectively.

Sudarshan & Marshak<sup>(86)</sup> have developed an equivalent theory on the basis of Chirality Invariance, i.e. on the assumption that a Dirac spinor is invariant under the transformation  $\psi \rightarrow \gamma_5 \psi$ , where  $\gamma_5^2 = +1$ , whilst Sakurai<sup>(87)</sup> obtained the same end results by considering all weak interactions to be invariant only under Mass Reversal.

Feynmann & Gell-Mann pointed out that the decay of strange particles can also be covered qualitatively by

this theory if the universality is extended to include a coupling constant involving the  $\Lambda$  or  $\Sigma$  fermion. This leads to non-conservation of parity even in decays such as  $K \rightarrow 2\pi$  and  $K \rightarrow 3\pi$  in which neutrinos do not participate.

It is possible to calculate the life-time of the  $\mu$ -meson on the basis of this universal theory, and the result obtained agrees with the determined value to within the experimental errors of about 2%. The comparable rates of the  $K_{e3}^{\pm}$  and  $K_{\mu3}^{\pm}$  decay modes, as found by Pias & Treiman<sup>(88)</sup>, are also in agreement with this theory.

The  $\pi \rightarrow (\mu \text{ or } e) + \nu$  and the  $K_{e3}$  and  $K_{\mu3}$  decay modes have been discussed by several authors<sup>(89) - (93)</sup> in the framework of this theory, and Taylor<sup>(89)</sup> showed that if  $\partial I_{\lambda}^A \equiv 0$  as well as  $\partial I_{\lambda}^V \equiv 0$  then the  $\pi \rightarrow e + \nu$  decay mode is forbidden. Later Anderson et al.<sup>(94)</sup>, in an attempt to find the  $\pi \rightarrow e + \nu$  decay mode, obtained a branching ratio

$$(\pi \rightarrow e + \nu) / (\pi \rightarrow \mu + \nu) = (1.03 \pm 0.20) \times 10^{-4}.$$

At this stage, it was not known if it was possible to construct a divergenceless axial vector current, but Taylor, in view of the similarity of the Fermi and Gamow-Teller interactions shown by the polarization experiments, and of the near equality of the Fermi and Gamow-Teller coupling constants ( $|C_A/C_V| = 1.14$ ), pointed

out that, if these coupling constants should in fact turn out to be identical, then the condition  $\partial \bar{J}_\lambda^A = 0$  would hold.

The problem of conserved axial vector currents has been discussed by Goldberger & Treiman<sup>(95)</sup> who showed that a scheme of conserved strangeness violating currents is ruled out, and by Polkinghorne<sup>(96)</sup> who pointed out that a conserved axial vector current can be constructed if the medium-strong K-meson interactions are neglected.

At first, the identity of the Fermi coupling constant for  $\beta$  and  $\mu$ -meson processes seemed strange, in view of the fact that nucleons also take part in strong interactions but  $\mu$ -mesons do not. However, Gell-Mann<sup>(97)</sup> has shown that the universal coupling constant is not appreciably altered by renormalization. He has also shown that the vector interaction gives rise to a "weak magnetism", analogous to the magnetic effects that induce the emission of M1 photons, which should be observable experimentally. Bernstein & Lewis<sup>(98)</sup> have extended this work by Gell-Mann to show the effects of this weak magnetism on spectral shapes,  $\beta - \gamma$  and  $\beta - \alpha$  directional correlations.

Some discrepancies between the effects observed in muon decay and those predicted by the Universal Fermi Interaction theory have been found. Lee & Yang<sup>(99)</sup>, discussing the difference between the observed Michel

parameter and the theoretical one have suggested that this may be due to non-local effects. (The original theory assumed that all interactions were purely local.) Sirlin<sup>(100)</sup>, considering this discrepancy, and also that between the expected ratio of the transition probabilities for the  $\pi \rightarrow e + \nu$  and  $\pi \rightarrow \mu + \nu$  decays, and the actual value found experimentally, also postulated the existence of non-local effects. If these effects have to be taken into account, then the original theory becomes a first order approximation to the complete theory.

As the similarity of the electron-nucleon and the electron-muon weak interactions had already been observed, Argo et al.<sup>(101)</sup> studied the absorption of negative cosmic ray muons stopped in  $C^{12}$  in order to investigate the third leg of the triangle, the muon-nucleon interaction. They compared the probability per second of the absorption resulting in the formation of  $B^{12}$  in the ground state to the known rate of  $\beta$ -decay of  $B^{12}$  to the ground state of  $C^{12}$ . Since, in the allowed approximation, the nuclear matrix elements for the two processes are the same, they were able to calculate the ratio of these rates in terms of the ratio of the coupling constants without assuming a nuclear model. To within the uncertainty imposed by this approximation, it was found that the electron-nucleon and muon-nucleon axial vector coupling constants are the same.

## 7. Time Reversal.

As violation of parity and charge conjugation invariance have been shown in both beta and muon-decay, the question now arises as to whether or not interactions are invariant under time-reversal.

### (i) Strong Interactions.

The question of time-reversal invariance in nuclear interactions has been discussed by Henley & Jacobsohn, (102) with particular reference to an experiment by Schrader, (103) in which the angular correlation of the  $\gamma$ -rays in the  $2(E2+M1)2(E2)0$  cascade of  $\text{Hg}^{108}$  was measured, and to the detailed balance experiments

$$p + \text{H}^3 \rightleftharpoons n + \text{He}^3; \quad p + \text{He}^3 \rightleftharpoons \gamma + \text{He}^4 \text{ and}$$

$$p + \text{Li}^7 \rightleftharpoons d + \text{Li}^6.$$

In angular correlations in which one of the radiations in the cascade consists of the superposition of two angular momenta, time-reversal invariance leads to an interference term with the phase  $0^\circ$  or  $180^\circ$ . Schrader's experiment indicated that the value of this phase was greater than  $159^\circ$ . Non-invariance of nuclear interactions under time-reversal leads to the non-reality of certain matrix elements, which would show up in the detailed balance experiments mentioned above. From the results of these experiments, Henley & Jacobsohn concluded that the forces which were odd with respect to time-reversal in strong interactions were present to not

more than (10 - 20)% of the total forces in the interactions.

Later data on the time-reversal invariance of strong interactions, obtained from detailed balance experiments, (104)-(105) and from experiments on the scattering of both polarized and unpolarized protons in hydrogen, lithium, beryllium and aluminium, (106) lead to a value of about 2 - 3% of odd forces in these interactions.

(ii) Weak Interactions.

At the time that the present experiment to test time-reversal invariance in weak interactions was started, although papers had been published on the effects of non-invariance with respect to time-reversal in beta and muon decay processes, no experiment had been reported which had been specifically designed to test these effects.

It has already been noted that, if parity is not conserved, then, by the PCT theorem, at least one of C and T must also be violated, and that violation of charge conjugation has been demonstrated by the magnitude of the asymmetries observed in the original "parity" experiments. This does not, however, rule out the possibility of non-invariance with respect to time-reversal in weak interaction.

Lee & Yang, in their original paper on parity

conservation in weak interaction, <sup>(1)</sup> pointed out that, if the interactions are invariant under time-reversal, then all the coupling constants  $C_i$  and  $C_i'$  must be real, except perhaps for a common phase factor, which can be normalised to unity, whereas, if the interactions are not invariant under time-reversal, then each of these constants will have both real and imaginary parts. This point was also discussed by Lee, Oehme & Yang <sup>(107)</sup>, who considered the behaviour of the interaction Hamiltonian under the operations of the parity, (P), charge conjugation (C), and time-reversal (T), operators and derived the restrictions placed on the coupling constants by the conservation and non-conservation of interactions under P, C and T and all possible combinations of them.

Pursey <sup>(108)</sup> has considered the effect of the assumption of zero neutrino mass on the conditions for invariance of the weak interaction Hamiltonian under the operations of P, C and T, and shown that, although the conditions: all  $C_i' = 0$ ; all  $C_i$  real and  $C_i'$  imaginary; and all  $C_i$  and  $C_i'$  real, are sufficient conditions for P, C and T invariance respectively, they are not necessary conditions. He has, therefore, derived the sufficient and necessary conditions for P, C and T invariance

which are:  $C_i C_j'^* + C_i' C_j^* = 0$  for all  $i$  and  $j$ ;

$$\text{Im}(C_i C_j^* + C_i' C_j'^*) = 0 \text{ and}$$

$$\text{Im}(C_i C_j'^* + C_i' C_j^*) = 0 \text{ for all } i \text{ and } j;$$

and  $\text{Im}(C_i C_j^* + C_i' C_j'^*) = 0$  and  $\text{Re}(C_i C_j^* + C_i' C_j'^*) = 0$ ; respectively.

He also quoted the equivalent conditions imposed on the coupling constants involved in muon decay by invariance under these operations.

Three experimental situations, which could serve as a test of time-reversal invariance in  $\beta$ -decay, have been discussed by Jackson et al. (14) These are experiments in which the nuclei are oriented and either the electron and neutrino momenta, or the electron momentum and polarization are observed, and experiments in which the nuclei are not oriented but the recoil momentum and the electron momentum and polarization are measured.

In the absence of Coulomb terms, in order to test time-reversal invariance, terms which include either the nuclear orientation or the electron polarization must be detected. In the first type of experiment mentioned, the quantities observed are the nuclear polarization  $\langle \underline{J} \rangle$ , the electron momentum  $\underline{p}_e$  and the neutrino momentum  $\underline{p}_\nu$ . In the distribution function for an allowed beta transition these quantities appear in a term proportional to  $(\langle \underline{J} \rangle / J) \cdot (\underline{p}_e \times \underline{p}_\nu) / E_e E_\nu$  which is invariant under space rotation, but not under time-reversal. This term can be distinguished from other terms in the distribution function, of the form  $\langle \underline{J} \rangle \cdot \underline{p}_e$  and  $\langle \underline{J} \rangle \cdot \underline{p}_\nu$  which violate parity but not time-reversal, by experiments in which

the nuclei are polarized along the + z axis and the coincidence rates are observed between the recoil nuclei travelling in the + x direction and the electrons travelling along the + y and - y directions. A difference between these coincidence rates shows the presence of the required term in the distribution function and hence a violation of time-reversal invariance in the decay process.

In experiments in which the nuclear polarization,  $\langle J \rangle$ , the electron polarization,  $\underline{n}$ , and the electron momentum  $\underline{p}_e$  are observed, in order to detect a violation of time-reversal invariance in the decay process, a term of the form  $\underline{n} \cdot \langle J \rangle \times \underline{p}_e$  must be observed. Jackson has shown that this combination of vectors appears in the distribution function in electron energy, angle and polarization for allowed beta decay from oriented nuclei in a term proportional to  $R \underline{n} \cdot (\langle J \rangle / J) \times (\underline{p}_e / E_e)$ , where R depends on the imaginary parts of the cross-products  $C_x C_y'^*$  and  $C_x' C_y^*$ , and on the nuclear matrix elements.

Since the transverse polarization of the electrons produced in the decay also depends on R, the observation of such a polarization would show a non-zero value of R, and hence that time-reversal invariance is violated in the interaction.

For the analysis of experiments with unpolarized parent nuclei Jackson has given the distribution function

in electron and neutrino directions, electron energy and polarization for allowed transitions. This includes terms of the form  $(\underline{n} \cdot \underline{p}_e)$ ,  $(\underline{n} \cdot \underline{p}_\nu)$ , and  $(\underline{n} \cdot \underline{p}_e)(\underline{p}_e \cdot \underline{p}_\nu)$ , which violate parity conservation but not time-reversal invariance, and also a term of the form  $(\underline{n} \cdot \underline{p}_e \times \underline{p}_\nu)$  which changes sign under time-reversal. As the coefficient of this term involves the same combination of coupling constants and matrix elements as does the expression for the transverse polarization of the electrons produced in the decay, the detection of such a polarization will give evidence of non-invariance with respect to time-reversal in the decay of unpolarized nuclei.

Morita & Morita<sup>(109)</sup> have considered the term in the electron distribution function in allowed beta decay which violates time-reversal invariance and which depends on  $\propto Z/p$ , that is, on the Coulomb distortion of the electron wave function. This term is of the form  $(\underline{p}_e \cdot \underline{p}_\nu)(\frac{\alpha Z}{p})$ . They assumed that  $C_i$  and  $C_i'$  have equal absolute magnitudes and only a very small phase difference, and defined  $C_A/C_T = g \exp(i\theta)$  where  $g$  and  $\theta$  are real. Under these conditions, the electron-neutrino angular correlation function reduces to

$$W(\theta) = 1 + (P/3W)f(g) \cos \theta,$$

$$\text{where } f(g) = [1 \mp 2g(\alpha Z/p) - g^2]/(1 + g^2),$$

and the negative and positive signs refer to electron and positron decay respectively. From this it can be

seen that the invariance properties of the decay under time-reversal can be determined by observing the  $Z$  or  $p$  dependence of the function  $f(g)$ . Morita & Morita, however, suggested that a more convenient method would be to measure and compare the values of  $f(g)$  for electron and positron decay in the same energy range, since this would lead to a value for  $f_1(g) - f_2(g)$  which equals  $(2g \propto Z/p)(Z_1 + Z_2)/(1 + g^2)$ , where the subscripts 1 and 2 refer to positron and electron decay respectively. An observed value of  $f_1(g) - f_2(g)$  different from zero would indicate non-invariance of the  $\beta$ -decay process under time-reversal.

In a later paper, Morita & Morita<sup>(110)</sup> pointed out that distribution and correlation functions which have terms of the form  $(P/W) \text{Im}(C_T^* C_A^{(\prime)})$  (where  $(\prime)$  denotes primed or unprimed) as a main asymmetry term also have terms of the form  $(\propto Z/W) \text{Re}(C_T^* C_T^{(\prime)})$  as a Coulomb correction, whilst those with a main asymmetry term of the form  $(P/W) \text{Im}(C_T^* C_S^{(\prime)})$  have terms of the form  $(\propto Z/W) \text{Re}(C_A^* C_S^{(\prime)})$  as a Coulomb correction, and that these correction terms mask the effects due to non-invariance under time-reversal. They suggested an experiment to detect the invariance properties of beta-decay processes in which the  $\beta - \chi$  angular correlation in the decay of oriented nuclei, which has an asymmetry of the form  $\langle \underline{J} \cdot \underline{p} \times \underline{k} \rangle (\underline{p} \cdot \underline{k})^x$ , is observed. Here  $\langle \underline{J} \rangle$

defines the orientation axis of the nucleus,  $\underline{p}$  and  $\underline{k}$  the directions of the emitted electron and  $\gamma$ -ray respectively, and  $x = 1$  and  $3$ . Assuming the Coulomb corrections to be small, this asymmetry, which is proportional to  $(P/W)\text{Im}(C_T^* C_S' + C_T'^* C_S - C_A^* C_V' - C_A'^* C_V)$ , will only arise if time-reversal invariance is violated. If  $\langle \underline{J} \rangle$  and  $\underline{k}$  are perpendicular this asymmetry will vanish, but an asymmetry, which is related to the circular polarization  $P$  of the  $\gamma$ -rays, will still exist in the  $\beta - \gamma$  angular correlation if time-reversal invariance does not hold. This asymmetry term is of the form  $P \langle \underline{J} \rangle (\underline{p} \times \underline{k})$ , and is of the same order of magnitude as the asymmetry mentioned above, but changes sign with opposite senses of the circular polarization  $P$ .

Curtis & Lewis<sup>(66)</sup> have also considered the measurement of the  $\beta - \gamma$  correlation in the decay of oriented nuclei as a means of testing time-reversal invariance. They discussed, in particular, the case of a  $1^+(\beta)1^+(\gamma)0^+$  transition, the correlation function of which contains a term of the form  $E \langle \underline{J} \rangle (\underline{p} \times \underline{k}) (\underline{J} \cdot \underline{k})$  (where  $E$  depends on cross-products of the coupling constants) which may be observed by measuring the  $\beta - \gamma$  coincidence asymmetry. However, as the coefficient of the asymmetry term depends also on factors other than  $E$ , a measurement of the magnitude of this asymmetry will only lead to definite information on time-reversal

invariance if all other factors are known.

In their paper on electron polarization in the decay of unoriented nuclei, Curtis & Lewis<sup>(15)</sup> considered transverse as well as longitudinal polarization and gave the correlation function between the transverse electron polarization and the electron and  $\gamma$ -ray directions in a simple cascade. Since no such correlation exists for allowed transitions they considered the case of a first forbidden transition. This correlation function, in the absence of Coulomb corrections, is of the form

$$W(\underline{p}_e, \underline{k}, \underline{n}) = 1 + A [\beta(\underline{p}_e \cdot \underline{k})^2 - 1] + B(\underline{p}_e \cdot \underline{k})(\underline{n} \cdot \underline{k}) + C(\underline{n} \cdot \underline{p}_e \times \underline{k})(\underline{p}_e \cdot \underline{k}),$$

where  $\underline{p}_e$  is a unit vector in the direction of the electron momentum,  $\underline{n}$  is a unit vector in the direction of the electron spin (orthogonal to  $\underline{p}_e$ ), and  $\underline{k}$  is a unit vector in the direction of the  $\gamma$ -ray. The first two terms give the ordinary  $\beta - \gamma$  directional correlation; the third term, which violates parity, appears in the correlation function only if the transverse polarization is in the plane of  $\underline{p}_e$  and  $\underline{k}$ ; the final term, which violates time-reversal invariance, is present only if the electron polarization is perpendicular to the plane containing  $\underline{p}_e$  and  $\underline{k}$ . Observation of such a polarization would therefore give conclusive proof that beta-decay processes are not invariant under time-reversal.

Since the parameter C depends on the electron

energy, the Fermi and Gamow-Teller matrix elements and the coupling constants in combinations of the form  $C_i C_j^* + C_i' C_j'^*$ , this transverse polarization will arise only in mixed Fermi and Gamow-Teller transitions.

Most of the experiments to test parity conservation in beta-decay and to measure the degree of longitudinal electron polarization were not sensitive to time-reversal invariance and the results obtained were consistent with the assumption of real coupling constants. However the experimental results of Burgy et al. (111) on the electron asymmetry from the decay of polarized neutrons, and also those of Ambler et al. (29(ii)) on the electron asymmetry from the decay of polarized  $\text{Co}^{58}$  nuclei, are difficult to explain on this assumption.

In view of the lack of data on the behaviour of weak forces under time-reversal, the present experiment - an attempt to detect the transverse polarization predicted by Curtis & Lewis - was undertaken.

Chapter II.Introduction to Experiment.1. General.

The transverse polarization of an electron beam may be observed by measuring the asymmetry in the electron distribution after the beam has been scattered in a thin foil of high  $Z$  value.

When a transversely polarized electron approaches a nucleus, it experiences a force due to the interaction between the Coulomb field of the nucleus and the electron spin. If an electron approaches a nucleus, as shown in fig. 1, with its momentum vector directed along the  $+z$  axis and its spin vector pointing along the  $+y$  axis, the nucleus lying in the  $x-z$  plane, then it will experience a force which will deflect it along the  $-x$  direction. Whereas, if the electron spin is reversed, all other factors remaining the same, the force will deflect it along the  $+x$  axis. Thus Mott scattering of a transversely polarized electron beam leads to an asymmetry in the resultant distribution of the scattered electrons.

In the present experiment, electrons from the source were scattered from a gold foil, and the scattered electrons were observed in coincidence with their cascade  $\gamma$ -rays. That an asymmetry in this coincidence

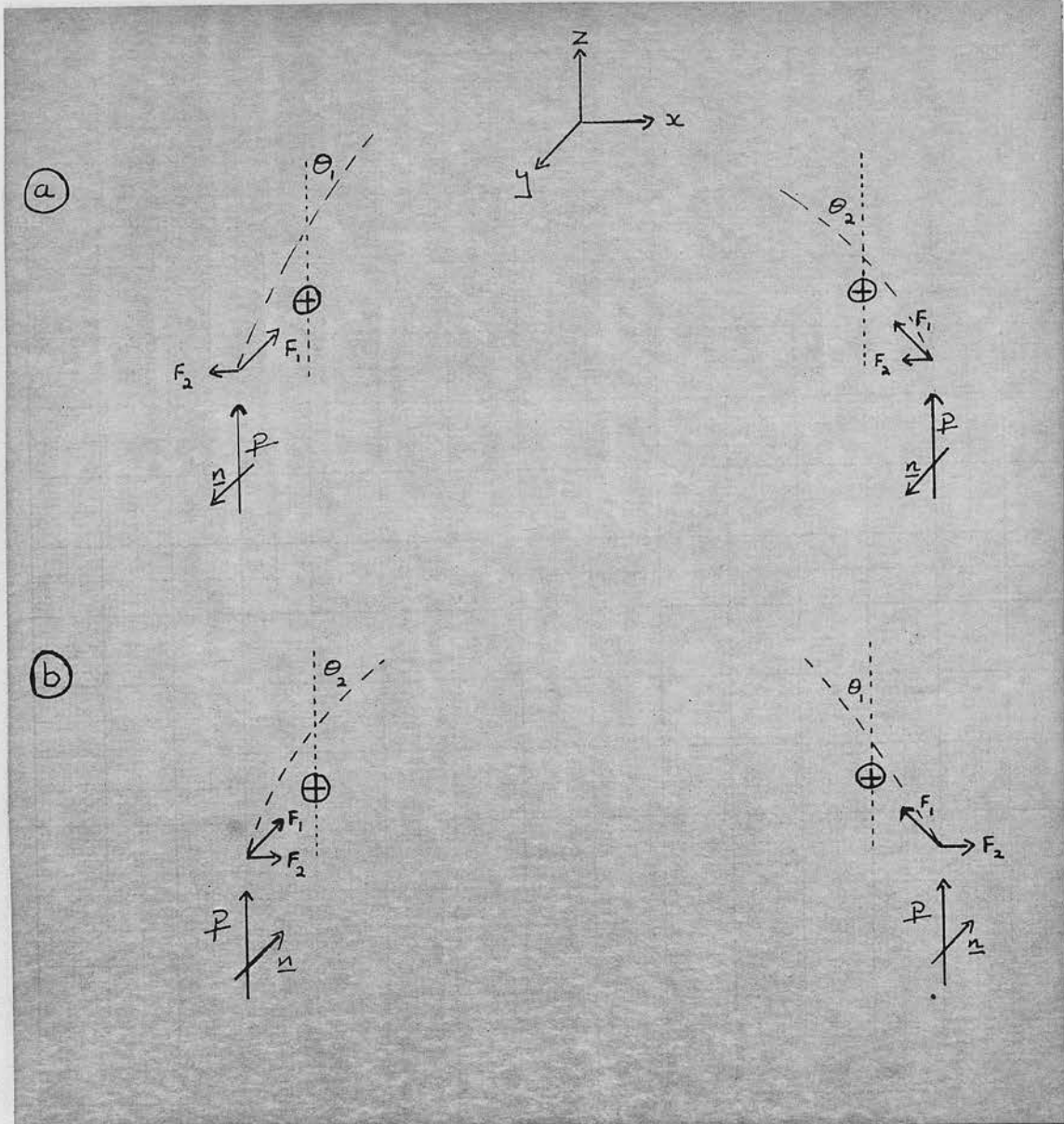


Figure 1. To illustrate Mott scattering of a transversely polarized electron.

In each diagram an electron with momentum  $\underline{p}$  along the + z direction approaches a nucleus lying in the x-z plane and experiences two forces,  $F_1$  due to the Coulomb attraction and  $F_2$  due to the spin-orbit coupling.

In figure 1(a) the spin vector,  $\underline{n}$ , points along the + y direction and in figure 1(b) it is directed along the - y direction. The broken lines show the trajectory of the electron under the combined action of the two forces in each case. ( $\theta_2 > \theta_1$ ).

counting rate indicates the presence of a transverse electron polarization and hence a violation of time-reversal invariance in the decay process can be seen by considering the "normal" and the "time-reversed" situations.

The normal, experimental, situation is shown in fig. 2(a).  $\underline{p}$ , pointing along the + z axis, defines the direction of the momentum of the electron beam,  $\underline{n}$ , pointing along the + y axis, defines the direction of the polarization of the beam, and  $\underline{k}$  shows the direction of the detected  $\gamma$ -ray. Since the required correlation term is of the form  $(\underline{n} \cdot \underline{p} \times \underline{k})(\underline{p} \cdot \underline{k})$ , those  $\gamma$ -rays are detected which are emitted at an angle of  $\frac{3}{4} \pi$  from the direction of  $\underline{p}$ .  $\underline{p}$  and  $\underline{k}$  therefore define the x - z plane. If a scattering foil is placed at  $45^\circ$  both to the direction of incident electrons and to the x axis, then, by the argument given above, more electrons will be scattered along the - x axis than along the + x axis. Therefore, if the electrons which are scattered along the - x direction are observed in coincidence with the  $\gamma$ -rays, more coincidences will be recorded with the  $\gamma$ -counter in position 1 than with the  $\gamma$ -counter in position 2, obtained by rotating the counter through  $180^\circ$  in the x-y plane.

The time reversed situation is shown in fig. 2(b) and is obtained by reversing the directions of the

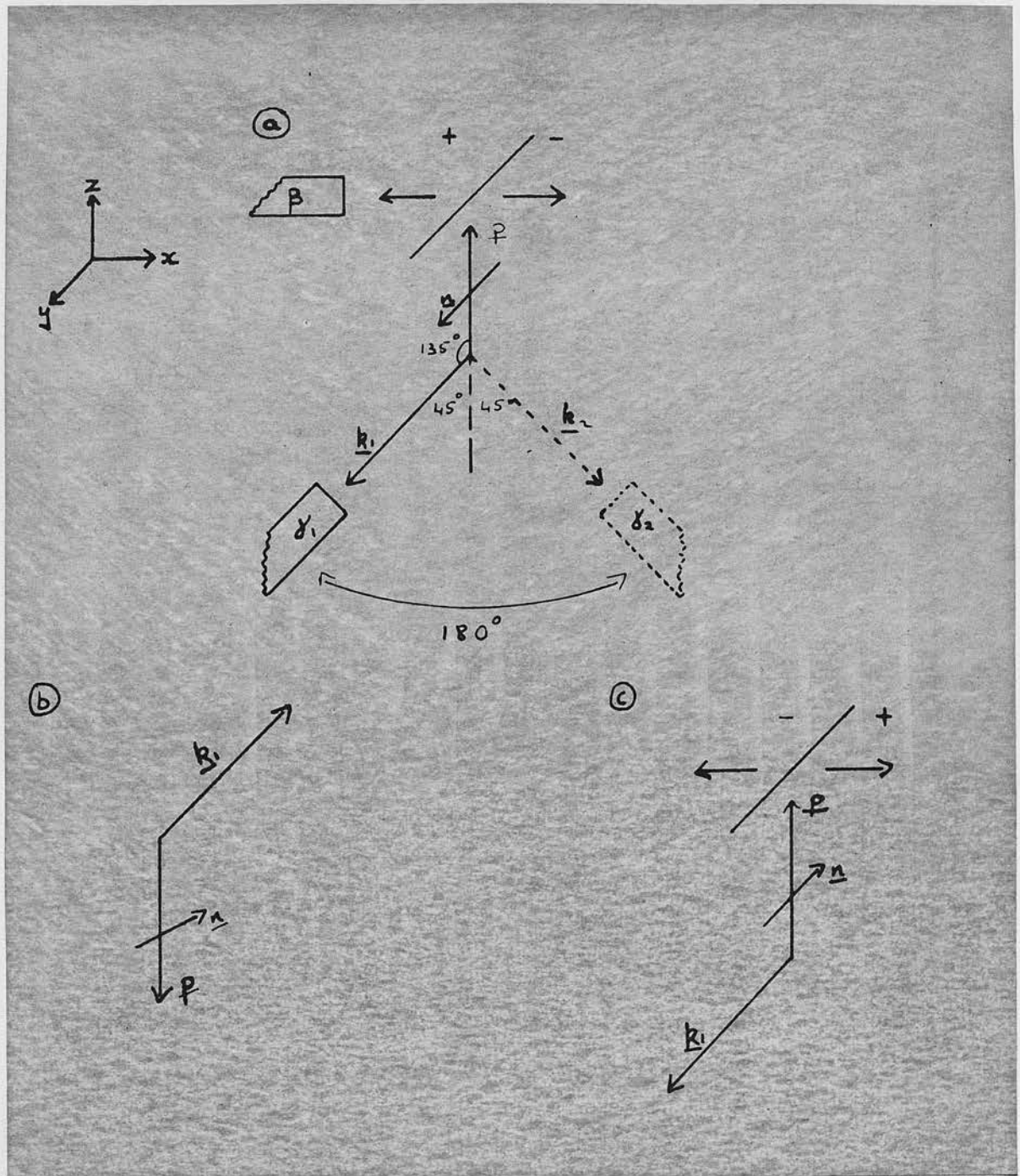


Figure 2. The detection of  $\gamma$ -rays in coincidence with transversely polarized electrons.

(a) shows the "normal" experimental situation, (b) and (c) the hypothetical "time-reversed" situation.

electron and  $\gamma$ -ray momenta and of the polarization vector. This is exactly equivalent to the situation shown in fig. 2(c) in which  $\underline{p}$  is directed along the + z axis as before,  $\underline{k}$  is also directed as in fig. 2(a) but  $\underline{n}$  is now directed along the - y axis. In this case if a scattering foil is placed at  $45^\circ$  to the direction of the incident electrons a preponderance of scattered electrons occurs in the + x direction. If coincidences were recorded, in this situation, between the electrons scattered along the - x direction and the  $\gamma$ -rays given off in the two directions already considered, the counting rate obtained with the  $\gamma$ -counter in position 2 would exceed that with the  $\gamma$ -counter in position 1.

Since the "normal" and "time-reversed" situations are distinguishable when the electron beam has a polarization orthogonal to the plane containing the  $\beta$  - and  $\gamma$ -rays, the process in which such electrons and  $\gamma$ -rays are produced must be non-invariant under time-reversal. Hence the detection of an asymmetry in the coincidence counting rates in the normal situation for the two  $\gamma$ -counter positions would give conclusive proof, not only of the existence of a transverse electron polarization, but also of non-invariance of the  $\beta$  - decay process with respect to time-reversal.

## 2. Apparatus.

The apparatus is shown in figs. 3 - 9. Figs. 3(a), (b) and (c) show the main vacuum chamber and the positions of the  $\beta$  and  $\gamma$  counters. The main body of the vacuum chamber is  $12\frac{1}{2}$  in. in length and  $5\frac{1}{2}$  in. in internal diameter, and, during the experiment, was maintained at a pressure of  $\sim 10^{-3}$  mm. Hg by means of a rotary pump. Limbs X and Y, of internal diameter 4 in., contain rails along which the foil holder (see fig. 4) can move so that an aluminium or a gold foil may be placed in the path of the electrons from the source, at  $45^\circ$  to the directions of both the incident and detected beams. Limb Z contains the  $\beta$ -counter.

The foil holder is  $10\frac{1}{2}$  in. long and  $3\frac{3}{4}$  in. wide, and has three recessed holes into which rings of  $2\frac{1}{2}$  in. internal diameter and made of  $\frac{1}{8} \times \frac{1}{8}$  in. aluminium may be placed. During the experiment, the rings in positions A and C held gold and aluminium foils respectively, whilst the centre position was left empty. The external pointer lies against a scale with three marks to indicate whether the centre of hole A, B or C is at the centre of the chamber, thus showing which foil is in the path of the electron beam.

The source holder, shown in fig. 5, is made of  $\frac{1}{8}$  in. aluminium. The source itself is evaporated on to a 1 mgm./sq. cm. aluminium foil which is then placed on

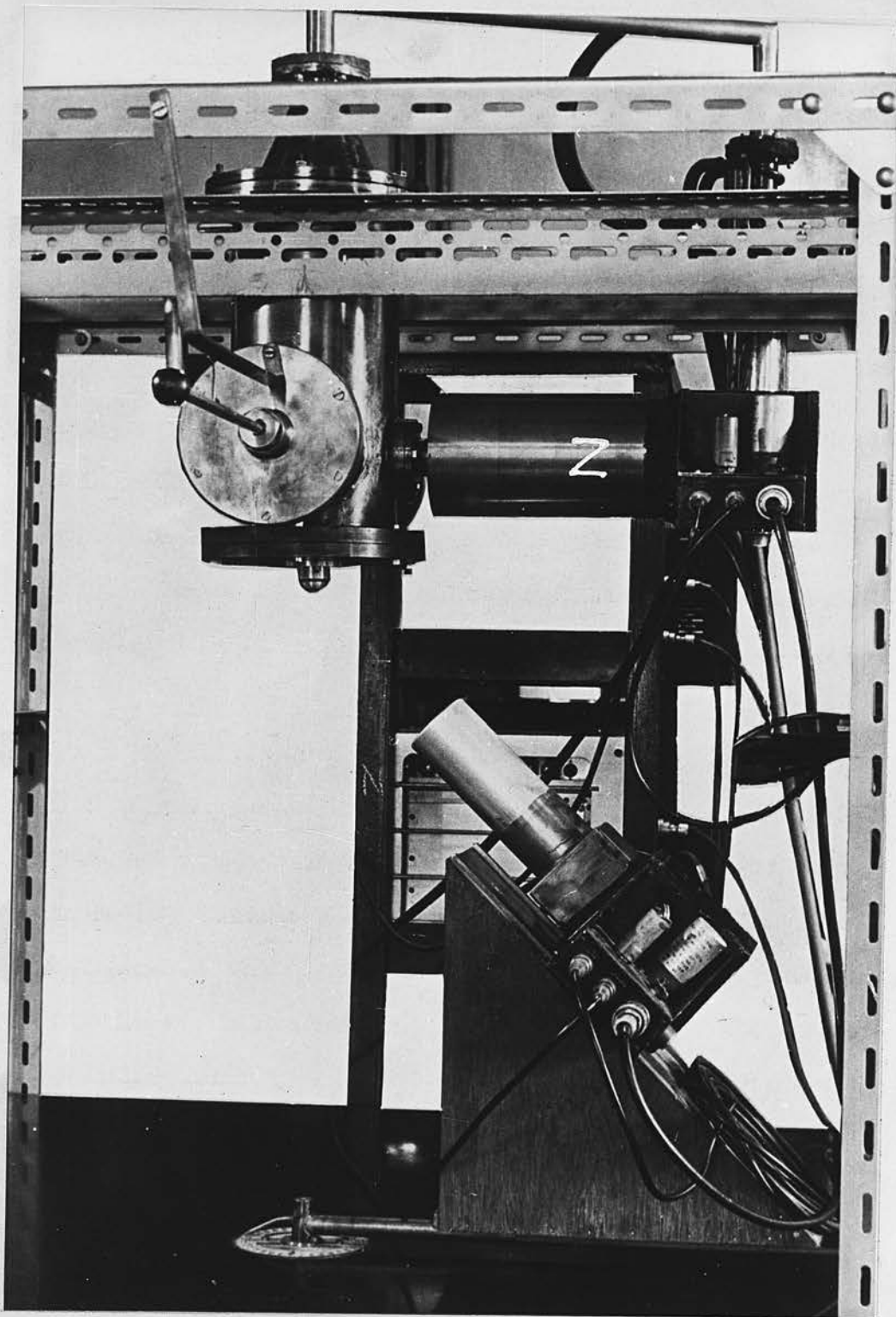


Figure 3(a). The main vacuum chamber showing the  $\beta$ -counter and the  $\gamma$ -counter in the EAST position.

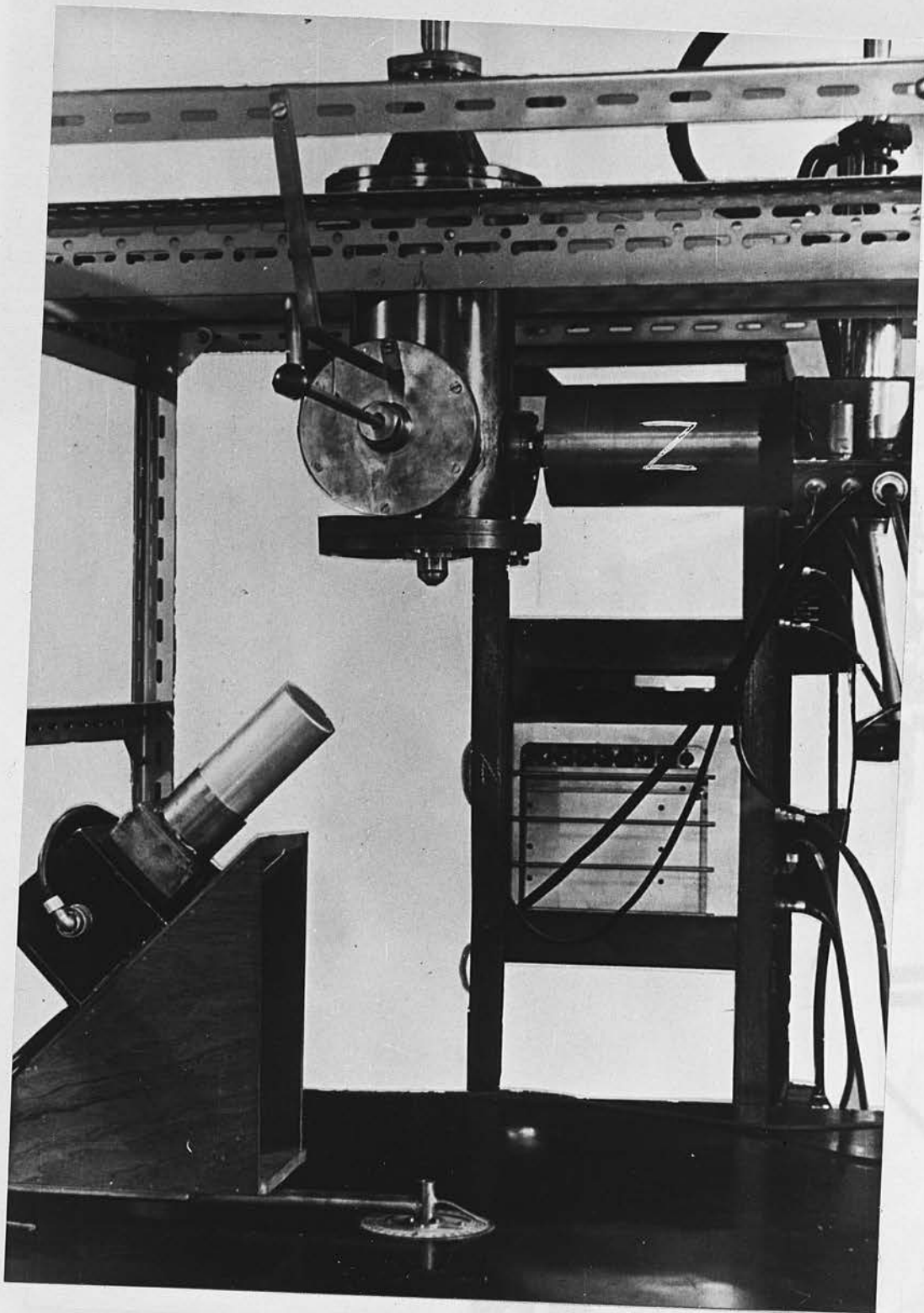


Figure 3(b). The main vacuum chamber with the  $\gamma$ -counter in the WEST position.

Figure 3(a). The main vacuum chamber mounted on the steel frame along which the collimator may be moved.

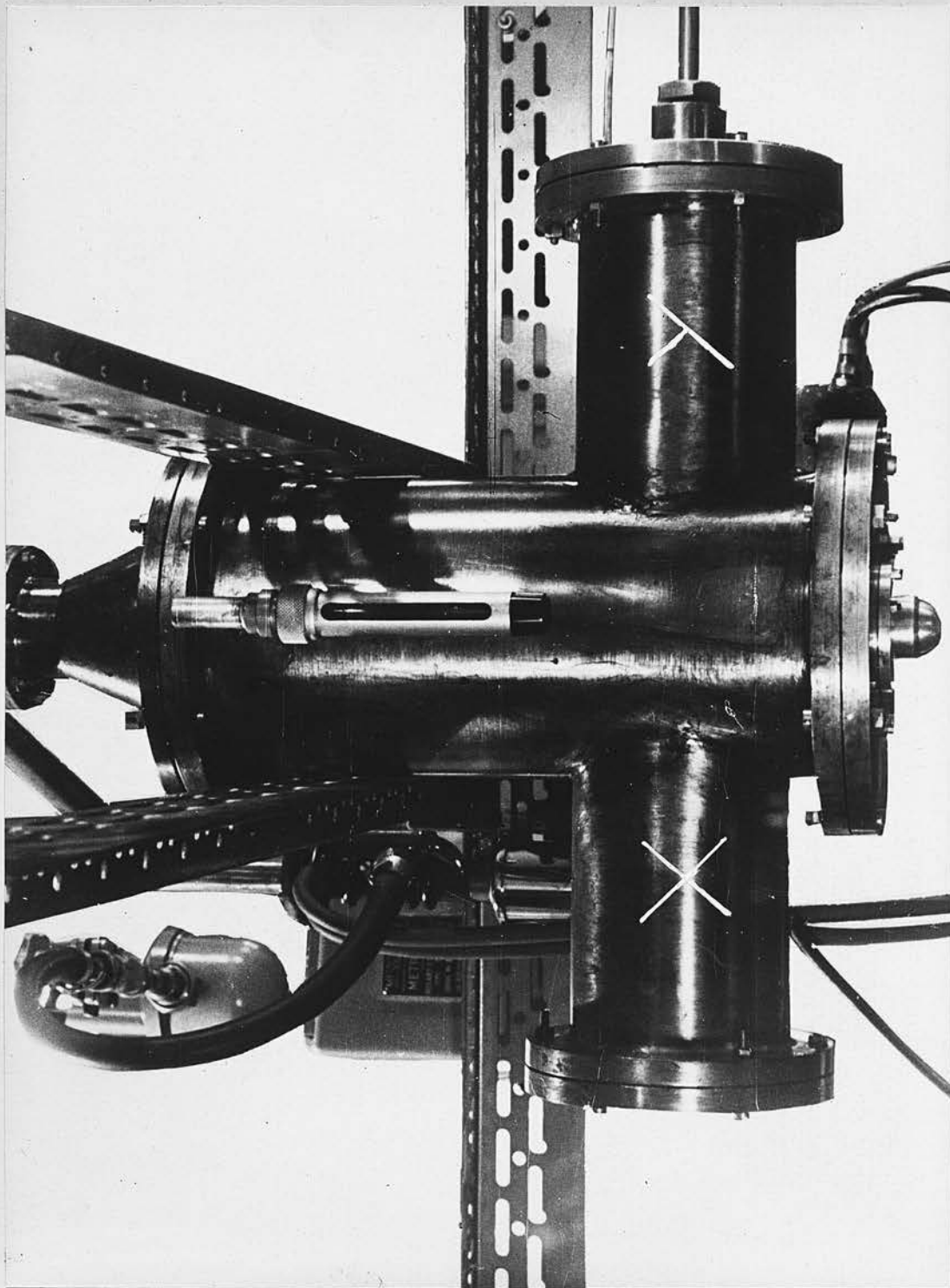


Figure 3(c). The main vacuum chamber showing the limbs containing the rails along which the foil holder may be moved.

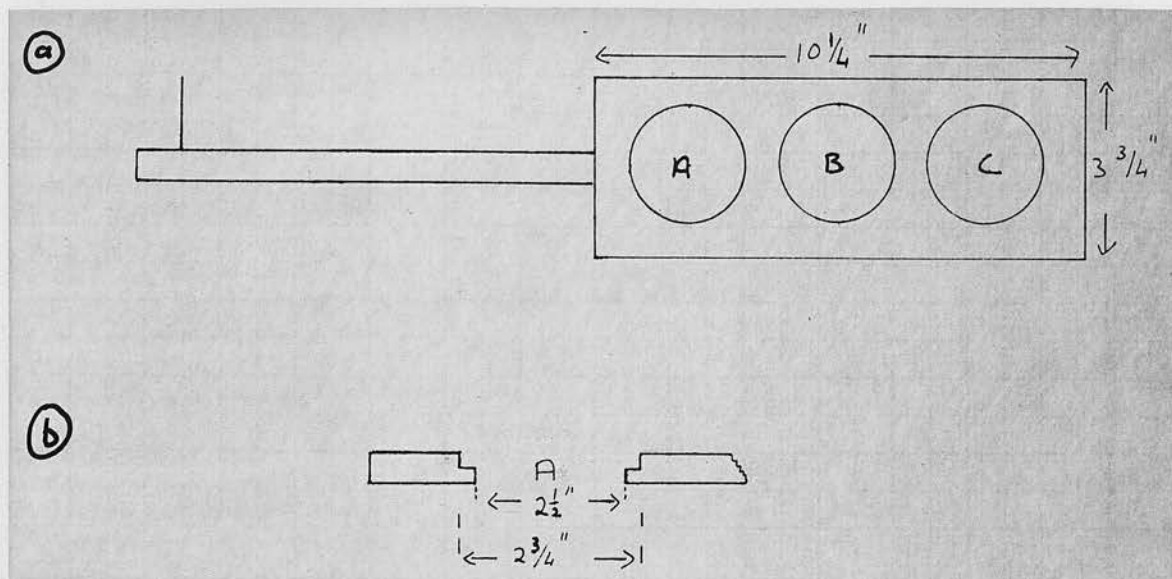


Figure 4. The foil holder.

- (a) shows the holder with external pointer.
- (b) shows the dimensions of the recessed holes.

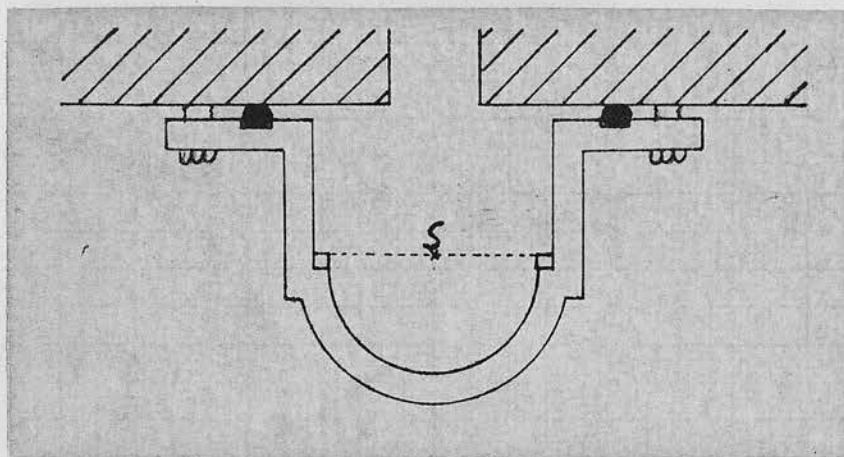


Figure 5. The source holder.

an aluminium ring which fits into the recess shown. The lower part of the holder forms a hemisphere with the source at the centre. The source ring has grooves running along its under surface and up the outer edges so that, when the chamber is being evacuated, air may pass from the space below the source without damaging the supporting foil.

The base plate of the chamber and the lead, which shields the crystal in the  $\beta$ -counter from direct radiation, are shown in fig. 6(a). The lead block is  $5\frac{1}{2}$  in. in diameter and has a 1 in. hole through its centre. The groove shown allows the passage of the foil holder. A can of  $\frac{1}{8}$  in. <sup>Duralumin,</sup> XXXXXXXXXX shown in fig. 6(b), fits into the hole in the lead. In the base of this can there is a  $\frac{1}{4}$  in. diameter hole which restricts the beam of electrons from the source, so that all the electrons which reach the scattering foil are incident on it at approximately  $45^\circ$ .

Fig. 7 shows the  $\beta$ -crystal, with an aluminium shield to prevent electrons scattered from parts of the apparatus other than the foil reaching it. The crystal itself is 1 in. in diameter and  $\frac{1}{8}$  in. thick, and is a plastic phosphor type N.E.102 made by Nuclear Enterprises Ltd. The front face of the crystal is covered with a thin aluminium foil to reflect into the crystal any light scattered back out of it instead of

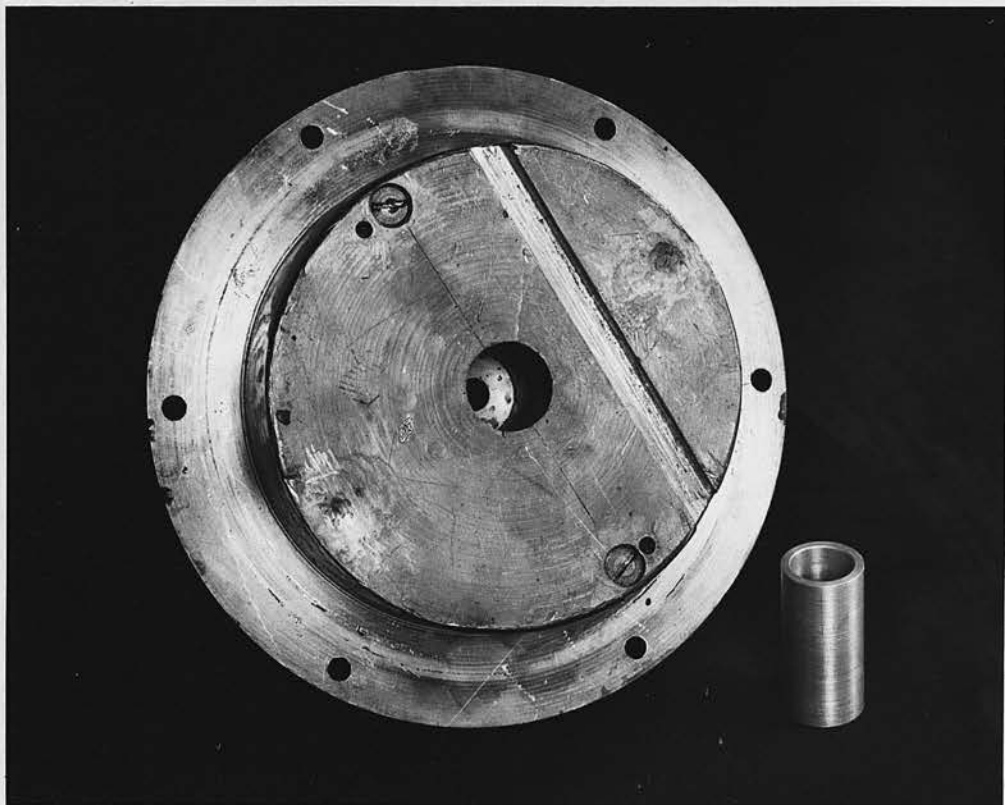


Figure 6(a). The base-plate of the vacuum chamber and the duralumin can.

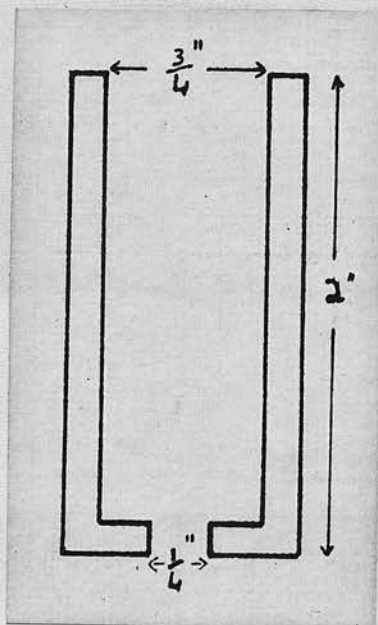


Figure 6(b). To show the dimensions of the duralumin can.

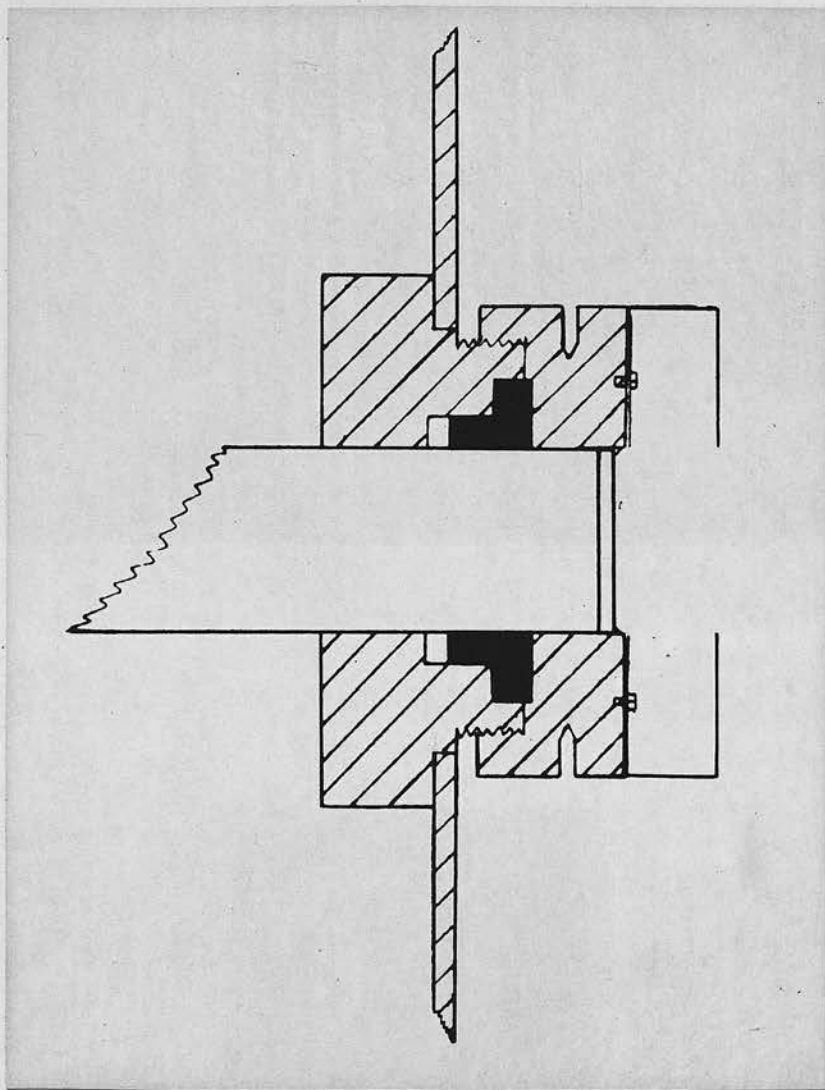


Figure 7. The crystal for detecting the scattered electrons, showing the aluminium shield and also the light guide passing through the wall of the vacuum chamber.

into the light guide. Optical contact is made between the crystal and light guide, and between the light guide and photomultiplier tube, by means of a thin layer of white petroleum jelly well compressed between the surfaces. The photomultiplier used in this counter was an eleven-stage tube type 5311.

An anthracene crystal was used as the  $\gamma$ -ray detector. This crystal is 1 in. in diameter and 1 in. high. In this counter the crystal is in direct contact with the photomultiplier which is an eleven-stage tube type 6097B, optical contact again being made by means of a thin layer of petroleum jelly.

The paths of the electrons and  $\gamma$ -rays to be detected are shown schematically in fig. 8.  $\gamma_1$  and  $\gamma_2$  are the two positions of the  $\gamma$ -counter, the first position being directly under the  $\beta$  counter and the second being obtained by rotating the  $\gamma$ -counter through  $180^\circ$  in the horizontal plane.

A block diagram of the electronics used with the above apparatus is given in fig. 9. The coincidence set, which consists of a discriminator unit type 1153A, a coincidence mixer unit type 1153A, power units, and head amplifiers, was used in conjunction with the detectors already described and scaling units type 1009A and 200A.

Single channel counts of the scattered electrons

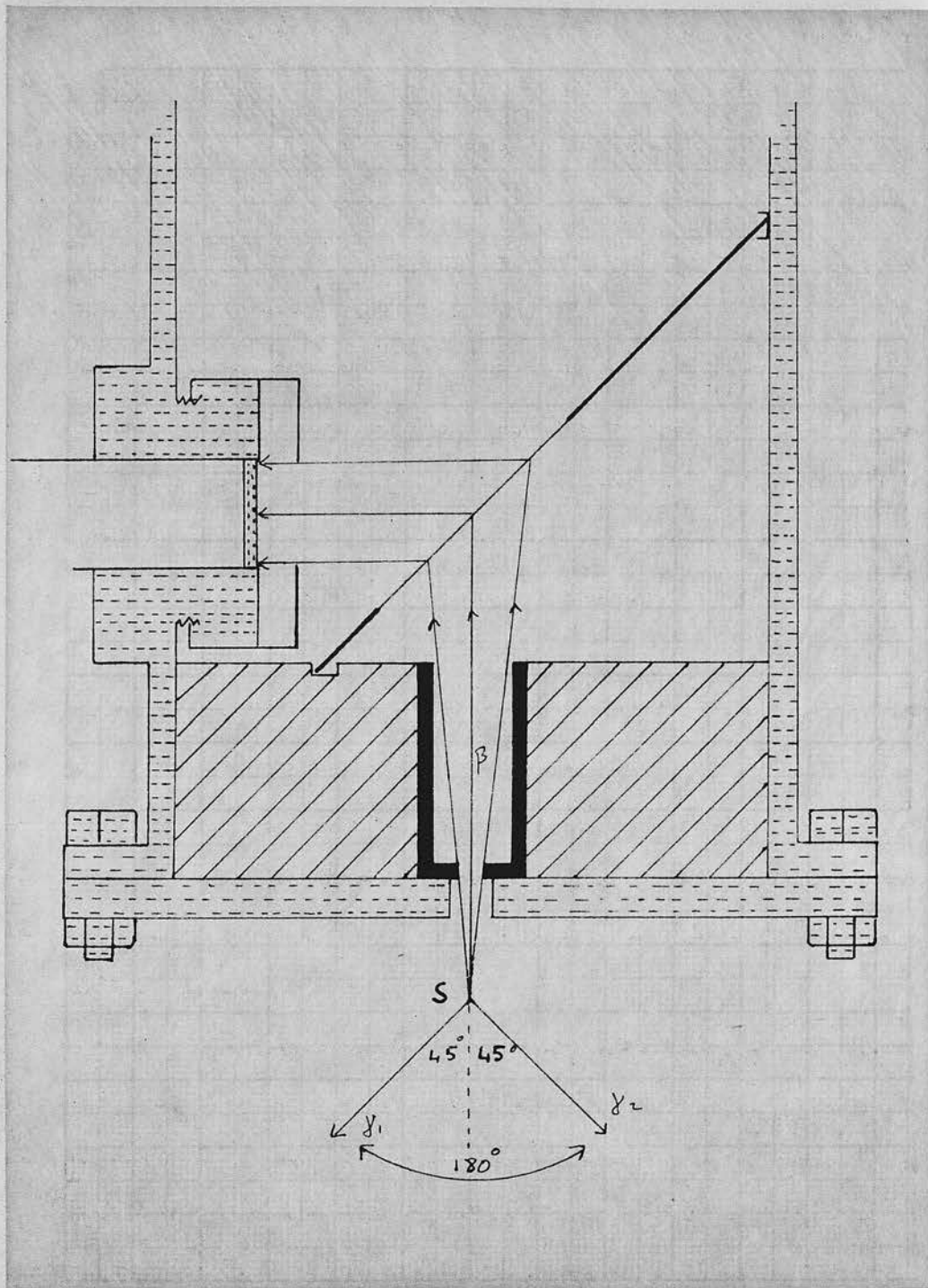


Figure 8. The paths of the electrons and  $\gamma$ -rays before detection.

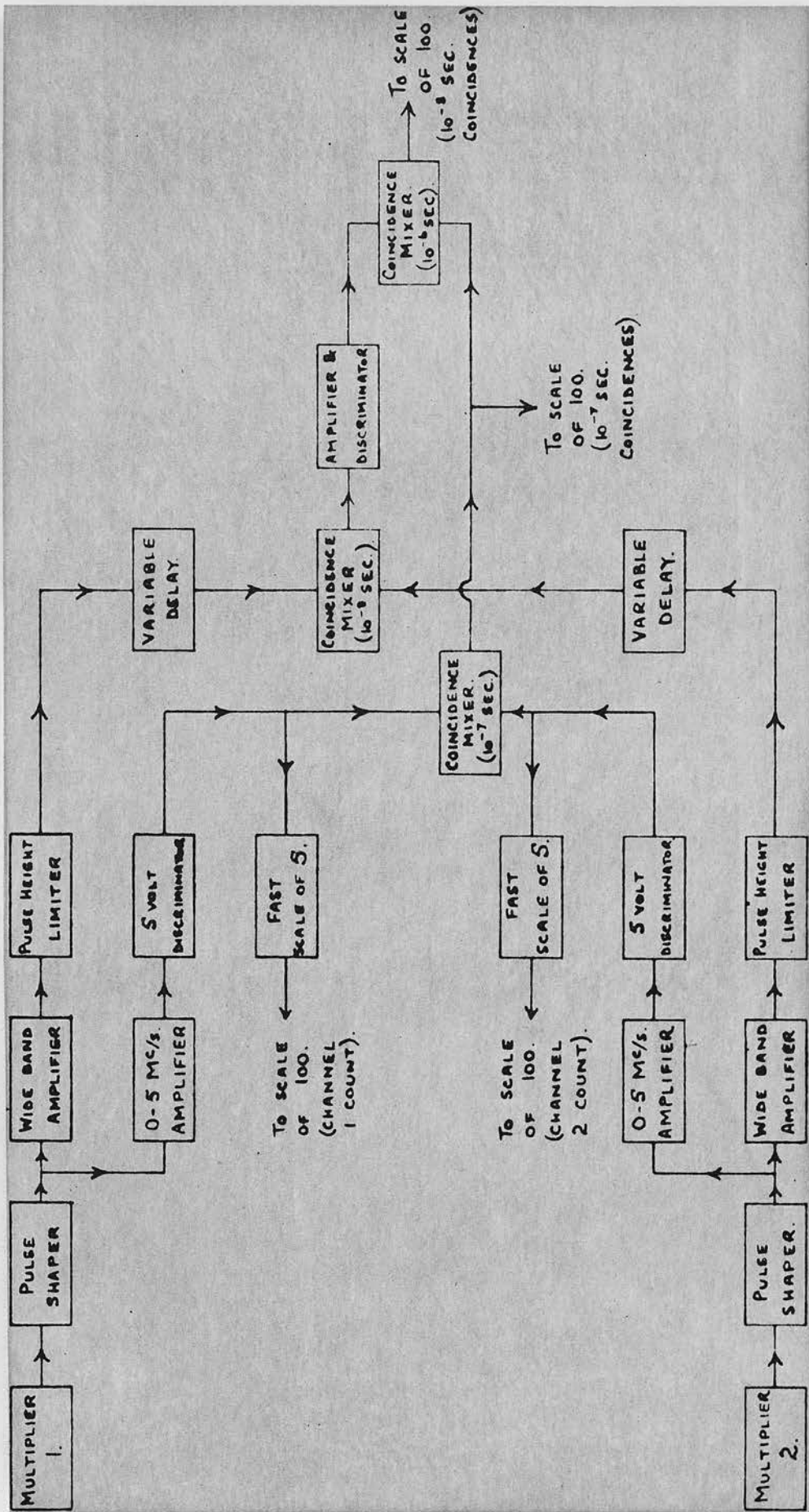


Figure 9. Block diagram of the electronics.

and direct  $\gamma$ -rays were recorded, as well as coincidences occurring due to electrons and  $\gamma$ -rays being counted within, approximately,  $10^{-7}$  seconds and  $10^{-8}$  seconds of each other.

This "fast-slow" coincidence unit has already been described by F.H. Wells<sup>(112)</sup> who originally designed it, so no further comment will be made here.

### 3. Choice of Source.

As the transverse electron polarization- $\gamma$ -ray correlation was given by Curtis & Lewis for first forbidden transitions a source suitable for this experiment would be an isotope in which a high percentage of the decay occurs through a first forbidden  $\beta$ -transition followed by a direct  $\gamma$ -transition to the ground state of the daughter nucleus. The original choice of source was the isotope  $\text{Au}^{198}$ , which decays 98.6% through  $\beta$ -emission from its  $2^-$  ground state to a 0.412 MeV  $2^+$  state in  $\text{Hg}^{198}$ , which, in turn, decays by the emission of an E2  $\gamma$ -ray to the  $0^+$  ground state of  $\text{Hg}^{198}$  (see fig. 10).

A few preliminary measurements were made with this type of source, but, owing to its short half-life of 2.7 days, and to the slow coincidence counting rates obtained, it was considered advisable to look for another isotope which decays under the required correlation conditions.

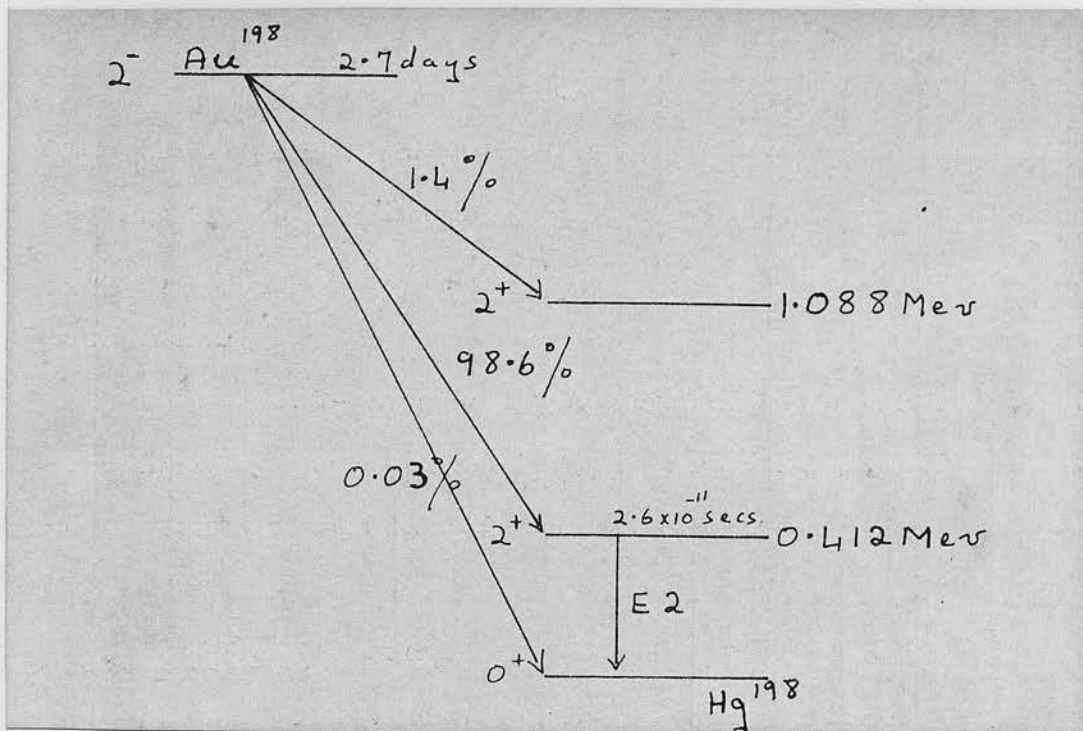


Figure 10. Decay scheme of the  $\text{Au}^{198}$  isotope.

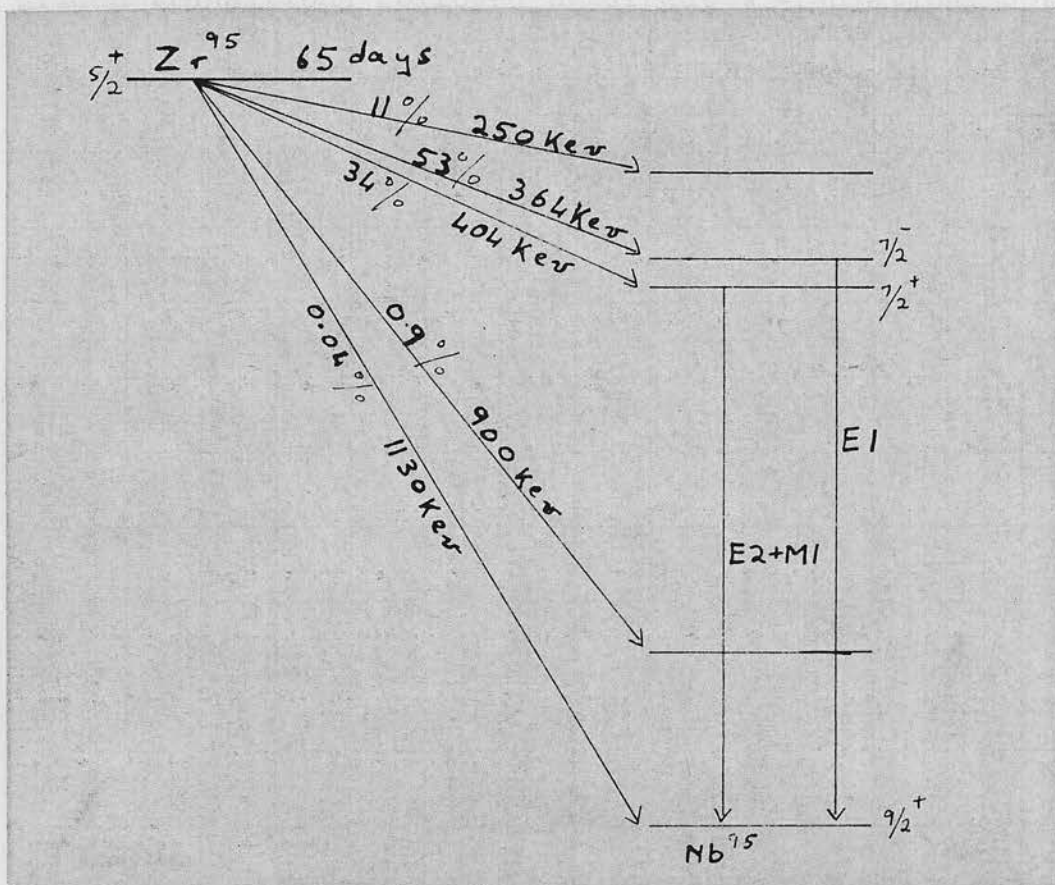


Figure 11. Decay scheme of the  $\text{Zr}^{95}$  isotope.

53% of the decay of  $Zr^{95}$  occurs through  $\beta$  -emission to a 756 keV,  $\frac{7^-}{2}$  level in  $Nb^{95}$ , which in turn decays to the ground state by emission of E1  $\gamma$  -radiation. Since the ground state of  $Zr^{95}$  is a  $\frac{5^+}{2}$  state, this decay process satisfies the conditions stipulated by Curtis & Lewis. A further 34% of the  $Zr^{95}$  decay occurs through an allowed  $\beta$  -transition to a 723 keV,  $\frac{7^+}{2}$  level in  $Nb^{95}$ , which then decays to the ground state by emission of (E2 + M1)  $\gamma$  -radiation (see fig.11). Since Pursey<sup>(115)</sup> has shown that, for an allowed  $\beta$  -transition which is followed by mixed  $\gamma$  -radiation, there is a correlation similar to that given by Curtis & Lewis for first forbidden transitions followed by direct  $\gamma$  -radiation, both these decay processes, amounting to 87% of the total decay, will contribute to the required asymmetry effect, if the decay interaction is not invariant under time-reversal.

As  $Zr^{95}$  has a 65 day half-life, it was considered to be a more suitable isotope than  $Au^{198}$ , and all results quoted were obtained using this isotope.

Chapter III.Preliminary Measurements.1. Adjustment of Voltages on the Photomultiplier Tubes.

In order to pick out the required  $\beta$ -particles from the  $Zr^{95}$  decay, and at the same time to exclude most of those from the 11% transition of end point 250 keV, the voltage on the  $\beta$ -channel photomultiplier tube, which was supplied by a 2 KV 0.1% stable power unit, was adjusted by means of a potentiometer until the counter just ceased to detect the 167 keV electrons from  $S^{35}$ .

The voltage on the second photomultiplier was adjusted so that only  $\gamma$ -rays of  $\sim 700$  keV would be recorded in this channel.

2. Resolving Times of the Coincidence Channels.

As the experiment involves the recording of coincidence counts, it is important to know the resolving times of the coincidence channels accurately, so that the chance coincidence counting rates may be subtracted from the recorded counting rates to obtain the genuine coincidence counting rates.

These resolving times were found in the following way. The two detectors were moved as far from each other as was possible and  $Co^{60}$  sources were placed beside them. They were then well screened with lead, so

that no counts were recorded in either due to the source lying near to the other, and the number of counts recorded in the single channels and in the two coincidence channels in a known period of time were noted.

The chance coincidence rate is related to the single channel counting rates and to the resolving time of the coincidence channel by the equation  $N_{12} = 2N_1N_2T_{12}$ , where  $N_{12}$  is the number of chance coincidences per second,  $N_1$  and  $N_2$  are the number of counts recorded in the two single channels per second, and  $T_{12}$  is the resolving time, in seconds, of the coincidence channel concerned.

By applying this formula to each of the coincidence channels in turn, their resolving times were accurately determined. These resolving times were checked regularly throughout the experiment.

### 3. Source Preparation.

1 millicurie sources of  $Zr^{95}$  were obtained from the U.K.A.E.A. Radiochemical Centre at Amersham. These were in solution in oxalic acid, no other impurity being present to more than 1%. The sources used in the experiment were prepared by evaporating this solution onto 1 mgm./sq. cm. aluminium foil, great care being taken to ensure that the final source should cover an area of diameter not greater than  $\sim 4$  mm. The aluminium foil

was then fixed to the source-holding ring so that the source was centrally placed. The strengths of the sources thus obtained were between 0.2 mC and 0.4 mC (certainly not greater than 0.5 mC).

#### 4. Choice of Scattering Foils.

With the  $Zr^{95}$  source in position, the  $\gamma$ -counter directly below the  $\beta$ -counter, and the chamber evacuated, the number of electrons scattered from a 1 mgm./sq. cm. gold foil in a given time, and the number of coincidences occurring between the scattered electrons and direct  $\gamma$ -rays in that time, were recorded. It was found that, with this foil, both the  $\beta$ -counting rate and the coincidence counting rate were far too small for convenience. Several gold foils, of various thicknesses, were therefore tested in a like manner and a foil of  $\sim 5$  mgm./sq. cm. was eventually chosen for use in the experiment. Even with this foil, the greatest  $\beta$ -counting rate obtained was only 350 per minute greater than the background, and the greatest coincidence rate recorded due to these scattered electrons was 36 per hour.

To correct for any instrumental asymmetry, since the expected Mott scattering asymmetry depends on the  $Z$  value of the scattering foil, a comparison experiment was performed using an aluminium foil, with which the asymmetry produced should be so much reduced as to be



negligible. Several aluminium foils of thickness from  $\sim 3$  mgm./sq. cm. to  $\sim 30$  mgm./sq. cm. were tested in the same manner as were the gold foils. It was found that above a certain thickness no appreciable increase in the  $\beta$ -counting rate occurred with further increase of the foil thickness. In the actual experiment, two aluminium foils were used, one of  $\sim 10$  mgm./sq. cm. and the other of  $\sim 15$  mgm./sq. cm., the coincidence counting rates per detected  $\gamma$ -ray per scattered  $\beta$ -particle, after the background counting rates had been subtracted from each, being consistent to within the statistical errors for both of these foils.

##### 5. Instrumental Asymmetries.

Although the use of an aluminium scattering foil in a comparison experiment should eliminate instrumental asymmetries, several additional tests for such asymmetries were carried out.

In the construction of the apparatus it was ensured that the centre of the scattering foil, and of the holes in the lead block and duralium can all lay on the axis of the main vacuum chamber. Great care was also taken to make sure that the source holder and  $\gamma$ -counter positions were also symmetric with respect to this axis.

To ensure that the source itself was centrally placed, the counting rate in the  $\gamma$ -channel was noted

for various positions of the  $\gamma$ -counter, which could be rotated through  $360^\circ$  in the plane perpendicular to the initial direction of the detected electrons. In particular, the counting rate was noted with the  $\gamma$ -counter directly under the  $\beta$ -counter and with the  $\gamma$ -counter turned through  $180^\circ$  from this position. These two  $\gamma$ -counter positions are those used in the main experiment and will hereafter be referred to as the East and West positions respectively.

To ensure that no radiation was scattered from the material of the  $\beta$ -counter into the  $\gamma$ -counter when in the East position, having ensured that the  $\gamma$ -counting rate was the same in both the experimental positions, a replica  $\beta$ -counter was supported above the  $\gamma$ -counter when in the West position, and the counting rate again recorded. No change was observed.

To check for scattered radiation entering the  $\beta$ -detector, the counting rate in this channel was noted for various positions of the  $\gamma$ -counter, again, most particular attention being focused on the two experimental positions. No variation in the  $\beta$ -counting rate was obtained due to changing the position of the  $\gamma$ -counter.

Since the only other asymmetry arising from the change in the relative positions of the parts of the apparatus during the experiment occurs due to the movement of the foil holder, the  $\beta$ -counting rate was observed

with gold foils on each of the rings and with the foil holder in each of its possible positions. Similar observations were made with no foil in the holder. It was found that the position of the foil holder did not affect the counting rate.

From these tests it was assured that no asymmetry in the counting rates arose due to the construction of the apparatus.

Corresponding to the six possible configurations of the apparatus, i.e. with the  $\beta$ -counter directly below the  $\beta$ -counter (East position) and the foil holder in each of its three positions, corresponding to a gold scattering foil, an aluminium scattering foil and no scattering foil in the path of the electron beam, and with the  $\gamma$ -counter in the West position and the foil holder again in each of its possible positions. Before and after each one hour count the single channel counting rates were noted over short periods to ensure the stability of the electronics.

From each set of six counts, a value of the asymmetry in the coincidence counting rates produced by the presence of the gold and aluminium foils was calculated.

Since the total time covered by the six sets of observations, between six and seven hours, is short compared to the 55 day half-life of the  $\text{Er}^{135}$  isotope, the correction required to allow for source decay during this period is negligible.

Chapter IV.Experimental Procedure and Treatment of Results.1. Normalization and Correction Factors.

With the main chamber of the apparatus evacuated and the source in position the counting rates in the single channels and in the two coincidence channels were recorded, observations being taken in sets of six, one hour counts corresponding to the six possible configurations of the apparatus, i.e. with the  $\gamma$ -counter directly below the  $\beta$ -counter (East position) and the foil holder in each of its three positions, corresponding to a gold scattering foil, an aluminium scattering foil and no scattering foil in the path of the electron beam, and with the  $\gamma$ -counter in the West position and the foil holder again in each of its possible positions. Before and after each one hour count the single channel counting rates were noted over short periods to ensure the stability of the electronics.

From each set of six counts, a value of the asymmetry in the coincidence counting rates produced by the presence of the gold and aluminium foils was calculated.

Since the total time covered by the six sets of observations, between six and seven hours, is short compared to the 65 day half-life of the  $Zr^{95}$  isotope, the correction required to allow for source decay during this period is negligible.

As the  $\gamma$ -counting rate was high and the noise level comparatively very low in this channel, the correction required to eliminate the counts recorded due to noise pulses in the photomultiplier was also negligible. In order to obtain the counting rate in the  $\beta$ -channel due to electrons scattered from either the gold or aluminium foil, however, a correction had to be made. This counting rate was found by subtracting the counting rate recorded when no foil was in the path of the electrons from the source from that obtained when each of the foils was present, thus eliminating background counts due either to direct radiation falling on the detecting crystal or to electrons scattered from parts of the apparatus other than the foil concerned.

The genuine coincidence rates in each channel for the different experimental situations were found by subtracting the chance coincidence rates, obtained from the single channel counting rates and the resolving times of the channels, as described above, from the actual counting rates recorded in the channels. As the number of coincidences recorded per hour in each channel was small, a further correction was applied to find the most probable, as opposed to the recorded, counting rate. This correction factor has been described by D.J. Behrens<sup>(116)</sup> of Harwell and was used here because on a few occasions the number of genuine coincidences

per hour obtained with no scattering foil was equal to, or greater than, the number obtained with a scattering foil present.

This correction factor assumes that both the genuine background counting rate, obtained with no foil present, and the genuine coincidence counting rate with a foil in position have Poisson distributions. The expected number of genuine counts, above the background level, can then be expressed in terms of the actual number of genuine counts recorded and the measured background. If the genuine background coincidence count is denoted  $B$ , and the genuine coincidence counting rate obtained with a foil present is denoted  $N$ , then the expectation value of  $N$  above the background is given by  $\bar{A}$  where

$$\bar{A} = \frac{\sum_{a=0}^{\infty} a (B+a)^N e^{-(B+a)}}{\sum_{a=0}^{\infty} (B+a)^N e^{-(B+a)}}$$

which can be rewritten as

$$\bar{A} = \frac{\sum_{a=0}^{\infty} (B+a)^{N+1} e^{-(B+a)} - B \sum_{a=0}^{\infty} (B+a)^N e^{-(B+a)}}{\sum_{a=0}^{\infty} (B+a)^N e^{-(B+a)}}$$

which, by replacing  $B + a$  by  $x$ , may be simplified to

$$\bar{A} = \frac{\sum_{x=B}^{\infty} x^{(N+1)} e^{-x} - B \sum_{x=B}^{\infty} x^N e^{-x}}{\sum_{x=B}^{\infty} x^N e^{-x}}$$

$$= \frac{(N+1)! - \sum_{x=0}^{B-1} x^N e^{-x} - B \left[ N! - \sum_{x=0}^{B-1} x^N e^{-x} \right]}{N! - \sum_{x=0}^{B-1} x^N e^{-x}}$$

Using this formula each genuine coincidence rate measured was corrected with its expectation value.

Using the corrected values of the coincidence and  $\beta$ -channel counting rates, the number of coincidences occurring per detected  $\gamma$ -ray was found. In order to evaluate the East-West asymmetry produced by the scattering foils, each of these coincidence per  $\gamma$  ratios was further normalised to the same  $\beta$ -counting rate so that the background could be eliminated from each value by direct subtraction of this normalised ratio calculated for the case when no scattering foil was present from that calculated from the observations made when a foil was present. Thus the number of coincidences occurring per detected  $\gamma$ -ray per scattered  $\beta$ -particle was found for the two positions of the  $\gamma$ -counter for each of the scattering foils and since these values had been

normalised to the same  $\beta$  -counting rate a direct comparison could be made between the calculated asymmetry due to the presence of the gold foil and that due to the presence of the aluminium foil.

Thus, for the gold scattering foil, the values of  $(\bar{N}/\gamma)/(\beta_{Au} - \beta_{Bl})$ , where  $\bar{N}$  is the expectation value of the coincidence counting rate ( $= \bar{A} + B$ ),  $\gamma$  is the  $\gamma$  -counting rate, and  $(\beta_{Au} - \beta_{Bl})^{\times}$  is the rate at which electrons are scattered from the gold foil, were calculated from the counting rates obtained with the  $\gamma$  -detector in the East and in the West positions.

Similar values were calculated from the measurements taken when no foil was in the path of the electrons.

To obtain the corresponding results from the measurements taken when the aluminium foil was present the factor  $(\beta_{Au} - \beta_{Bl})$  was replaced by  $(\beta_{Al} - \beta_{Bl})$ , which is the rate at which the electrons were scattered from this foil. In order to eliminate the background in this case the value  $(\bar{N}/\gamma)_{no\ foil} [\equiv (B/\gamma)_{no\ foil}]$  must also be divided by  $(\beta_{Al} - \beta_{Bl})$  to normalise this value to the same  $\beta$  -counting rate.

In order that a direct comparison between the

$\times$  The subscripts Au, Al, and Bl refer to measurements taken when the gold, aluminium and no scattering foil are present, respectively.

asymmetries produced by the gold and aluminium foils could be made, the gold asymmetry value was found by taking  $\frac{W - E}{W + E}$ , where W is defined by

$$W = \left[ \left( \bar{N}/\gamma \right) \left( \frac{\beta_{Au} - \beta_{Be}}{\beta_{Au} - \beta_{Be}} \right) \right]_{Au} - \left[ \left( \bar{N}/\gamma \right) \left( \frac{\beta_{Au} - \beta_{Be}}{\beta_{Au} - \beta_{Be}} \right) \right]_{Be}$$

where the values of  $\bar{N}$ ,  $\gamma$  and the  $\beta$ -counting rates were all obtained with the  $\gamma$ -counter in the West position, and E is defined in exactly the same way but involves the measurements taken with the  $\gamma$ -counter in the East position. The aluminium asymmetry value was found by taking  $\frac{W' - E'}{W' + E'}$ , where W' is defined by  $W' = (\bar{N}/\gamma)_{Al} - (\bar{N}/\gamma)_{Be}$ , all measurements being made with the  $\gamma$ -counter in the West position, and E' is defined in exactly the same way, using observations made with the  $\gamma$ -counter in the East position.

The value  $\bar{N}$  per detected  $\gamma$ -ray was taken for each individual count, so that no correction would be required for source decay, when the results obtained on successive days were compared. It also corrects for any slight variations in the gains of the photomultiplier tubes due to variations of the mains voltage. The use of the factor  $(\beta_{Al} - \beta_{Be})/(\beta_{Au} - \beta_{Be})$  applied to each value of  $\bar{N}/\gamma$  in the calculation of the asymmetry produced by the gold foil also eliminates the necessity of a correction for source decay.

Since no asymmetry should be produced by the aluminium foil, any such asymmetry found must be due to an instrumental effect not previously foreseen, and the true asymmetry produced by the gold foil will be given by the difference between that calculated from the results obtained with the gold foil and that calculated from the results obtained with the aluminium scatterer.

The two coincidence channels were used throughout, to ensure that all the genuine coincidences were recorded since the genuine coincidence counting rate in each channel should be the same.

In order to clarify the method of calculation of the asymmetry values an example is given in tables I and II.

Table I.

Results obtained with the  $\gamma$ -counter  
in the WEST position.

(a)

| Foil | $\gamma$ -counts in<br>a given time<br>(t)(N <sub>1</sub> ) | $\beta$ -particles<br>recorded in<br>t(N <sub>2</sub> ) | $\beta$ 's per<br>minute | ( $\beta - \beta_{Bl}$ )<br>per<br>minute |
|------|---|---|--------------------------|---|
| Au   | 848671  | 20040   | 334.0                    | 212.8                                     |
| Bl   | 849301  | 7271  | 121.2                    | -   |
| Al   | 856819  | 13107   | 218.5                    | 97.3                                      |

(b) Coincidence measurements.

| Foil | Coincidences recorded | Chance | N  | $\bar{A}$ | $\bar{N}$ |
|------|-----------------------|--------|----|-----------|-----------|
| Au   | 12                    | 0.9    | 11 | 10        | 12        |
| B1   | 2                     | 0.3    | 2  |           |           |
| Al   | 6                     | 0.6    | 5  | 4         | 6         |

## (c)

| Foil | Coincidences/<br>detected<br>$\gamma$ -ray ( $\bar{N}/\gamma$ ) | $\frac{\beta_{Al} - \beta_{B1}}{\beta_{Au} - \beta_{B1}}$ | $(\bar{N}/\gamma) \times \frac{\beta_{Al} - \beta_{B1}}{\beta_{Au} - \beta_{B1}}$ |
|------|---|---|---|
| Au   | $1.4140 \times 10^{-5}$   | 0.4572  | $0.6465 \times 10^{-5}$<br>( $\pm 0.1886 \times 10^{-5}$ )                        |
| B1   | $0.2002 \times 10^{-5}$   |   | $0.0915 \times 10^{-5}$<br>( $\pm 0.0641 \times 10^{-5}$ )                        |

## (d)

| Foil | $(\bar{N}/\gamma)$                                      |
|------|---|
| Al   | $0.7003 \times 10^{-5}$ ( $\pm 0.2917 \times 10^{-5}$ ) |
| B1   | $0.2002 \times 10^{-5}$ ( $\pm 0.1401 \times 10^{-5}$ ) |

Thus, with the  $\gamma$ -counter in the West position, the number of coincidences recorded per detected  $\gamma$ -ray per electron scattered from the gold foil, normalised to the rate at which electrons are scattered from the aluminium foil, is  $0.5550 \times 10^{-5}$ , and the number of coincidences

recorded per detected  $\gamma$ -ray, when the electrons are scattered from the gold foil is  $0.5001 \times 10^{-5}$ .

Table II.

Results obtained with the  $\gamma$ -counter  
in the EAST position.

(a)

| Foil | $N_1$ in time $t$ | $N_2$ in time $t$ | $\beta$ 's<br>per minute | $(\beta - \beta_{Bl})$<br>per minute |
|------|-------------------|-------------------|--------------------------|--------------------------------------|
| Au   | 919698            | 21050             | 323.8                    | 202.4                                |
| Bl   | 854394            | 7284              | 121.4                    |                                      |
| Al   | 855796            | 12608             | 210.1                    | 88.7                                 |

(b)

Coincidence measurements.

| Foil | Counting<br>rate | Chance<br>rate | Genuines<br>( $N$ ) | $\bar{A}$ | $\bar{N}$<br>in time $t$ |
|------|------------------|----------------|---------------------|-----------|--------------------------|
| Au   | 18               | 1.0            | 17                  | 11        | 18                       |
| Bl   | 7                | 0.3            | 7                   |           |                          |
| Al   | 11               | 0.6            | 10                  | 4         | 11                       |

(c)

| Foil | $\bar{N}/\gamma$        | $\frac{\beta_{Al} - \beta_{Bl}}{\beta_{Au} - \beta_{Bl}}$ | $(\bar{N}/\gamma) \times \frac{\beta_{Al} - \beta_{Bl}}{\beta_{Au} - \beta_{Bl}}$ |
|------|-------------------------|---|---|
| Au   | $1.9572 \times 10^{-5}$ | 0.4382  | $0.8576 \times 10^{-5}$<br>( $\pm 0.2001 \times 10^{-5}$ )                        |
| Bl   | $0.7842 \times 10^{-5}$ |   | $0.3436 \times 10^{-5}$<br>( $\pm 0.1276 \times 10^{-5}$ )                        |

(d)

| Foil | $(\bar{N}/\chi)$                                    |
|------|---|
| Al   | $1.3321 \times 10^{-5} (\pm 0.3398 \times 10^{-5})$ |
| Bl   | $0.7842 \times 10^{-5} (\pm 0.3996 \times 10^{-5})$ |

In this case, the results lead to a normalised value of the number of coincidences recorded per detected  $\chi$ -ray per scattered  $\beta$ -particle due to the presence of the gold foil of  $0.5140 \times 10^{-5}$ , and a similar value due to the presence of the aluminium foil of  $0.5479 \times 10^{-5}$ .

From these results, the asymmetry in the coincidence counting rate due to the presence of the gold foil, defined by  $(W - E)/(W + E)$  is 0.0384, whilst that due to the presence of the aluminium foil is - 0.0456.

The errors on these calculated asymmetry values occur mainly through the statistical errors in the coincidence counts, and, since these counts are small, the resultant errors on the asymmetry values are large. In fact, considering this source of error alone leads, in the above example, to an asymmetry, in the case of the gold foil of  $(4 \pm 30)\%$ , and in the case of the aluminium foil of  $(- 5 \pm 62)\%$ .

In order to reduce these errors, a large number of observations was taken, and the asymmetries in the coincidence rates produced by the gold and aluminium

foils were calculated from each set, using the method shown. The final error in the average values of these asymmetries was then calculated from the statistical spread in each case.

From the calculation shown, it can be seen that, when the genuine coincidence rate  $N$  is well above the background  $N_{B1}$  (or  $B$ ), the application of the correction term to find the expectation value  $\bar{N}$  only increases the original value by unity. Since the error in  $N$  is greater than this, the difference between the values of the asymmetry calculated using the measured value ( $N$ ) and the expectation value ( $\bar{N}$ ) is well within the error in either result.

In the few cases in which the genuine coincidence counting rate in the presence of a scattering foil appears to be equal to or less than the genuine background, the use of the expectation value of the coincidence counting rate reduces the calculated asymmetry value from 100% or greater to a more reasonable value, although, in fact, the difference between these calculated asymmetries lies within the errors in the values, and the difference between  $\bar{N}$  and the background, and between  $N$  and the background, agrees to within the errors in the individual counts.

This can be seen from the following example. On one occasion, with the  $\chi$ -counter in the East position,

seventeen coincidences were recorded in an hour in the  $10^{-8}$  channel, both when a gold foil and when no foil was in the path of the electron beam. Since the number of chance coincidences occurring in this time for the "gold" case was 1.4 and for the "blank" case was only 0.5, this leads to a negative value of the factor

$$\left[ \left( \bar{N}/\gamma \right) \times \frac{\beta_{Al} - \beta_{Bl}}{\beta_{Au} - \beta_{Bl}} \right]_{Au} - \left[ \left( B/\gamma \right) \times \frac{\beta_{Al} - \beta_{Bl}}{\beta_{Au} - \beta_{Bl}} \right]_{Bl} \text{ East,}$$

and hence in the calculation of the asymmetry  $W - E$  becomes very large and  $W + E$  comparatively small leading to a value of the asymmetry of  $> 100\%$ . It must, however, be noted that the error in this value is greater than the value obtained. On the other hand, when the expectation value of  $N$  is used, this value of  $E$  once more becomes positive and, in fact, the resultant value of the asymmetry calculated using  $\bar{N}$  instead of  $N$  is  $7.8\%$ , although the difference between  $\bar{N}$  and  $B$  is only 3 and the errors in each of the observed coincidence counting rates is  $\pm 4$ .

## 2. Results.

The individual asymmetry values obtained are shown in tables III and IV. Owing to the fact that the errors in these values are greater when aluminium was used as the scattering foil rather than gold, a larger number of results were taken in this case.

Table III.

Asymmetry values obtained using a gold scattering foil.

Expressed in the form  $(W - E)/(W + E)$ .

|          |          |          |          |          |          |
|----------|----------|----------|----------|----------|----------|
| + 0.2685 | + 0.6239 | - 0.0332 | - 0.0034 | - 0.2416 | + 0.2842 |
| + 0.1518 | - 0.2310 | + 0.4683 | + 0.3142 | - 0.5998 | + 0.5542 |
| - 0.3953 | - 0.0481 | - 0.0427 | + 0.4272 | + 0.0403 | - 0.2737 |
| + 0.1012 | + 0.0593 | - 0.0631 | + 0.4405 | + 0.6065 | - 0.1063 |
| + 0.0389 | + 0.1612 | - 0.0935 | + 0.2160 | - 0.3130 | + 0.8149 |
| + 0.3269 | + 0.2644 | - 0.0507 | - 0.4366 | - 0.1931 | - 0.2078 |
| - 0.0029 | + 0.3409 | - 0.2886 | + 0.1627 | + 0.1535 | + 0.2711 |
| + 0.1076 | - 0.1725 | - 0.4544 | - 0.0558 | + 0.0225 | - 0.2102 |
| - 0.0259 | + 0.4271 | - 0.0907 | + 0.3171 | + 0.0768 | - 0.0909 |
| + 0.0384 | - 0.4883 | - 0.1245 | - 0.1067 | + 0.5556 | - 0.2707 |
| + 0.2006 | + 0.0628 | - 0.1044 | - 0.3937 | - 0.1198 | - 0.4024 |
| - 0.0085 | - 0.2657 | - 0.1017 | + 0.2282 | + 0.3380 | - 0.0961 |
| - 0.0088 | - 0.0346 | - 0.0449 | - 0.0943 | - 0.3135 | + 0.0502 |
| + 0.0025 | + 0.1235 | - 0.2187 | + 0.5099 | - 0.1749 | - 0.1473 |
| - 0.0043 | - 0.2959 | + 0.3716 | + 0.0434 | - 0.6008 | + 0.2667 |
| - 0.1864 | + 0.2563 | + 0.3181 | - 0.6142 | - 0.1251 | + 0.0105 |
| - 0.2971 | + 0.4233 | - 0.3168 | - 0.0731 | - 0.0078 | - 0.1786 |
| + 0.0776 | + 0.0040 | + 0.0812 | - 0.4956 | - 0.3638 | + 0.4967 |
| + 0.0036 | - 0.6265 | + 0.0537 | - 0.2619 | + 0.6779 | + 0.6731 |

Table IV.

Asymmetry values obtained using an aluminium scattering foil. Expressed in the form  $(W - E)/(W + E)$

|          |          |          |          |          |          |
|----------|----------|----------|----------|----------|----------|
| - 0.4585 | + 0.0674 | - 0.3070 | + 0.3554 | - 0.5163 | + 0.2890 |
| - 0.7080 | + 0.2336 | + 0.5456 | - 0.5895 | + 0.1927 | - 0.3155 |
| - 0.1148 | - 0.0828 | - 0.4011 | + 0.1582 | - 0.2838 | - 0.3143 |
| - 0.2769 | - 0.8249 | - 0.5437 | + 0.2967 | - 0.1398 | + 0.5684 |
| + 0.1490 | - 0.2765 | - 0.0972 | + 0.5058 | + 0.0543 | - 0.1885 |
| - 0.4583 | + 0.0677 | - 0.2241 | - 0.0456 | + 0.1483 | - 0.5683 |
| - 0.3300 | - 0.3433 | - 0.3063 | - 0.0647 | - 0.2803 | + 0.2146 |
| - 0.4671 | - 0.4189 | + 0.6341 | + 0.4806 | - 0.2471 | - 0.0405 |
| + 0.3047 | - 0.7318 | - 0.5222 | + 0.2524 | - 0.4586 | - 0.1192 |
| - 0.0334 | + 0.5812 | + 0.8970 | + 0.2563 | + 0.0042 | - 0.0442 |
| + 0.2810 | - 0.6716 | + 0.2950 | + 0.5994 | - 0.7237 | - 0.5946 |
| + 0.1547 | - 0.1263 | - 0.0034 | - 0.5198 | + 0.2615 | - 0.1552 |
| - 0.3006 | - 0.2099 | - 0.1153 | + 0.1560 | + 0.5969 | - 0.3515 |
| + 0.5561 | - 0.1507 | - 0.1763 | + 0.2746 | - 0.0925 | - 0.4844 |
| + 0.3908 | - 0.7916 | - 0.6622 | + 0.4465 | - 0.3452 | - 0.3188 |
| - 0.1766 | - 0.0316 | + 0.2328 | - 0.4397 | - 0.0470 | + 0.3975 |
| + 0.2251 | + 0.3554 | - 0.4816 | + 0.1185 | - 0.3081 |          |
| + 0.3227 | + 0.0709 | - 0.4476 | + 0.1055 | - 0.0426 |          |
| + 0.5098 | - 0.4846 | - 0.1942 | + 0.6761 | - 0.5503 |          |
| - 0.4313 | - 0.1680 | + 0.3352 | - 0.0790 | - 0.1809 |          |
| - 0.0910 | - 0.2674 | - 0.3670 | + 0.1973 | - 0.0179 |          |
| + 0.2783 | - 0.1057 | - 0.5571 | + 0.1053 | - 0.1733 |          |
| + 0.6333 | - 0.7873 | - 0.0931 | + 0.4501 | + 0.0346 |          |
| - 0.3163 | - 0.1437 | - 0.4592 | - 0.7156 | - 0.4335 |          |

These results lead to a value of the asymmetry in the presence of the gold foil of  $(+ 0.011 \pm 0.028)$ , and to an asymmetry in the presence of the aluminium foil of  $(- 0.082 \pm 0.032)$ . Since this last asymmetry should be due purely to instrumental effects, the actual asymmetry caused by the presence of the gold scattering foil is  $(+ 0.093 \pm 0.043)$ .

In order to calculate the degree of electron polarization from this asymmetry value, Sherwin's<sup>(117)</sup> tables of the asymmetries produced when fully polarized electron beams of different energies are scattered from targets of various Z values were used. Since the electrons used in this experiment were not monoenergetic, but had, in fact, an energy range from 167 keV to 404 keV, this factor was also taken into account. A graph of the  $\beta$ -spectrum of  $Zr^{95}$  for  $\beta$ -energies greater than 167 keV was plotted against the electron momentum, with the aid of the appropriate Fermi functions<sup>(118)</sup>. See table V and fig. 12. This graph was then divided up into equal momentum intervals, and the area under each section of the curve, corresponding to the number of electrons in each momentum interval, was found. Using Sherwin's tables, a graph was plotted of the asymmetries expected when a 100% polarized electron beam is scattered from a target of Z value 80, the scattering angle being  $90^\circ$ , against the electron momentum. See fig. 13.

Table V.

Fermi functions and  $\beta$ -spectra.

$$y = \sqrt{N/F} = 1(\epsilon_0 - \epsilon) \quad E_0 = 404 \text{ keV} \quad \epsilon_0 = 1.791 \quad \epsilon = E/mc^2$$

| P<br>momentum<br>in units<br>of $mc$ | $\epsilon$<br>in units<br>of $mc^2$ | $\epsilon_0 - \epsilon$ | N/F    | F     | N      |
|--------------------------------------|-------------------------------------|-------------------------|--------|-------|--------|
| 0.85                                 | 1.312                               | 0.479                   | 0.2294 | 2.283 | 0.5237 |
| 0.90                                 | 1.345                               | 0.446                   | 0.1989 | 2.483 | 0.4939 |
| 0.95                                 | 1.379                               | 0.412                   | 0.1697 | 2.692 | 0.4568 |
| 1.00                                 | 1.414                               | 0.377                   | 0.1421 | 2.910 | 0.4135 |
| 1.05                                 | 1.449                               | 0.342                   | 0.1170 | 3.142 | 0.3676 |
| 1.10                                 | 1.487                               | 0.302                   | 0.0924 | 3.373 | 0.3117 |
| 1.15                                 | 1.524                               | 0.267                   | 0.0713 | 3.624 | 0.2584 |
| 1.20                                 | 1.562                               | 0.229                   | 0.0524 | 3.874 | 0.2030 |
| 1.25                                 | 1.601                               | 0.190                   | 0.0361 | 4.144 | 0.1496 |
| 1.30                                 | 1.640                               | 0.151                   | 0.0228 | 4.414 | 0.1006 |
| 1.35                                 | 1.680                               | 0.111                   | 0.0123 | 4.703 | 0.0578 |
| 1.40                                 | 1.720                               | 0.071                   | 0.0050 | 4.991 | 0.0250 |
| 1.45                                 | 1.761                               | 0.030                   | 0.0009 | 5.299 | 0.0047 |
| 1.486                                | 1.791                               | 0                       |        |       | 0      |

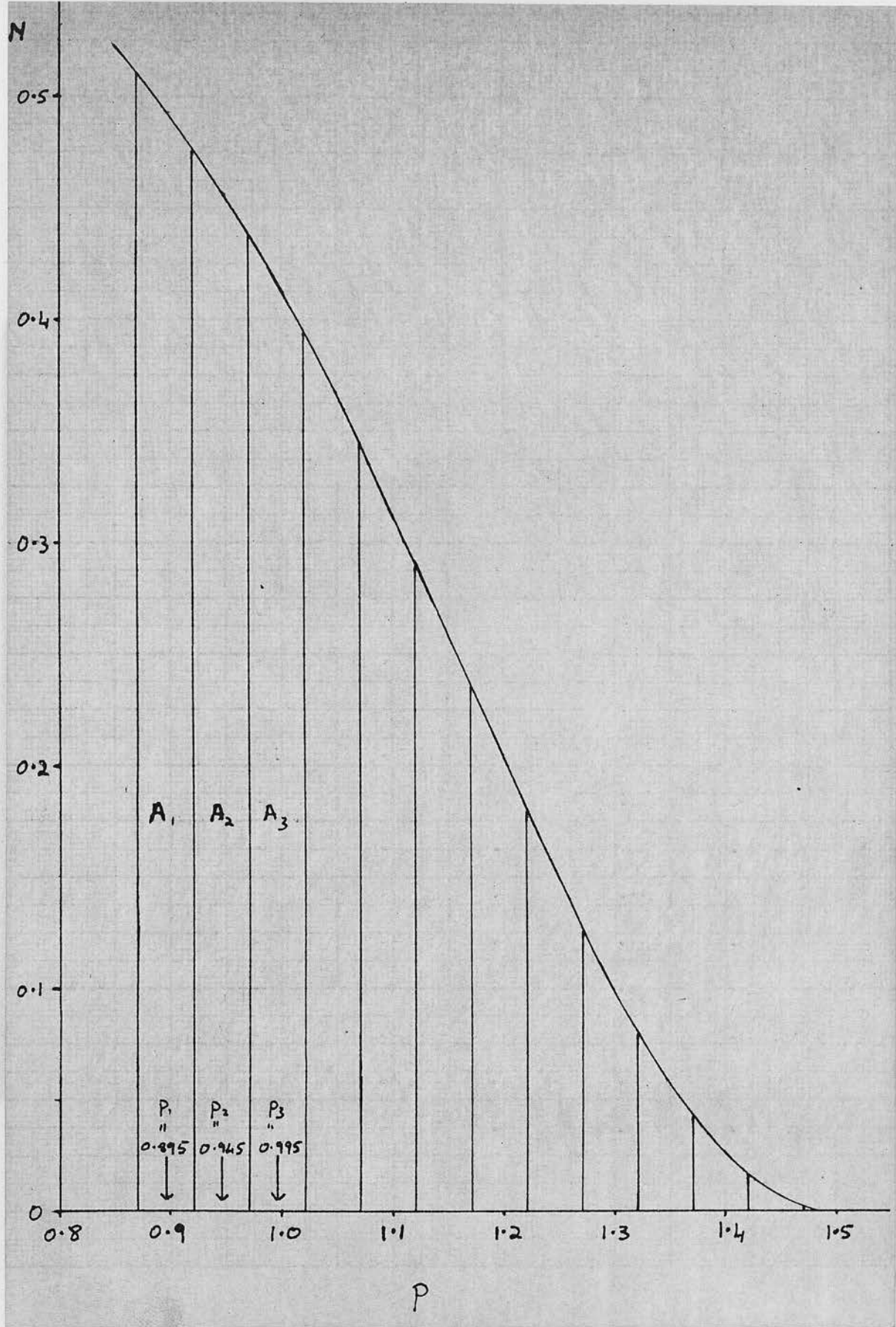


Figure 12. The  $\beta$ -spectrum of  $Zr^{95}$  for energies  $> 167$  keV.

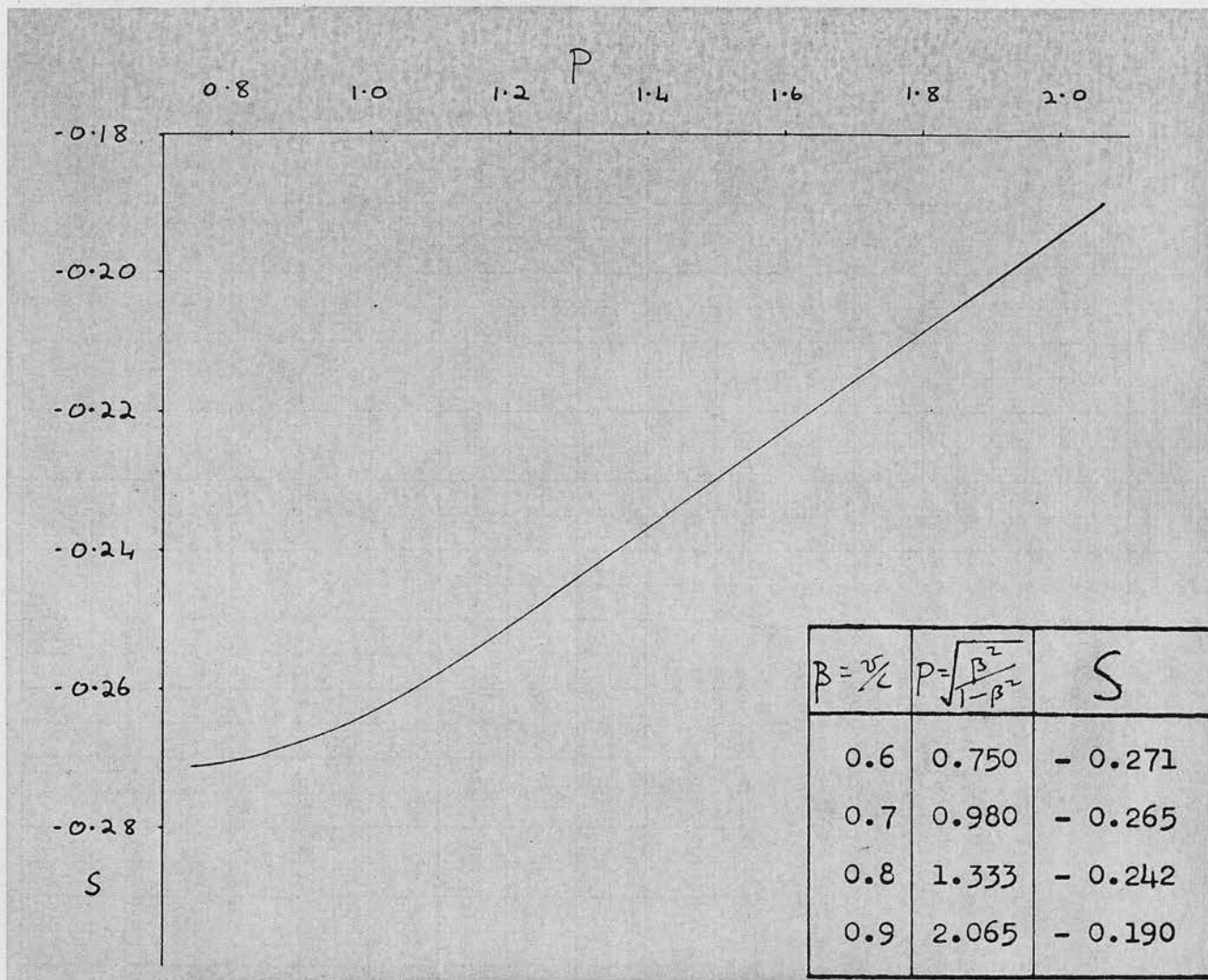


Figure 13. Graph of Sherwin's values for the expected asymmetry produced by Mott scattering, through  $90^\circ$ , of a 100% polarized electron beam  $v$ . the electron momentum, for a scattering material of Z value 80.

Using these two graphs, a weighted average value of the asymmetry, which would have occurred had the experimental electron beam been fully polarized, was calculated. See table VI. By comparing this calculated asymmetry with that experimentally obtained, the degree of polarization of the electrons from the  $Zr^{95}$  source was found.

Table VI.

| P in units<br>of mc | S        | A          | -SA            |
|---------------------|----------|------------|----------------|
| 0.895               | - 0.2695 | 19.74      | 5.3199         |
| 0.945               | - 0.2665 | 18.25      | 4.8636         |
| 0.995               | - 0.2640 | 16.66      | 4.3982         |
| 1.045               | - 0.2613 | 14.80      | 3.8672         |
| 1.095               | - 0.2580 | 12.71      | 3.2792         |
| 1.145               | - 0.2548 | 10.51      | 2.6779         |
| 1.195               | - 0.2515 | 8.27       | 2.0799         |
| 1.245               | - 0.2480 | 6.12       | 1.5178         |
| 1.295               | - 0.2445 | 4.19       | 1.0245         |
| 1.345               | - 0.2410 | 2.49       | 0.6001         |
| 1.395               | - 0.2370 | 1.12       | 0.2654         |
| 1.445               | - 0.2338 | 0.25       | 0.0584         |
|                     |          | 0          | 0              |
|                     |          | A = 115.11 | SA = - 29.9521 |

∴ Asymmetry produced by a 100% polarized beam = 0.2602.

Chapter V.Discussion of Possible Sources of Instrumental Asymmetries and Further Results.1. Instrumental Asymmetries.

If it is assumed that there is no instrumental asymmetry then the value ( $+ 0.011 \pm 0.028$ ) of the asymmetry produced by the presence of the gold foil leads to a value of  $(4 \pm 11)\%$  for the degree of <sup>transverse</sup> polarization of the electrons from the  $Zr^{95}$  source. However, if the apparent instrumental asymmetry ( $- 0.082 \pm 0.032$ ), found from the observations taken when aluminium was used as the scattering material, is taken into account, the degree of polarization of the electrons becomes  $(36 \pm 17)\%$  which indicates that the  $\beta$ -interaction is not invariant under time-reversal. As this positive result depends entirely on the instrumental asymmetry it was thought advisable to look for the source of such an asymmetry.

The tests to ensure that the source was centrally placed with respect to the  $\gamma$ -counter positions were repeated as were those to ensure that no counts were being recorded due to radiation scattered from the material of the apparatus. No asymmetries due to these causes were found.

Observations were made to see if any Compton

electrons, caused by  $\gamma$ -rays from the source striking the foil, were being recorded in the  $\beta$ -channel since, if this were the case, the difference between the  $\beta$ -counting rates with a scattering foil and with no scattering foil in the path of the electron beam would be due not only to scattered electrons but also to these Compton electrons. If these Compton electrons are present, then the values of the ratios of the coincidence per recorded  $\gamma$ -ray to scattered  $\beta$ -particle, used in the above calculations, would be incorrect and the actual number of Compton electrons recorded, and any coincidences due to their presence, would have to be taken into account. It must be noted that the counting rates due to these Compton electrons would not be the same for the two scattering foils.

In order to discover whether any such Compton electrons were present the single and coincidence channel counting rates were measured with no source in the source holder and the foil holder in each of its three positions. These give the noise levels in the photomultipliers together with any counts due to cosmic rays. These background counting rates were found to be unaffected by the different foil holder positions. Measurements were then taken with the source in position but the aperture through the base-plate of the vacuum chamber blocked with a piece of aluminium sufficiently thick to prevent any

electrons entering the chamber while still allowing the passage of  $\gamma$ -rays. Again the three foil holder positions were used. In the case in which no foil was present at the centre of the chamber the counting rates recorded in the  $\beta$  and coincidence channels were due to the background of noise and cosmic rays already measured and also to  $\gamma$ -rays from the source. Any difference between these counting rates and those recorded when a scattering foil was in position at the centre of the chamber would be due to Compton electrons from the foil. It was found that the  $\beta$ -channel and coincidence counting rates remained statistically the same for the three positions of the foil holder showing that Compton electrons were not contributing to these counting rates. The stop was then removed and the counting rates noted once more when no foil was in the path of the electrons. These were found to be the same as the corresponding counting rates obtained when the  $\beta$ -stop was in position showing that the background in the  $\beta$  and coincidence channels under the conditions of the actual experiment was due to noise in the photomultipliers, cosmic rays and  $\gamma$ -rays reaching the  $\beta$ -detecting crystal and that the contribution due to electrons being scattered from the residual gas in the chamber, from the material of the foil holder or the walls of the chamber was negligible. As the background has been taken into account when

calculating the results any asymmetry in it (and an asymmetry due to cosmic rays was actually found to exist) has been eliminated from the final calculated asymmetry values.

A possible source of instrumental asymmetry not so far considered is the finite size of the source. Since the source covered a circular area of 4 mm. diameter, the solid angles subtended by the  $\gamma$ -detecting crystal at various points on the source were not the same. The solid angles subtended by a scattering foil at different points along the source also varied, as did the appropriate angles for collection of the scattered electrons. In order to find the maximum asymmetry due to an extended, but centrally placed, source, the source was regarded as two equal point sources at the ends of the East-West diameter of the source area; see fig. 14. Fig. 14(a) is drawn to scale and shows the paths of electrons from the extreme points of the source, i.e. from one point 2 mm. to the East and from another 2 mm. to the West of the central position, in broken lines. (The solid lines show the paths of electrons from the central point.) Fig. 14(b) is not drawn to scale but shows, in an exaggerated manner, the difference in the solid angles subtended by the  $\gamma$ -detecting crystal at the extremities of the source.

Denoting the solid angles subtended by the  $\gamma$ -

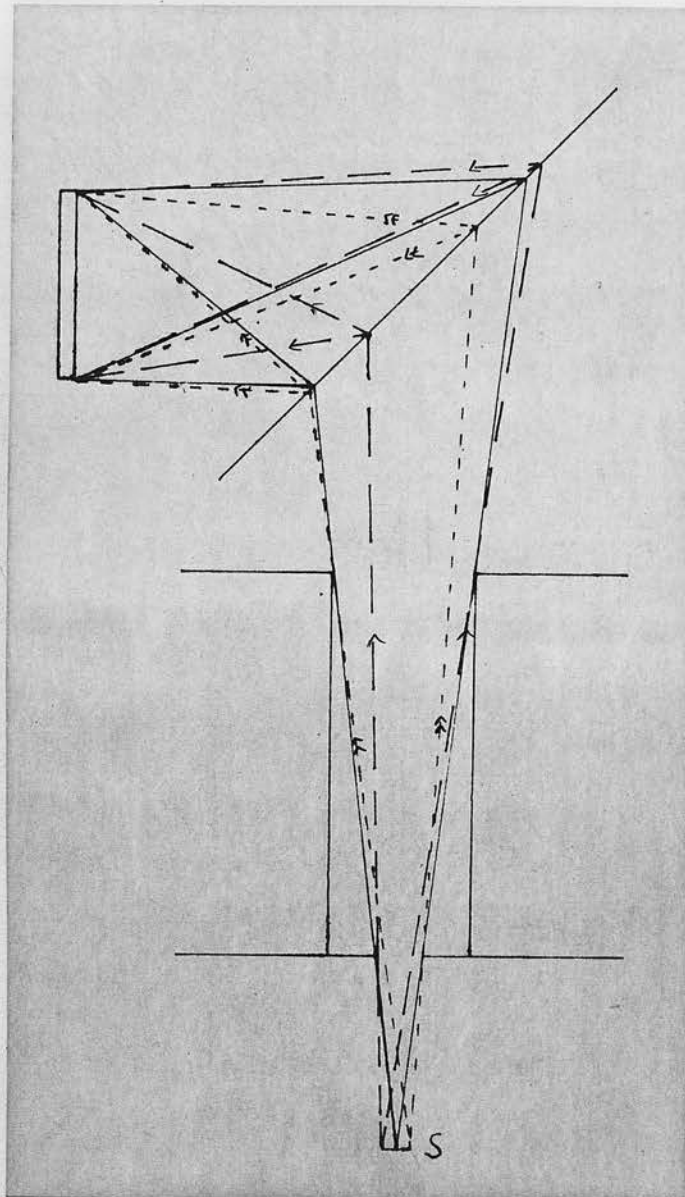


Figure 14(a). To show the effects of a source of finite size centrally placed with respect to the axis of the vacuum chamber.

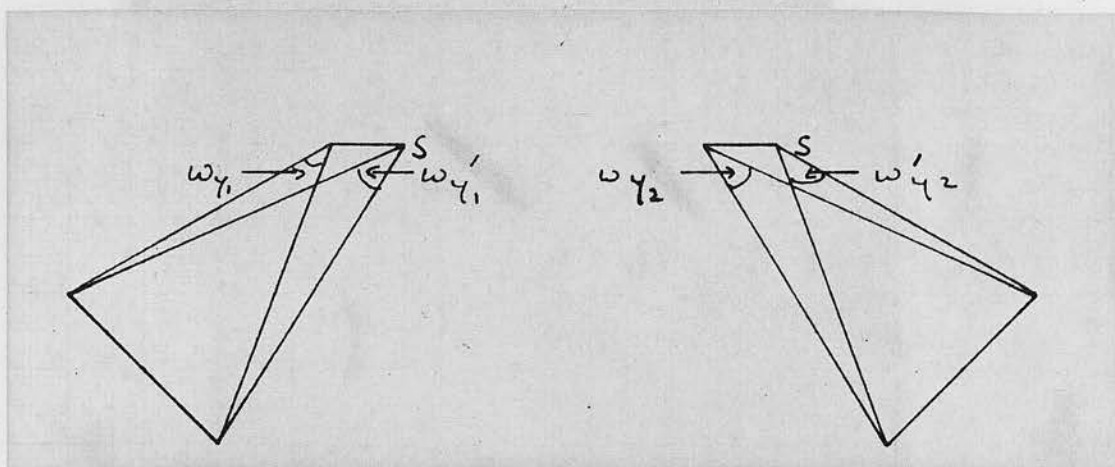


Figure 14(b). To show the different solid angles subtended by the  $\gamma$ -detecting crystal at the extremities of the source. (The size of the source is greatly exaggerated compared to that of the detecting crystal.)

Figure 14(c). To show the effect of a source of finite size displaced 2 mm. towards the slit from the central position.

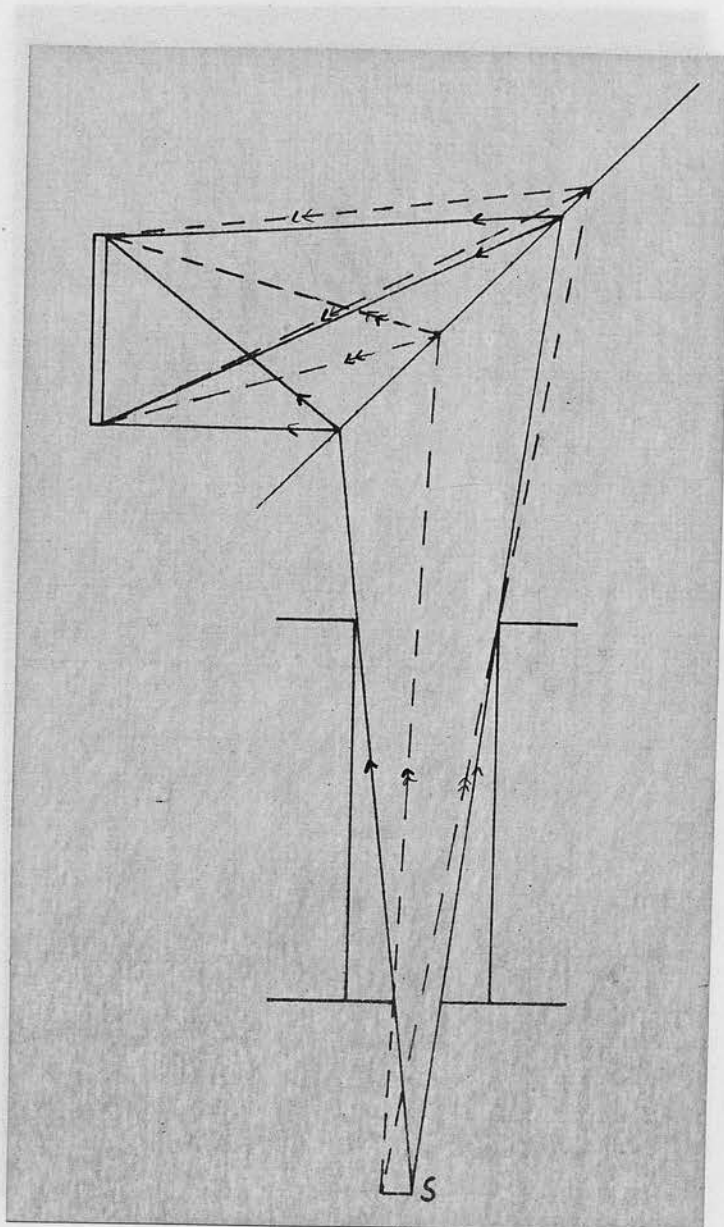


Figure 14(c). To show the effect of a source of finite size displaced 2 mm. towards the East from the central position.

detecting crystal at the East position and  
the counter is in the East position and  
the counter is in the West position

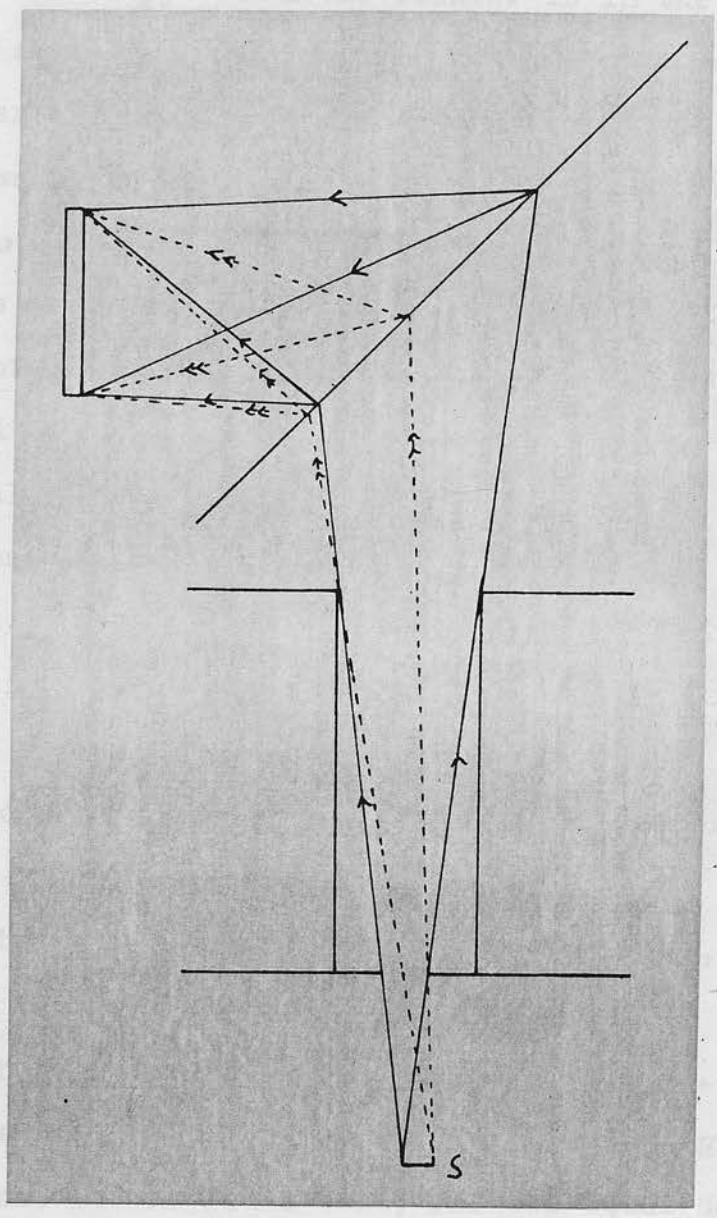


Figure 14(d). To show the effect of a source of finite size displaced 2 mm. from the central position towards the West.

detecting crystal at the two point sources  $\omega_{\gamma_1}$  and  $\omega_{\gamma_1}'$  when the counter is in the East position and  $\omega_{\gamma_2}$  and  $\omega_{\gamma_2}'$  when the counter is in the West position, as in the diagram, since the  $\gamma$ -counter positions were arranged so that the counting rates in each position were the same it follows that  $\omega_{\gamma_1}$  equals  $\omega_{\gamma_2}'$  and  $\omega_{\gamma_1}'$  equals  $\omega_{\gamma_2}$ . If the solid angles subtended by the scattering foil at the point source 2 mm. to the East of the centre point is denoted  $\omega_{\beta_2}$  and that subtended by the foil at the point 2 mm. to the West of the central position is denoted  $\omega_{\beta_2}'$ , and the corresponding scattering cross-sections for the electrons from these points and solid angles for the collection by the  $\beta$ -detecting crystal of the scattered electrons are denoted  $\sigma_{\beta_2}$ ,  $\sigma_{\beta_2}'$ ,  $\omega_{e_2}$  and  $\omega_{e_2}'$  respectively, then the coincidence counting rate is proportional to

$$\omega_{\gamma_1} \omega_{\beta_2} \sigma_{\beta_2} \omega_{e_2} + \omega_{\gamma_1}' \omega_{\beta_2}' \sigma_{\beta_2}' \omega_{e_2}'$$

when the  $\gamma$ -counter is in the East position, and to

$$\omega_{\gamma_1}' \omega_{\beta_2} \sigma_{\beta_2} \omega_{e_2} + \omega_{\gamma_1} \omega_{\beta_2}' \sigma_{\beta_2}' \omega_{e_2}'$$

when the  $\gamma$ -counter is in the West position.

Using these solid angles and scattering cross-sections, it was found that, for two equal sources deposited at the extremities of the East-West diameter of the source area, the coincidence counting rate would be approximately 6% higher with the  $\gamma$ -counter in the West position than with the  $\gamma$ -counter in the East position.

If a 2 mm. shift of the source towards the East is considered (fig. 14(c)), the solid angles for  $\gamma$  collection remain unaltered, since the  $\gamma$ -counter was positioned so that the source was symmetrically placed with respect to the East and West  $\gamma$ -counting positions, but the appropriate electron solid angles and scattering cross-sections become  $\omega_{\beta_4}$ ,  $\omega_{\beta_0}$ ,  $\sigma_{\beta_4}$ ,  $\sigma_{\beta_0}$ , and  $\omega_{e_4}$ ,  $\omega_{e_0}$ . Under these conditions a West-East asymmetry of  $\sim 9\%$  is expected, whereas a 2 mm. shift of the source from the central position towards the West (fig. 14(d)) leads to a 1.4% West-East asymmetry.

As the source had been very carefully positioned so that it lay as nearly as possible symmetrically with respect to the axis of the vacuum chamber a shift of more than  $\sim 2$  mm. off centre in either direction is unlikely. However, to put an outside limit to the asymmetry produced by a misplaced source, a shift of the source centre of 4 mm. to either side of the axis of the chamber was considered. It was found that a displacement of 4 mm. towards the East would lead to a West-East asymmetry of  $\sim 11\%$ , and that a similar displacement towards the West would lead to an East-West asymmetry of  $\sim 5.6\%$ . Such a shift in the source position would mean that no part of the source would lie directly under the aperture in the duralium can and consequently no greater asymmetries than these would, in practice,

occur.

Since the condition assumed of two point sources 4 mm. apart did not in fact exist, the source being deposited over a circular area of 4 mm. diameter, the actual asymmetry caused by an extended source, or by faulty alignment of the source would be considerably smaller than the values quoted above. As the relationship between the displacement of the source from the central position and the percentage asymmetry in the coincidence counting rate is approximately linear, the effect of an extended, uniformly deposited, centrally placed source was calculated knowing the asymmetry arising from two equal, symmetrically placed, point sources to be 6.3% and knowing that a point source on the axis can lead to no asymmetry in the coincidence counting rates, (see fig. 15). By integrating over the area of the source, the expected value of the West-East asymmetry was found to be  $\sim \frac{2}{3}\%$ . Owing to the approximately linear relationship between the source displacement and the expected percentage asymmetry the other calculated values should be reduced by a similar factor when a uniformly deposited source is considered.

It can be seen from these calculations that, even although the source may not have been uniformly deposited, the instrumental asymmetry due to an extended and faultily aligned source should not exceed  $\sim 2 - 3\%$  in

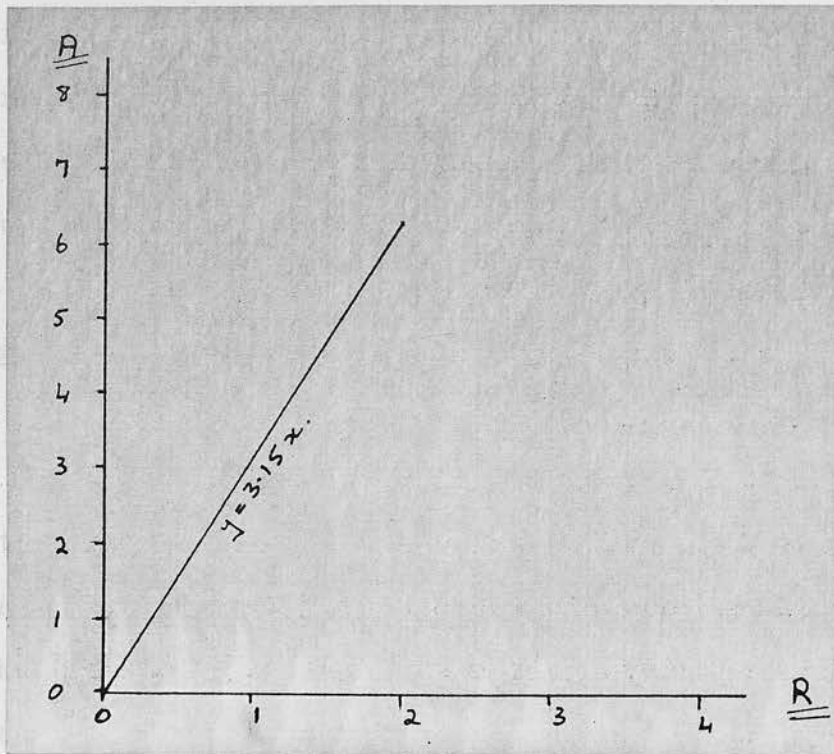


Figure 15. Graph of the percentage asymmetry (A) due to a centrally placed source v. source radius (R) in mm.

either direction. No cause being found for the East-West instrumental asymmetry of  $(8 \pm 3)\%$  calculated from the observations made with an aluminium scattering foil in the electron beam, it was considered advisable to neglect this result and to repeat the experiment under different conditions, since the final positive value obtained for the degree of polarization of the electrons from the  $Zr^{95}$  source depended entirely on this instrumental effect.

## 2. Further Observations.

As has been stated previously, the original choice of gold scattering foil was made by measuring the number of electrons scattered per minute from foils of various thicknesses and the number of coincidences due to these scattered electrons, and then selecting a foil which gave about twenty to thirty coincidence counts per hour, in order that the statistical errors in the counting rates should not be too great. In this way a foil of thickness  $\sim 5$  mgm./sq. cm. was chosen. However, with such a foil multiple scattering will occur, and although the transmitted rather than the reflected electrons were detected in order to minimize <sup>this</sup> effect, the recording of multiply scattered electrons will increase the and coincidence channel counting rates but will not lead to any asymmetry. Thus, in the equations for the

asymmetry value,  $\alpha = (W - E)/(W + E)$ , the values of  $W$  and  $E$  will both be increased by the recording of multiply scattered electrons. This will leave the numerator in the above expression unaltered but will increase the denominator, so reducing the value of  $\alpha$  and thus masking any asymmetry due to the non-invariance of the  $\beta$ -decay process under time-reversal.

In view of this, a separate set of results was obtained using a second gold scattering foil, this time of thickness  $\sim 0.7$  mgm./sq. cm., observations being taken in sets of four, one-hour, counts, i.e. with this gold foil as scatterer and the  $\gamma$ -counter in each of its two positions, and then with no scattering foil in the path of the electron beam and the  $\gamma$ -counter once more in each of its experimental positions. Since two sets of results were taken per day, and as there is no reason why a "gold" count should be coupled with a "blank" count taken immediately before it rather than one taken subsequently, more than two asymmetry values could be obtained from each day's counting provided that the number of equations used did not exceed the number of independent variables measured. The asymmetry values calculated from the counting rates obtained with the thinner gold foil are shown in table VII and lead to a final West-East asymmetry value of  $(+ 0.027 \pm 0.022)$ . Owing to the fact that the counting rates obtained with

this thin gold foil as scatterer were very much smaller than those recorded when the original gold foil was in use, the scattered  $\beta$  counting rate using the thin gold foil being  $\sim 10 - 15$  electrons per minute, a larger number of asymmetry values was required in this case.

The result of these observations was then compared with that obtained using the thicker gold scatterer. As any instrumental asymmetry must remain constant, and as the scattering foils are of the same material, any difference between the two asymmetry values must be due purely to a change in the number of multiply scattered electrons recorded. Since the multiple scattering and any consequent masking of time-reversal effects are reduced by using a thinner gold foil any difference between the two asymmetry values must be due to time-reversal effects.

From these two asymmetry values of  $+ 0.011$ , produced by the presence of the original gold foil in the path of the electron beam, and of  $+ 0.027$ , produced by the presence of the thinner gold foil, there would appear to be a small effect due to non-invariance under time-reversal; however, when the errors in these values are taken into account this difference is found to be not significant. In fact, if it is assumed that in the first case any time-reversal effects are completely masked by multiple scattering, and that therefore this

asymmetry value of  $(0.011 \pm 0.028)$  can be considered as a measure of the instrumental assymetry, the second set of results leads to a genuine asymmetry of  $(+ 0.016 \pm 0.036)$  which corresponds to a  $(6 \pm 14)\%$  <sup>Transverse</sup>  $\lambda$  polarization of the electrons from  $Zr^{95}$ .

|          |          |          |          |          |          |
|----------|----------|----------|----------|----------|----------|
| - 0.1892 | - 0.2778 | + 0.6053 | + 0.4913 | - 0.2109 | - 0.2183 |
| - 0.0287 | - 0.2011 | + 0.5674 | - 0.1375 | + 0.2058 | + 0.5537 |
| + 0.0106 | + 0.0508 | - 0.1843 | - 0.0286 | - 0.2072 | + 0.4932 |
| - 0.1460 | + 0.0405 | - 0.4163 | - 0.2864 | - 0.1046 | + 0.2444 |
| - 0.4435 | + 0.0884 | - 0.0514 | + 0.5288 | + 0.8120 | - 0.0497 |
| - 0.3507 | + 0.0692 | - 0.1293 | + 0.0069 | + 0.2887 | - 0.1106 |
| - 0.1493 | + 0.0343 | + 0.2600 | + 0.5176 | + 0.1460 | - 0.1174 |
| - 0.0665 | + 0.0802 | + 0.1965 | + 0.3935 | + 0.4055 | + 0.2604 |
| + 0.3016 | - 0.4050 | + 0.5708 | + 0.7734 | - 0.3702 | + 0.3304 |
| - 0.1578 | - 0.3362 | - 0.1610 | + 0.4939 | - 0.0328 | + 0.3305 |
| - 0.4718 | - 0.2006 | + 0.0065 | + 0.1767 | + 0.2453 | + 0.2998 |
| - 0.3183 | + 0.3244 | + 0.1712 | - 0.0333 | + 0.4566 | - 0.1293 |
| - 0.6725 | + 0.1305 | - 0.5775 | + 0.3649 | + 0.7307 | + 0.5607 |
| + 0.0732 | + 0.2708 | - 0.0755 | - 0.0860 | - 0.1432 | + 0.0465 |
| + 0.4006 | + 0.2245 | - 0.1060 | - 0.0484 | - 0.0562 | - 0.4940 |
| - 0.0611 | - 0.0013 | + 0.8753 | + 0.0587 | - 0.4959 | + 0.2158 |
| + 0.5641 | - 0.1851 | - 0.4034 | - 0.3884 | - 0.8597 | - 0.5509 |
| + 0.5208 | - 0.1549 | - 0.4347 | - 0.6482 | - 0.7302 | + 0.0810 |
| - 0.5013 | + 0.1520 | + 0.7696 | - 0.0312 | - 0.8533 | - 0.2078 |
| + 0.5275 | - 0.0328 | + 0.0053 | + 0.0009 | + 0.2584 | - 0.4898 |
| + 0.5838 | + 0.8568 | + 0.0038 | - 0.2153 | + 0.2062 | + 0.7346 |
| - 0.4307 | + 0.8486 | + 0.1071 | - 0.2633 | + 0.1273 | - 0.5276 |

Table VII.Asymmetry values obtained using the  $\sim 0.7$  mgm./sq.cm.thick gold foil. Expressed in the form  $(W - E)/(W + E)$ .

|          |          |          |          |          |          |
|----------|----------|----------|----------|----------|----------|
| + 0.0258 | - 0.2488 | + 0.8214 | + 0.4901 | - 0.2331 | - 0.3551 |
| - 0.0336 | - 0.6327 | + 0.5404 | + 0.4088 | + 0.1389 | + 0.0771 |
| - 0.1892 | - 0.2772 | + 0.6253 | + 0.4913 | - 0.1109 | - 0.2103 |
| - 0.0187 | - 0.2011 | + 0.5674 | - 0.1375 | + 0.2058 | + 0.5537 |
| + 0.0108 | + 0.0508 | - 0.1849 | - 0.0284 | - 0.2071 | + 0.4931 |
| - 0.1460 | + 0.0405 | - 0.4163 | + 0.2864 | - 0.1046 | + 0.2444 |
| - 0.4435 | + 0.0864 | - 0.0514 | + 0.5284 | + 0.2120 | - 0.0497 |
| - 0.3307 | + 0.0692 | - 0.1293 | + 0.0060 | + 0.2887 | - 0.1106 |
| - 0.1893 | + 0.0343 | + 0.2600 | + 0.3176 | + 0.1460 | - 0.1194 |
| - 0.0665 | + 0.0802 | + 0.1565 | + 0.3939 | + 0.4055 | + 0.2604 |
| - 0.3016 | - 0.4050 | + 0.5708 | + 0.7734 | + 0.3702 | + 0.3384 |
| - 0.1578 | - 0.3362 | - 0.1810 | + 0.4939 | - 0.0328 | + 0.3305 |
| - 0.4718 | - 0.2006 | + 0.0065 | + 0.1767 | + 0.2453 | + 0.2598 |
| - 0.3183 | + 0.3244 | + 0.1712 | + 0.0333 | + 0.4556 | - 0.1253 |
| - 0.6725 | + 0.1305 | - 0.5776 | + 0.3649 | + 0.7347 | + 0.5607 |
| + 0.0732 | + 0.2708 | - 0.0755 | - 0.0860 | + 0.5432 | + 0.0465 |
| + 0.4006 | + 0.2248 | - 0.1060 | - 0.0484 | - 0.0542 | - 0.4940 |
| - 0.0611 | - 0.0013 | + 0.8751 | + 0.0587 | - 0.4950 | + 0.2150 |
| + 0.5641 | - 0.1851 | - 0.4034 | - 0.3884 | - 0.8597 | - 0.5509 |
| + 0.5208 | - 0.1649 | - 0.4147 | - 0.0482 | - 0.7302 | + 0.0810 |
| - 0.5013 | + 0.1520 | + 0.7696 | - 0.0312 | - 0.8533 | - 0.2078 |
| + 0.5275 | - 0.0328 | + 0.0057 | + 0.0009 | + 0.2564 | - 0.4898 |
| + 0.5835 | + 0.8568 | + 0.0038 | - 0.2153 | + 0.2082 | - 0.7346 |
| - 0.4307 | + 0.8486 | + 0.1071 | - 0.2633 | + 0.1273 | - 0.5276 |

Table VII (continued).

|          |          |          |          |          |          |
|----------|----------|----------|----------|----------|----------|
| - 0.7419 | + 0.1822 | + 0.3277 | - 0.0324 | - 0.3077 | + 0.1167 |
| + 0.2322 | - 0.6394 | + 0.0520 | - 0.6379 | - 0.0926 | + 0.4987 |
| + 0.2622 | - 0.0641 | - 0.3499 | + 0.3009 | - 0.3889 | - 0.5736 |
| - 0.0990 | + 0.5328 | - 0.1927 | - 0.4437 | + 0.1055 | + 0.2880 |
| - 0.0768 | + 0.4827 | - 0.2100 | - 0.2747 | + 0.4103 | - 0.5503 |
| + 0.1650 | + 0.3229 | + 0.0224 | - 0.1078 | + 0.5032 | - 0.4179 |
| - 0.3904 | + 0.3887 | - 0.0955 | + 0.0753 | - 0.1036 | - 0.1508 |
| + 0.7870 | - 0.2868 | - 0.4996 | + 0.0447 | + 0.8028 | - 0.0831 |
| + 0.8491 | - 0.2380 | - 0.6151 | - 0.1435 | - 0.5834 | + 0.1594 |
| + 0.5877 | + 0.3355 | - 0.5045 | + 0.0514 | + 0.3670 | - 0.0229 |
| + 0.3201 | + 0.1670 | - 0.2108 | - 0.2520 | - 0.7055 | + 0.0914 |
| + 0.1244 | + 0.0609 | - 0.1156 | - 0.3103 | + 0.4298 | + 0.7655 |
| + 0.2368 | - 0.0157 | - 0.2298 | + 0.3655 | + 0.0430 | - 0.1943 |
| - 0.0382 | + 0.1789 | + 0.0702 | + 0.8083 | - 0.2908 | + 0.0435 |
| + 0.0432 | + 0.2156 | - 0.0987 | + 0.6434 | + 0.2685 | + 0.3915 |
| + 0.1583 | - 0.1117 | - 0.4171 | + 0.4462 | - 0.2824 | + 0.2449 |
| - 0.0735 | - 0.1923 | - 0.1711 | - 0.3453 | + 0.0197 | + 0.4316 |
| - 0.4345 | - 0.8601 | - 0.5920 | - 0.1603 | - 0.2790 | + 0.0964 |
| + 0.0787 | - 0.3581 | + 0.2371 | + 0.2883 | - 0.0065 | - 0.1484 |
| - 0.0671 | + 0.6078 | + 0.2360 | - 0.1133 | + 0.3420 | + 0.0318 |
| - 0.3451 | - 0.0180 | + 0.6226 | + 0.4481 | + 0.5142 | - 0.2755 |

such effects should be small. Both these groups look  
 for a term in the angular distribution function of the  
 decay products of the form  $D(\langle J \rangle / J) \cdot (p_x / E_x) \times (p_y / E_y)$ .

Chapter VI.Discussion of Results.1. Comparison of the Present Results with Those of Other Experimenters.

As has already been noted, any difference in the asymmetry values obtained using the two different gold scattering foils can only be due to time-reversal effects. The original value, taken as a measure of the instrumental asymmetry, is consistent with no such asymmetry being present and, on this assumption, a small asymmetry of  $(2.7 \pm 2.2)\%$  may be attributed to time-reversal effects in the decay process. However, when the errors in both the asymmetry values are taken into account, the final result is consistent with invariance of the  $\beta$ -decay interaction under the operation of time-reversal, or, at most, with only a small breakdown occurring. This conclusion is in agreement with the results of other experimenters.

The fact that Coulomb effects might tend to mask time-reversal effects was mentioned in the introduction and in view of this Burgy et al.<sup>(119)</sup> and Clark et al.<sup>(120)</sup> studied the decay of polarized neutrons where such effects should be small. Both these groups looked for a term in the angular distribution function of the decay products of the form  $D(\langle \underline{J} \rangle / J) \cdot (\underline{p}_e / E_e) \times (\underline{p}_\nu / E_\nu)$ ,<sup>(14)</sup>

where  $\langle \underline{J} \rangle / J$  is the average nuclear polarization, and  $\underline{p}_e$ ,  $\underline{p}_{\bar{\nu}}$ ,  $E_e$  and  $E_{\bar{\nu}}$  are the electron and antineutrino momenta and energies respectively.

Burgy et al. considered the decay of polarized neutrons under "normal" and "time-reversed" conditions as shown in fig. 16. If, under normal conditions, (fig. 16(a)) a neutron, with polarization vector pointing along the + z direction, decays at the point X resulting in an electron with its momentum vector directed along the + x axis and an antineutrino with its momentum vector along the + y axis, then, assuming that these two momenta are of equal magnitude, the slit system shown in the figure would allow the recoil proton to pass into the proton detector and a coincidence between the proton and the electron travelling into the appropriate detector on the x-axis would be recorded. Under the "time-reversed" conditions, since all the vectors are reversed, the slit and detector positions would have to be in the positions indicated in fig. 16(b) in order that a coincidence might be recorded. Since, by pure rotation about the z-axis, these two figures may be made to coincide, except for the direction of the nuclear spin, a measurement of the electron-proton coincidence rate per neutron decay, with the detector and slit positions as indicated in fig. 16(a), for the decay of neutrons polarized along

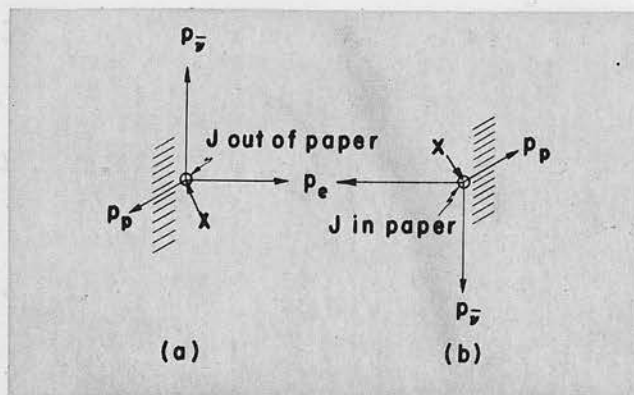


Figure 16. The decay of a polarized neutron under (a) "Normal", (b) "Time-reversed" conditions. (119)

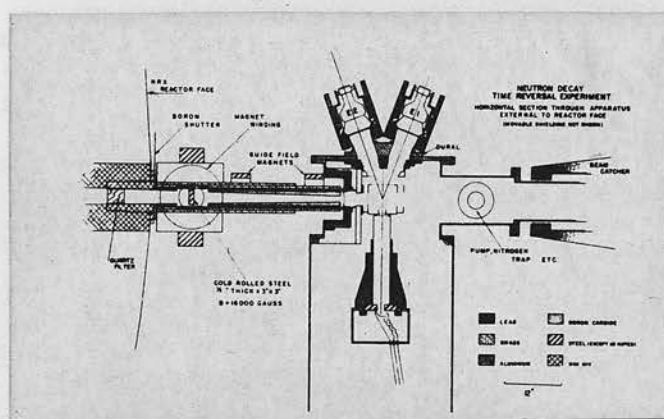


Figure 17. Apparatus used by Clark et al. (120) in their study of the time-reversal invariance properties of the neutron decay process.

the + z axis, and a similar measurement made with neutrons polarized along the - z axis will lead to information about the time-reversal properties of the decay. Any difference in these measured coincidence rates would show a breakdown of time-reversal invariance. Burgy et al., in an attempt to find an asymmetry in coincidence measurements of this type, obtained an asymmetry value of  $|0.015 \pm 0.017|$ , which leads to a value of  $|0.04 \pm 0.07|$  for D.

Clark et al., in their attempt to find the same term in the distribution function of the decay products of polarized neutrons, used the apparatus shown in fig. 17. In this case, the electron detectors were placed at  $160^\circ$  to the proton recoil direction in order to obtain a maximum value of the product  $p_e \times p_p$ . The coincidence rates were obtained between the proton and the two electron counters separately, and the asymmetry between these coincidence rates was found for both polarized and unpolarized neutrons. The value of D given by this experiment was  $|0.02 \pm 0.28|$  where the error is primarily statistical.

Since D can be expressed in terms of the coupling constants and is given by the expression (14)

$$D = \frac{2 \operatorname{Im} [C_S C_T^* - C_V C_A^* + C_S' C_T'^* - C_V' C_A'^*]}{|C_S|^2 + |C_T|^2 + |C_S'|^2 + |C_T'|^2 + 3 [ |C_A|^2 + |C_V|^2 + |C_A'|^2 + |C_V'|^2 ]}$$

if it is assumed that the interaction is VA in nature with an equal admixture of the vector and axial vector components and with  $C_i' = C_i$ , then the result  $D = 0$  implies that the  $\beta$ -decay is invariant under the operation of time-reversal, whereas the result  $|D| = 0.5$  implies a maximum breakdown of such an invariance. The results of these two experiments are therefore consistent with time-reversal invariance in the decay of neutrons, and show that a complete breakdown cannot occur.

A further experiment to test the time-reversal invariance of the  $\beta$ -decay interaction is that of Steffen<sup>(121)</sup> who looked for the transverse polarization of electrons from the decay of  $\text{Au}^{198}$ . This experiment is very similar to that undertaken by the author, the main differences being that the scattering foils were placed at  $90^\circ$  to the incident electrons and that the electron counter was placed so that it detected electrons which had been reflected through  $135^\circ$ . The apparatus is shown in fig. 18. In this experiment gold and aluminium scattering foils, both of thickness  $\sim 2$  mgm./sq. cm., were used, but no background measurements in the absence of a scattering foil were taken. Observations were taken in a series of fifteen minute counting periods. In addition to the East-West asymmetry, the North-South asymmetry due to each foil

was found. Such an asymmetry leads to a determination of the transverse polarization in the plane of the detected electron and  $\gamma$ -ray, i.e. it shows the presence of the term  $B(p \cdot E)(n \cdot E)$ , which violates parity, but not time-reversal, in the  $\beta$  -  $\gamma$  correlation function. In the first report to the presence of this term the value was given as  $(1.023 \pm 0.006)$  (1957).

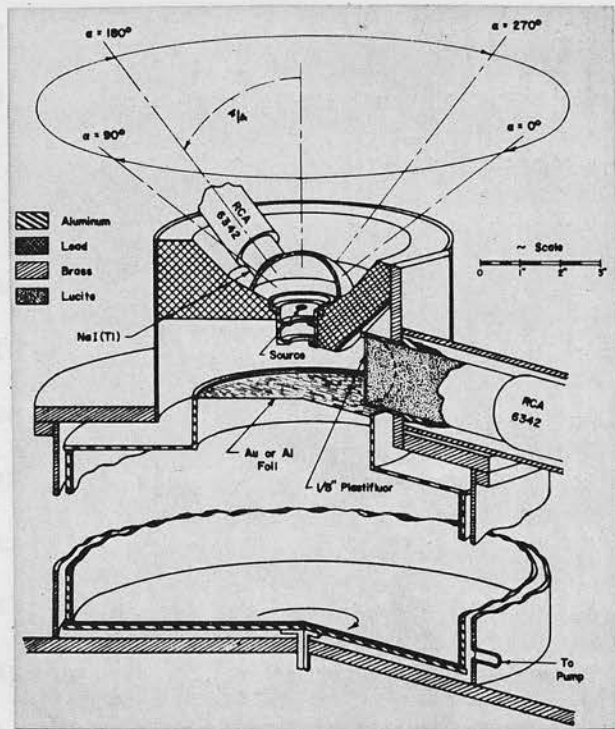


Figure 18. Apparatus used by Steffen<sup>(121)</sup> in his attempt to find a transverse polarization of the electrons from the decay of Au<sup>198</sup>.

this value for the degree of electron polarization from the above result an instrumental asymmetry of the order of  $(-0.002 \pm 0.005)$  must have been taken into account.

was found. Such an asymmetry leads to a determination of the transverse polarization in the plane of the detected electron and  $\gamma$ -ray, i.e. it shows the presence of the term  $B(\underline{p}, \underline{k})(\underline{n}, \underline{k})$ , which violates parity, but not time-reversal, in the  $\beta$ - $\chi$  correlation function. In the first report of this experiment, the asymmetry due to the presence of the gold scattering foil is quoted as  $(1.020 \pm 0.006)$  and that due to the presence of the aluminium foil as  $(0.986 \pm 0.012)$ , (these results are expressed in the form  $W/E$ ) which by comparison with the appropriate value of the expected asymmetry produced by a 100% polarized electron beam of average  $v/c \sim 0.85$  as given by Sherwin<sup>(117)</sup>, leads to a value of the degree of transverse electron polarization perpendicular to the plane of the detected electron and  $\gamma$ -ray of  $(5 \pm 3)\%$ . In the later paper, the results of four hundred and fifty days of continuous counting are given and, in this case, the asymmetry produced by the presence of the gold foil is quoted as  $(-0.0035 \pm 0.0015)$  (expressed in the form  $(W - E)/(W + E)$ ) and the final value of the degree of polarization of the electrons is given as  $(0.3 \pm 1.3)\%$ , no result being quoted for the asymmetry produced by the aluminium scattering foil, although in order to obtain this value for the degree of electron polarization from the above result an instrumental asymmetry of the order of  $(-0.002 \pm 0.005)$  must have been taken into account.

It must be noted that in both papers the asymmetry caused by the aluminium, as well as the gold, scattering foil is given for the North-South case and only in the final paper is this result omitted in the East-West case; that only in the case of the omission is this asymmetry due to the aluminium foil in the same sense as that due to the gold foil, and also that only in this case is the error in the experimentally measured asymmetry greater than the asymmetry value itself although, as the second paper gives the result of a much longer counting time than the first, this result would be expected to be more accurate than the preliminary one.

The careful consideration of all possible sources of an instrumental asymmetry in the present experiment and the reconsideration of the original results were, to some extent, due to this omission on the part of Steffen which lead to a doubt about the reliability of the results obtained with the aluminium scattering foil.

If, however, this unquoted instrumental error is taken into account, Steffen's results are also consistent with the invariance of the  $\beta$ -decay interaction under time-reversal if it is assumed that the Coulomb effects are small.

## 2. Consideration of Coulomb Correction Terms.

Unfortunately this assumption does not hold in

either Steffen's, or the present, experiment and it has been shown by Iben<sup>(122)</sup> that when Coulomb effects are taken into account asymmetries similar to those produced by non-invariance of the decay process under the operation of time-reversal are present, whether or not this invariance property is violated, and that the coefficient of the  $(\underline{n.p} \times \underline{k})(\underline{p.k})$  term in the correlation function depends on an energy, momentum and Z dependant function which is given by the expression

$$\begin{aligned} & \frac{3}{8} (p\varepsilon^{-1}) \left[ 2\alpha Z \left( \xi + \frac{1}{3} \eta \right) \beta_{\nu\nu} |M_{\nu}|^2 - \alpha Z \left( \xi - \frac{1}{3} \eta \right) \beta_{AA} |M_A|^2 \right. \\ & + \alpha Z \left( \xi - \eta \right) \text{Re} \beta_{\nu A} M_{\nu}^* M_A + \alpha Z \left( 3\alpha Z/p \right) \left[ \xi + \frac{1}{3} \varepsilon - \frac{1}{9} \eta \right] \text{Im} \beta_{\nu A} M_{\nu}^* M_A \\ & \left. + \frac{4}{3} p \text{Im} \beta_{\nu A} M_{\nu}^* M_A \right] \end{aligned}$$

where  $\alpha$  is the fine structure constant,  $p$  and  $q$  are the electron and antineutrino momenta in units of  $m_e c$ ;  $\varepsilon$  is the total electron energy in units of  $m_e c^2$ ;  $M_{\nu}$  and  $M_A$  are the nuclear matrix elements;  $\xi = Z/2R$ , where  $R$  is the nuclear radius in units of the electron Compton wavelength, and

$$\beta_{ik} = C_i C_k^* + C_i' C_k'^* = \text{Re} \beta_{ik} + i \text{Im} \beta_{ik}.$$

Iben has considered Steffen's experiment, taking into account these Coulomb terms, and has shown that a determination of the magnitude or even the energy dependence of this coefficient would not give definite

information about the time-reversal invariance properties of the decay.

In view of the presence of Coulomb effects, the use of the  $Zr^{95}$  isotope, in the present experiment, as the source of electrons whose transverse polarization was to be studied, has certain advantages over the use of the  $Au^{198}$  isotope, since the  $Z$  value of zirconium is approximately one half of that of gold, and thus any such effects should be greatly reduced. These effects are also reduced in the present experiment owing to the fact that the transition studied in the  $Au^{198}$  decay is a first forbidden transition (98.6% of the total decay) in which all the electrons, on leaving the nucleus, travel through a non-uniform electro-magnetic field which is expected to alter the relative orientation of the electron spin and momentum vectors, whereas two branches of the  $Zr^{95}$  decay can contribute to the time-reversal asymmetry effect, the first forbidden transition (53% of the total decay) followed by a direct  $\gamma$  transition to the ground state, and the allowed transition (34% of the total decay) which is followed by a mixed  $\gamma$  transition to the ground state, and since in an allowed transition the electron leaves the nucleus radially no such Coulomb effects should be present in this case.

However, in spite of the fact that Coulomb effects are greatly reduced in the present experiment they are

not completely eliminated and thus, although the results are consistent with the invariance of the  $\beta$ -decay interaction under the operation of time-reversal, no more definite conclusions are possible. It has, however, been suggested by Iben<sup>(122)</sup> that since, when the Coulomb corrections are taken into account, the coefficient of the term in the  $\beta - \gamma$  correlation function, which gives the anisotropy in the ordinary  $\beta - \gamma$  directional correlation, also depends on a function of the same variables as does the coefficient of the time-reversal asymmetry term, this function being

$$\frac{1}{3}(\rho^2 \epsilon^{-1}) \left[ 2\left(\xi + \frac{1}{2}\epsilon + \frac{1}{3}g\right) \beta_{\nu\nu} |M_{\nu}|^2 - \left(\xi + \frac{1}{4}\epsilon - \frac{1}{3}g\right) \beta_{AA} |M_A|^2 \right. \\ \left. + (\xi - g) \operatorname{Re} \beta_{\nu A} M_{\nu}^* M_A + (g \alpha Z \epsilon / 4 \rho) \left[ \xi + \frac{1}{3} \rho^2 \epsilon^{-1} - \frac{1}{9} g \right] \operatorname{Im} \beta_{\nu A} M_{\nu}^* M_A \right]$$

a determination of these two coefficients might lead to information of the time-reversal invariance property of the decay process, since, if they were shown to be of opposite sign, it could then be concluded that time-reversal invariance is violated although the extent to which such a violation occurs would not be known.

Acknowledgments.

1. T.D. Lee and C.N. Yang, (1956) Phys. Rev. 104, 254.

2. The author is indebted to Professor N. Feather, F.R.S. for extending the facilities of his laboratory and for his supervision of, and continuing interest in the investigation. *Mag. Series 5, 3, 801.*

3. Grateful thanks are due to Mr. J. Kyles, M.A. for his participation in, and supervision of the experimental work together with many helpful discussions and constant encouragement and advice. (1950) Phys. Rev. 23, 3430

In addition thanks are extended to Mr. A. Headridge and the technical staff of the Natural Philosophy Department for much valuable assistance in the construction of the apparatus. *E.W. Hayward, D.D. Hoopes and R.F. Hudson, (1957) Phys. Rev. 105, 1413.*

10. R.L. Garwin, L.H. Lederman and M. Weinrich, (1957) Phys. Rev. 105, 1415.

11. T.D. Lee and C.N. Yang, (1957) Phys. Rev. 105, 1671.

12. L. Landau, (1957) Nuclear Physics 3, 127.

13. A. Salam, (1957) Nuovo Cim. 2, 289.

14. J.D. Jackson, S.B. Treiman and H.W. Wylde, Jr.,

(1957) Phys. Rev. 106, 517.

15. R.B. Curtis and E.P. Lewis, (1957) Phys. Rev. 107, 543.

16. E. Alder, E. Steck and A. Winther, (1957) Phys. Rev. 107, 728.

References.

1. T.D. Lee and C.N. Yang, (1956) Phys. Rev. 104, 254.
2. D.H. Wilkinson, (1958) Phys. Rev. 109, 1603.
3. M. Tanner, (1957) Phys. Rev. 107, 1203.
4. R.E. Segel, J.V. Kane and D.H. Wilkinson, (1958)  
Phil. Mag. Series 8, 3, 204.
5. D.H. Wilkinson, (1958) Phys. Rev. 109, 1610.
6. D.H. Wilkinson, (1958) Phys. Rev. 109, 1614.
7. O. Chamberlain, E. Segre, R. Tripp, L. Wiegand and  
T. Ypsilantis, (1954) Phys. Rev. 93, 1430  
as quoted in ref. (1).
8. E.M. Purcell and N.F. Ramsay, (1950) Phys. Rev. 78,  
807 as quoted in ref. (1).
9. C.S. Wu, E. Ambler, R.W. Hayward, D.D. Hoppes and  
R.P. Hudson, (1957) Phys. Rev. 105, 1413.
10. R.L. Garwin, L.M. Lederman and M. Weinrich, (1957)  
Phys. Rev. 105, 1415.
11. T.D. Lee and C.N. Yang, (1957) Phys. Rev. 105, 1671.
12. L. Landau, (1957) Nuclear Physics 3, 127.
13. A. Salam, (1957) Nuovo Cim. 5, 299.
14. J.D. Jackson, S.B. Treiman and H.W. Wyld, Jr.,  
(1957) Phys. Rev. 106, 517.
15. R.B. Curtis and R.R. Lewis, (1957) Phys. Rev. 107,  
543.
16. K. Alder, B. Steck and A. Winther, (1957) Phys. Rev.  
107, 728.

17. M. Morita, (1957) Phys. Rev. 107, 1729.
18. M. Morita and R.S. Morita, (1958) Phys. Rev. 109,  
2048.
19. C.C. Bouchiat, (1958) Phys. Rev. 112, 877.
20. A.Z. Dolginov, (1958) Nuclear Physics 5, 512.
21. J.D. Jackson, S.B. Treiman and H.W. Wyld, Jr.,  
(1957) Nuclear Physics 4, 206.
22. M.E. Ebel and G. Feldman, (1957) Nuclear Physics  
4, 213.
23. V.B. Berestetsky, B.L. Ioffe, A.P. Rudick and  
K.A. Ter-Martirosyan, (1958)  
(i) Nuclear Physics 5, 464.  
(ii) Phys. Rev. 111, 522.
24. A.M. Bincer, (1958) Phys. Rev. 112, 244.
25. T. Kinoshita and A. Sirlin, (1957) Phys. Rev.  
106, 1110.
26. H. Uberall, (1957) Nuovo Cim. 6, 376.
27. J.D. Jackson, S.B. Treiman and H.W. Wyld, Jr.,  
(1957) Phys. Rev. 107, 327.
28. M.A. Grace, C.E. Johnson, R.G. Scurlock and C.V.  
Sowter, (1957) Phil. Mag. Series 8, 2, 1050.
29. (i) E.M. Ambler, R.W. Hayward, D.D. Hoppes, R.P.  
Hudson and C.S. Wu, (1957) Phys. Rev. 106,  
1361.  
(ii) E.M. Ambler, R.W. Hayward, D.D. Hoppes and R.P.  
Hudson, (1957) Phys. Rev. 108, 503.

30. H. Postma, W.J. Huiskamp, A.R. Miedema, M.J. Steenland, H.A. Tollhoek and C.J. Gorter,  
(i) (1957) *Physica* 23, 259.  
(ii) (1958) *Physica* 24, 157.
31. H. Frauenfelder, R. Bobone, E. von Goeler, N. Levine, H.R. Lewis, P.N. Peacock, A. Rossi and G. De Pasquali, (1957) *Phys. Rev.* 106, 386.
32. H. De Waard and O.J. Poppema, (1957) *Physica* 23, 597.
33. P.E. Cavanagh, J.F. Turner, C.F. Coleman, G.A. Gard and B.W. Ridley, (1957) *Phil. Mag. Series 8*, 2, 1105.
34. A. de-Shalit, S. Kuperman, H.J. Lipkin and T. Rothem, (1957) *Phys. Rev.* 107, 1459.
35. H. Frauenfelder, A.O. Hanson, N. Levine, A. Rossi and G. De Pasquali, (1957) *Phys. Rev.* 107, 643.
36. J.S. Geiger, G.T. Ewan, R.L. Graham and D.R. MacKenzie, (1958) *Phys. Rev.* 112, 1684.
37. F. Boehm and A.H. Wapstra, (1957) *Phys. Rev.* 106, 1364.
38. F. Boehm and A.H. Wapstra, (1957) *Phys. Rev.* 107, 1202.
39. F. Boehm and A.H. Wapstra, (1957) *Phys. Rev.* 107, 1462.
40. F. Boehm and A.H. Wapstra, (1958) *Phys. Rev.* 109, 456.

41. A. Lundby, A.P. Patro and J.P. Stroot, (1957)  
Nuovo Cim. 6, 745.
42. A. Lundby, A.P. Patro and J.P. Stroot, (1958)  
Nuovo Cim. 7, 891.
43. H. Schopper, (1957) Phil. Mag. Series 8, 2, 710.
44. H. Appel and H. Schopper, (1957) Zeits. für  
Physik 149, 103.
45. H. Appel, H. Schopper and S.D. Bloom, (1958)  
Phys. Rev. 109, 2211.
46. M. Goldhaber, L. Grodzins and A.W. Sunyar, (1957)  
Phys. Rev. 106, 826.
47. H. Schopper and S. Galster, (1958) Nuclear Physics  
6, 125.
48. (i) H. Frauenfelder, R. Bobone, E. von Goeler,  
N. Levine, H.R. Lewis, Jr., P.N. Peacock,  
A. Rossi and G. De Pasquali, (1957) Phys.  
Rev. 107, 909.
- (ii) H. Frauenfelder, A.O. Hanson, N. Levine,  
A. Rossi and G. De Pasquali, (1957)  
Phys. Rev. 107, 910.
49. F. Boehm, T.B. Novey, C.A. Barnes and B. Steck,  
(1957) Phys. Rev. 108, 1497.
50. M. Deutsch, B. Gittelman, R.W. Bauer, L. Grodzins  
and A.W. Sunyar, (1957) Phys. Rev. 107, 1733.
51. J.I. Friedman and V.L. Telegdi, (1957) Phys. Rev.  
105, 1681.

52. C. Castagnoli, C. Franzinetti and A. Manfredini,  
(1957) Nuovo Cim. 5, 684.
53. N.N. Biswas, M. Cecciaralli and J. Crussard, (1957)  
Nuovo Cim. 5, 756.
54. J. Heughebaert, M. Rene, J. Sacton and G. Vander-  
haeghe, (1957) Nuovo Cim. 5, 1808.
55. G.B. Chadwick, S.A. Durrani, L.M. Eisberg, P.B.  
Jones, J.W.G. Wignall and D.H. Wilkinson,  
(1957) Phil. Mag. Series 8, 2, 684.
56. D.F. Davis, A. Engler, C.J. Goebel, T.F. Hoang,  
M.F. Kaplon and J. Klarmann, (1957) Nuovo  
Cim. 6, 311.
57. B.M. Rustad and S.L. Ruby, (1953) Phys. Rev. 89, 880.
58. B.M. Rustad and S.L. Ruby, (1955) Phys. Rev. 97, 991.
59. J.S. Allen and W.K. Jentschke, (1953) Phys. Rev.  
89, 902.
60. W.P. Alford and D.R. Hamilton, (1954) Phys. Rev.  
94, 779.
61. D.R. Maxson, J.S. Allen and W.K. Jentschke, (1955)  
Phys. Rev. 97, 109.
62. J.M. Robson, (1955) Phys. Rev. 100, 933.
63. J.S. Allen, H.R. Paneth and A.H. Morrish, (1949)  
Phys. Rev. 75, 570.
64. D.R. Hamilton, (1947) Phys. Rev. 71, 456.

65. (i) M. Morita, R.S. Morita and M. Yamada, (1958)  
Phys. Rev. 111, 237.
- (ii) M. Morita and R.S. Morita, (1958) Phys. Rev.  
111, 1130.
- (iii) M. Morita, (1958) Phys. Rev. Letters I, 112.
66. R.B. Curtis and R.R. Lewis, (1957) Phys. Rev. 107,  
1381.
67. R.R. Lewis and R.B. Curtis, (1958) Phys. Rev. 110,  
910.
68. H. Frauenfelder, J.D. Jackson and H.W. Wyld, Jr.,  
(1958) Phys. Rev. 110, 451.
69. M.L. Good and E.J. Lauer, (1957) Phys. Rev. 105, 213.
70. W.P. Alford and D.R. Hamilton, (1957) Phys. Rev.  
105, 673.
71. W.B. Herrmannsfeldt, D.R. Maxson, P. Stählerin and  
J.S. Allen, (1957) Phys. Rev. 107, 641.
72. W.B. Herrmannsfeldt, R.L. Burman, P. Stählerin and  
J.S. Allen, (1958) Phys. Rev. Letters I, 61.
73. T. Lauritsen, C.A. Barnes, W.A. Fowler and C.C.  
Lauritsen, (1958) Phys. Rev. Letters I, 326.
74. C.A. Barnes, W.A. Fowler, H.B. Greenstein, C.C.  
Lauritsen and M.E. Nordberg, (1958) Phys.  
Rev. Letters I, 328.
75. K.H. Lauterjung, B. Schimmer and H. Maier-Leibnitz,  
(1958) Zeits. für Physik 150, 657.

76. G. Culligan, S.G.F. Frank, J.R. Holt, J.C. Kluyver  
and T. Massam, (1957) Nature 180, 751.
77. M. Bardon, D. Berley and L.M. Lederman, (1959)  
Phys. Rev. Letters II, 56.
78. T. Kinoshita and A. Sirlin, (1957)  
(i) Phys. Rev. 107, 593.  
(ii) Phys. Rev. 107, 638.
79. T. Kinoshita and A. Sirlin, (1957) Phys. Rev. 108,  
844.
80. L.A. Page, (1958) Nuovo Cim. 7, 727.
81. S.B. Treiman, (1958) Phys. Rev. 110, 448.
82. M. Goldhaber, L. Grodzins and A.W. Sunyar, (1958)  
Phys. Rev. 109, 1015.
83. M.T. Burgy, V.E. Krohn, T.B. Novey, G.R. Ringo and  
V.L. Telegdi, (1958) Phys. Rev. 110, 1214.
84. P.C. Macq, K.M. Crowe and R.P. Haddock, (1958)  
Phys. Rev. 112, 2061.
85. R.P. Feynman and M. Gell-Mann, (1958) Phys. Rev.  
109, 193.
86. E.C.G. Sudershan and R.E. Marshak, (1958) Phys. Rev.  
109, 1860.
87. J.J. Sakurai, (1958) Nuovo Cim. 7, 649.
88. A. Pias and S.B. Treiman, (1957) Phys. Rev.  
105, 1616.
89. J.C. Taylor, (1958) Phys. Rev. 110, 1216.
90. G. Morpurgo, (1957) Nuovo Cim. 5, 1159.

91. R. Gatto, (1958) Phys. Rev. 111, 1426.
92. F. Zachariasen, (1958) Phys. Rev. 110, 1481.
93. M. Sugawara, (1958) Phys. Rev. 112, 2128.
94. H.L. Anderson, T. Fujii, R.H. Miller and T. Lau,  
(1959) Phys. Rev. Letters II, 53.
95. M.L. Goldberger and S.B. Treiman, (1958) Phys. Rev.  
110, 1478.
96. J.C. Polkinghorne, (1958) Nuovo Cim. 8, 179.
97. M. Gell-Mann, (1958) Phys. Rev. 111, 362.
98. J. Bernstein and R.R. Lewis, (1958) Phys. Rev.  
112, 232.
99. T.D. Lee and C.N. Yang, (1957) Phys. Rev. 108, 1611.
100. A. Sirlin, (1958) Phys. Rev. 111, 337.
101. H.V. Argo, F.B. Harrison, H.W. Kruse and A.D.  
McGuire, (1959) Phys. Rev. 114, 626.
102. E.M. Henley and B.A. Jacobsohn,  
(i) (1958) Phys. Rev. 108, 502.  
(ii) (1959) Phys. Rev. 113, 225.
103. C.D. Schrader, (1953) Phys. Rev. 92, 928 as quoted  
in ref. (102)(i).
104. L. Rosen and J.E. Brolley, Jr., (1959) Phys. Rev.  
Letters II, 98.
105. D. Bodanski, S.F. Eccles, G.W. Farwell, M.E. Rickey  
and P.C. Robinson, (1959) Phys. Rev. Letters  
II, 101.

106. P. Hillman, A. Johansson and G. Tibell, (1958)  
Phys. Rev. 110, 1218.
107. T.D. Lee, R. Oehme, and C.N. Yang, (1957) Phys.  
Rev. 106, 340.
108. D.L. Pursey, (1957) Nuovo Cim. 6, 266.
109. M. Morita and R.S. Morita, (1957) Phys. Rev.  
107, 136.
110. M. Morita and R.S. Morita, (1957) Phys. Rev. 107,  
1316.
111. M.T. Burgy, R.J. Epstein, V.E. Krohn, T.B. Novey,  
S. Raboy, G.R. Ringo and V.L. Telegdi,  
(1957) Phys. Rev. 107, 1731.
112. (i) F.H. Wells, (1951) J. Brit. Instn. Rad. Engrs.  
11, 491.
- (ii) I.A.D. Lewis and F.H. Wells, Millimicrosecond  
Pulse Techniques, p. 161.
113. D. Strominger, J.M. Hollander and G.T. Seaborg,  
(1958) Rev. Mod. Phys. 30, 774.
114. P.P. Zarubin, (1954) Izvest. Akad. Nank. Ser. Fiz.  
S.S.S.R. 18, 563 as quoted in Nuclear Science  
Abstracts (1956) 10, No. 24B, 64.
115. D.L. Pursey, Private Communication.
116. D.J. Behrans, (1950) A.E.R.E. T/R 629.
117. N. Sherwin, (1956) Phys. Rev. 103, 1601.
118. Tables for the Analysis of Beta Spectra, (1952)  
National Bureau of Standards, Series 13.

119. M.T. Burgy, V.E. Krohn, T.B. Novey, G.R. Ringo and V.L. Telegdi, (1958) Phys. Rev. Letters I, 324.
120. M.A. Clark, J.M. Robson and R. Nathans, (1958) Phys. Rev. Letters I, 100.
121. (i) R.M. Steffen, Proceedings of the Rehovoth Conference on Nuclear Structure, (1958), p. 416.  
(ii) P.C. Simms and R.M. Steffen, (1958) Phys. Rev. Letters I, 289.
122. I. Iben, (1958) Phys. Rev. 112, 1240.